AD-768 617

EXTENDED ARRAY EVALUATION PROGRAM.
SPECIAL REPORT NO. 9. CONTINUED EVAL-
UATION OF THE NORWEGIAN SHORT-PERIOD
ARRAY

Frode Ringdal, et al

Texas Instruments, Incorporated

Prepared for:

Advanced Research Projects Agency
Air Force Technical Applications Center

10 August 1973

AD 768617

DOCUMENT CONTROL DATA - R & D

(Security classification of title, body of abstract and indexing annotation must be entered when the overall report is classified)

1 ORIGINATING ACTIVITY *(Corporate author)*	2a. REPORT SECURITY CLASSIFICATION
Texas Instruments Incorporated Equipment Group Dallas, Texas 75222	UNCLASSIFIED
	2b. GROUP

3. REPORT TITLE

Continued Evaluation of The Norwegian Short-Period Array, Special Report No. 9

4. DESCRIPTIVE NOTES *(Type of report and inclusive dates)*

Special

5. AUTHOR(S) *(First name, middle initial, last name)*

Frode Ringdal
Richard L. Whitelaw

6. REPORT DATE	7a. TOTAL NO. OF PAGES	7b. NO. OF REFS
10 August, 1973	107	7

8a. CONTRACT OR GRANT NO.	9a. ORIGINATOR'S REPORT NUMBER(S)
Contract No. F33657-72-C-0725	
b. PROJECT NO.	
AFTAC Project No. VELA T/2705/B/ASD	9b. OTHER REPORT NO(S) *(Any other numbers that may be assigned this report)*
c.	
d.	

10. DISTRIBUTION STATEMENT

APPROVED FOR PUBLIC RELEASE; DISTRIBUTION UNLIMITED

11. SUPPLEMENTARY NOTES	12. SPONSORING MILITARY ACTIVITY
ARPA Order No. 1714	Advanced Research Projects Agency Nuclear Monitoring Research Office Arlington, Virginia 22209

13. ABSTRACT

This report describes the continued evaluation of the Norwegian short-period Seismic Array (NORSAR), which was conducted by Texas Instruments Incorporated at the Seismic Data Analysis Center over the period 1 April 1972 to 31 March 1973.

The major areas of study presented in this report are:

- Signal analysis on a regional basis
- Signal amplitude response patterns across the array
- Array processing performance
- NORSAR seismic event detection capability
- Behavior of short-period seismic discriminants

The total data base for this study comprises 344 events.

DD FORM 1473
1 NOV 65

14. KEY WORDS	LINK A		LINK B		LINK C	
	ROLE	WT	ROLE	WT	ROLE	WT
NORSAR short-period array						
Signal characteristics						
Array beamforming						
Signal-to-noise improvement						
Detection threshold						
Discrimination capability						

AFTAC Project No. VELA T/2705/B/ASD

CONTINUED EVALUATION OF THE NORWEGIAN SHORT-PERIOD ARRAY

SPECIAL REPORT NO. 9

EXTENDED ARRAY EVALUATION PROGRAM

Prepared by
Frode Ringdal and Richard L. Whitelaw

T. W. Harley, Program Manager
Area Code 703, 836-3882 Ext. 300

TEXAS INSTRUMENTS INCORPORATED
Equipment Group
Post Office Box 6015
Dallas, Texas 75222

10 August 1973

Equipment Group

ABSTRACT

This report describes the continued evaluation of the Norwegian short-period Seismic Array (NORSAR), which was conducted by Texas Instruments Incorporated at the Seismic Data Analysis Center over the period 1 April 1972 to 31 March 1973.

The major areas of study presented in this report are:

- Signal analysis on a regional basis
- Signal amplitude response patterns across the array
- Array processing performance
- NORSAR seismic event detection capability
- Behavior of short-period seismic discriminants

The total data base for this study comprises 344 events.

TABLE OF CONTENTS

TABLE OF CONTENTS
(continued)

LIST OF FIGURES

LIST OF FIGURES
(continued)

LIST OF FIGURES
(continued)

LIST OF FIGURES
(continued)

LIST OF FIGURES
(continued)

x

LIST OF TABLES

SECTION I
INTRODUCTION

This report presents the results of an ongoing evaluation of the short-period (SP) Norwegian Seismic Array (NORSAR), using seismic data recorded during 1971 and 1972. The overall objectives of the NORSAR SP evaluation are:

- Determine the best processing methods for enchancing the signal-to-noise ratio of Eurasian events.

- Determine the array capability for Eurasian events.

- Evaluate the performance of short-period discriminants at NORSAR.

- In conjunction with long-period NORSAR data. determine the detection and discrimination capability of NORSAR for Eurasian events.

Substantial progress has been made toward achieving the first three objectives, but the results presented in this report may still be improved as the data base for the evaluation is expanded. Work toward meeting the fourth objective is still at an initial stage, and will be given more attention in our future analysis.

Five analysis tasks were undertaken in order to meet the first three objectives stated above:

- Noise analysis

- Signal analysis
- Array processing effectiveness
- Detection threshold estimation
- Behavior of SP discriminants

Results from noise analysis were presented in Special Report No. 6 under the Extended Array Evaluation program. No further work on this subject has been undertaken since then. Results from each of the four remaining tasks are presented in subsequent sections of this report.

The NORSAR SP array, centered about 100 km due north of Oslo, Norway, consists of 132 short-period seismometers and has an aperture of about 100 km. The sensors are grouped in 22 six-element subarrays; each subarray has a center sensor and a five-sensor ring and is about 7 km in diameter (Figure I-1). Throughout this report, the official nomenclature will be used whenever a NORSAR seismometer or subarray is referred to.

The results presented in the following sections are based primarily on events located on the Eurasian Continent. A total of 344 events have been analyzed; 106 of these were listed as the data base for Special Report No. 6. Table I-1 lists the parameters for the additional 238 events processed since then.

Geographically, the events are concentrated principally in the Northwestern Pacific (from Kamchatka to Taiwan) and in south central Asia (north and west of the Himalayan system). Thirty-nine events from the Mediterranean region are included as well eight from the Arctic Ocean and eight from Continental North America. Twenty-one events are presumed explosions; including eight from Eastern Kazakh, one from Western Kazakh, two from the Ural Mountains, three from Western Russia, one from Novaya Zemlya, one from the Aleutian Islands and five from Nevada.

01C (9)

02C (10)

03C (11)

14C (22)

04C (12)

13C (21)

01B (2)

02B (3)

07B (8)

03B (4)

05C (13)

12C (20)

01A (1)

06C (14)

06B (7)

04B (5)

11C (19)

05B (6)

10C (18)

N

08C (16)

07C (15)

09C (17)

|— 20 km —|
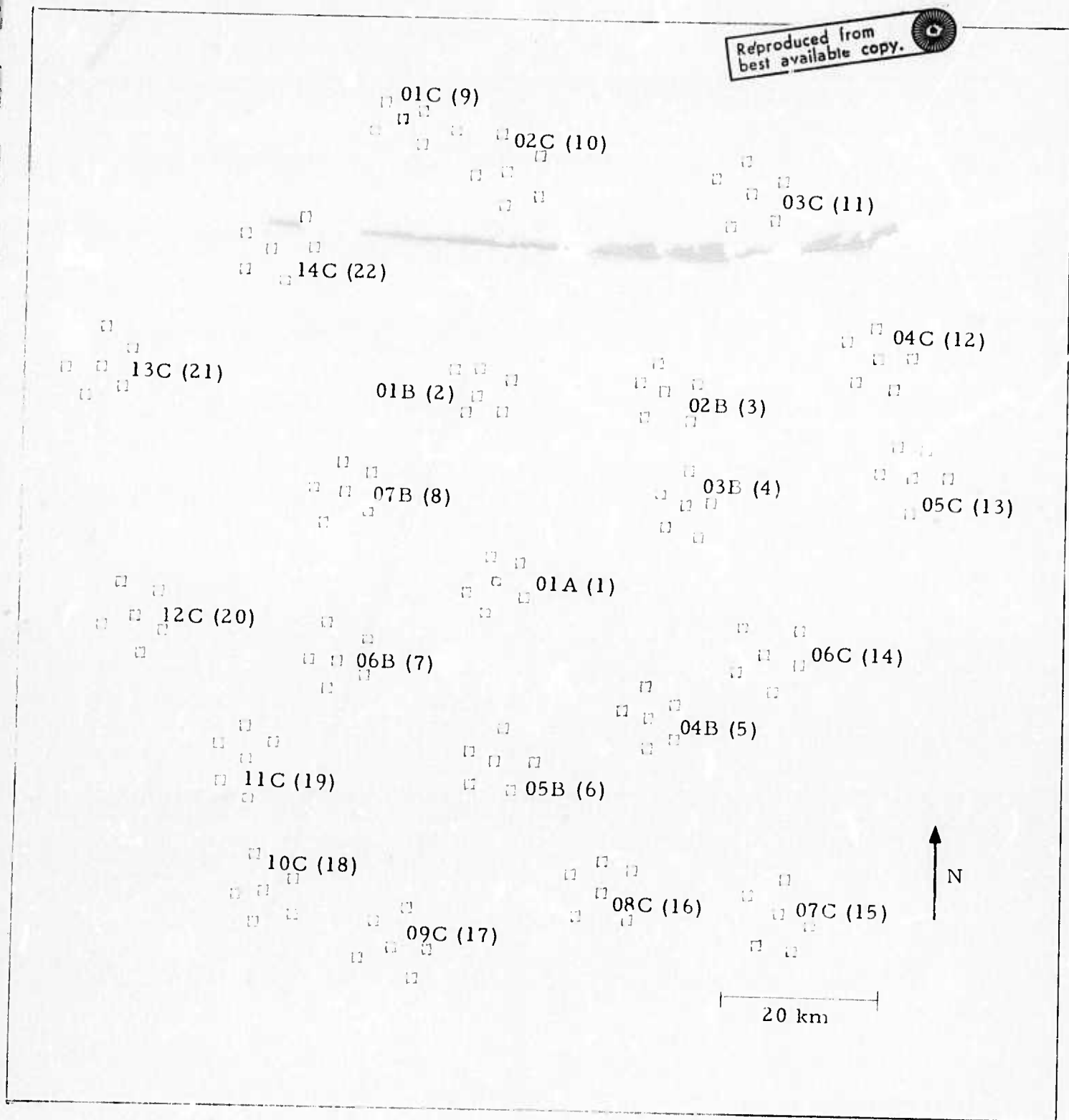
FIGURE 1-1

NORSAR SHORT PERIOD ARRAY

I-3

TABLE I-1

EVENT PARAMETERS
(PAGE 1 OF 6)

EVENT DESIGNATION	DATE	ORIGIN TIME	LAT	LON	DEPTH	MB	SOURCE BLTN	COMMENT
TUR/126/04N	05/06/71	04.24.33	39.0N	29.7E	23	4.6	P	
TUR/143/01N	05/23/71	01.02.54	37.6N	30.1E	NOR	4.4	P	
TUR/161/09N	06/10/71	09.31.54	39.1N	29.6E	NOR	4.0	P	
FRS/165/14N	06/14/71	14.25.56	56.2N	123.5E	NOR	4.6	P	
KAM/166/14N	06/15/71	14.04.08	52.8N	160.8E	55	5.1	P	
KIR/166/23N	06/15/71	23.17.33	41.6N	79.2E	NOR	4.0	P	
KUR/168/02N	06/17/71	02.32.05	44.4N	148.9E	NOR	4.0	P	
KIR/170/17N	06/19/71	17.23.02	41.5N	79.3E	NOR	5.2	P	
KIR/170/21N	06/19/71	21.08.45	41.5N	79.4E	NOR	4.7	P	
KUR/190/16N	07/09/71	16.44.15	43.5N	147.7E	46	4.0	P	
KUR/191/03N	07/10/71	03.05.00	43.6N	147.7E	36	4.8	P	
KUR/191/09N	07/10/71	09.01.34	45.0N	150.5E	NOR	4.6	P	
KAM/193/02N	07/12/71	02.12.29	53.1N	160.0E	NOR	4.0	P	
SZE/228/04N	08/16/71	04.58.00	28.9N	103.7E	NOR	5.5	P	
SZE/228/18N	08/16/71	13.29.24	28.8N	103.7E	NOR	4.8	P	
NEV/230/14N	08/18/71	14.00.00	37.1N	116.0W	0	5.4	P	E
TAI/231/08N	08/19/71	08.28.53	23.9N	121.9E	23	5.4	P	
KUR/231/22N	08/19/71	22.15.37	49.3N	155.4E	NOR	6.0	P	
IRA/234/17N	08/22/71	17.54.14	30.1N	50.7E	NOR	5.1	P	
SZE/235/05N	08/23/71	05.36.11	28.8N	103.7E	NOR	5.2	P	
KUR/235/21N	08/23/71	21.55.17	45.6N	151.0E	34	5.7	P	
CRS/236/16N	08/24/71	16.33.22	52.2N	91.4E	NOR	5.2	P	
IRA/237/00N	08/25/71	00.30.44	29.2N	52.3E	NOR	4.1	P	
HOK/237/10N	08/25/71	10.41.43	42.1N	142.3E	69	4.1	P	
IRA/238/06N	08/26/71	06.55.08	30.0N	50.7E	45	4.8	P	
IRA/239/05N	08/27/71	05.20.15	30.2N	50.7E	54	5.0	P	
IRA/239/07N	08/27/71	07.59.11	30.1N	50.7E	63	4.4	P	
HON/239/13N	08/27/71	13.49.59	40.8N	143.8E	NOR	4.9	P	
RYU/240/15N	08/28/71	15.57.47	28.3N	130.7E	35	5.7	P	
IRA/240/16N	08/28/71	16.34.44	37.6N	55.8E	NOR	4.8	P	
SIN/241/15N	08/29/71	15.16.56	36.5N	78.5E	NOR	5.0	P	
HIN/243/01N	08/31/71	01.52.16	36.5N	70.8E	87	4.3	P	
HON/245/09N	09/02/71	09.30.23	32.0N	131.7E	345	4.7	P	
IRA/245/18N	09/02/71	18.24.47	30.1N	50.8E	45	5.1	P	
IRA/245/22N	09/02/71	22.21.39	30.1N	50.8E	39	5.0	P	
SZE/246/18N	09/03/71	18.42.16	28.9N	103.7E	NOR	4.8	P	
TUR/248/12N	09/05/71	12.19.56	37.3N	30.3E	20	4.5	P	
FRS/248/21N	09/05/71	21.13.57	46.6N	140.9E	NOR	4.6	P	
SAK/249/06N	09/06/71	06.45.59	46.4N	141.1E	16	5.7	P	
SAK/249/13N	09/06/71	13.37.10	46.7N	141.4E	29	6.1	P	
SAK/249/20N	09/06/71	20.10.47	46.6N	141.2E	NOR	5.0	P	
RUM/251/04N	09/08/71	04.10.18	45.8N	27.0E	140	3.4	P	
HON/251/07N	09/08/71	07.25.14	37.2N	141.2E	56	5.5	P	
SAK/251/11N	09/08/71	11.48.23	46.4N	141.4E	6	5.9	P	
IRA/251/12N	09/08/71	12.53.34	29.2N	60.0E	12	5.4	P	

TABLE I-1

EVENT PARAMETERS
(PAGE 2 OF 6)

EVENT DESIGNATION	DATE	ORIGIN TIME	LAT	LON	DEPTH	MB	SOURCE BLTN	COMMENT
ERS/251/16N	09/08/71	16.59.52	46.2N	140.9E	16	5.9	P	
TUR/251/17N	09/08/71	17.01.09	37.3N	30.3E	6	4.8	P	
ERS/251/19N	09/08/71	19.22.15	45.4N	140.9E	19	5.3	P	
TUR/251/22N	09/08/71	22.35.15	41.1N	43.8E	32	4.8	P	
ERS/252/21N	09/09/71	21.06.20	46.6N	140.9E	NOR	4.5	P	
KUR/252/23N	09/09/71	23.01.06	44.4N	150.9E	7	6.0	P	
AFG/255/05N	09/12/71	05.03.25	37.0N	71.3E	130	4.5	P	
HIN/256/01N	09/13/71	01.45.35	35.7N	69.9E	120	4.8	P	
KUR/256/13N	09/13/71	13.01.29	48.5N	148.9E	120	4.8	P	
HON/258/14N	09/15/71	14.55.05	39.1N	143.4E	359	4.5	P	
RAT/261/02N	09/18/71	02.12.30	51.9N	178.6E	17	5.8	P	
NEV/262/00N	09/19/71	00.58.35	39.4N	118.9E	112	4.6	P	
WES/262/11N	09/19/71	11.00.06	57.8N	41.1E	10	4.5	P	
T /264/01N	09/21/71	01.04.18	38.3N	43.9E	NOR	4.5	P	F
TIR/264/09N	09/21/71	09.13.51	32.4N	01.8E	19	4.2	P	
TUR/264/16N	09/21/71	16.48.51	37.3N	30.2E	NOR	5.0	P	
ERS/265/14N	09/22/71	14.20.10	46.4N	140.8E	37	4.8	P	
AFG/268/08N	09/25/71	08.53.20	37.8N	69.7E	14	4.9	P	
GRE/269/05N	09/26/71	05.44.34	37.9N	69.7E	56	4.5	P	ND
TAL/269/15N	09/26/71	15.25.18	37.9N	22.2E	107	4.1	P	
HIN/269/23N	09/26/71	23.48.25	3.2N	125.8E	48	5.3	P	
TUR/271/05N	09/28/71	05.10.24	36.3N	70.2E	229	4.6	P	
TAL/271/14N	09/28/71	14.04.41	37.1N	30.1E	36	4.7	P	
HON/271/14N	09/28/71	14.13.09	3.7N	126.0E	169	5.9	P	
NEV/272/14N	09/29/71	14.00.00	40.2N	143.4E	45	4.2	P	
TUR/273/08N	09/30/71	08.45.58	37.0N	116.0W	0	4.4	P	ND F
RAT/273/11N	09/30/71	11.52.36	37.7N	30.1E	NOR	4.5	P	
SIB/273/21N	09/30/71	21.31.25	51.3N	178.8E	41	5.0	P	
TUR/276/07N	10/03/71	07.44.26	61.6N	140.3E	NOR	5.4	P	
TUR/276/17N	10/03/71	17.18.53	38.9N	29.9E	23	4.7	P	
SIB/278/01N	10/05/71	01.40.41	36.8N	29.9E	27	4.4	P	
IRA/278/18N	10/05/71	18.31.17	67.5N	172.8W	NOR	5.3	P	
TUR/278/18N	10/05/71	18.53.06	27.2N	55.8E	39	5.1	P	
IRA/278/22N	10/05/71	22.45.04	39.0N	29.9E	9	4.5	P	
TUR/279/01N	10/06/71	01.46.38	31.6N	50.7E	66	4.1	P	
RAT/279/11N	10/06/71	11.37.54	38.3N	30.2E	19	4.6	P	
NEV/281/14N	10/08/71	14.30.00	52.1N	178.2E	139	4.9	P	
KAZ/282/06N	10/09/71	06.02.57	37.1N	116.0W	0	4.7	P	E
IRA/288/14N	10/15/71	14.19.31	50.0N	77.7E	0	5.4	P	E
AFG/288/16N	10/15/71	16.22.13	37.3N	54.6E	39	4.7	P	
KAZ/356/06N	12/22/71	06.59.56	37.0N	71.8E	147	4.9	P	
SIB/001/15N	01/01/72	15.04.19	47.9N	48.2E	0	6.0	P	E
KUR/001/16N	01/01/72	16.55.06	59.7N	153.8E	NOR	4.1	S	ND
KUR/001/18N	01/01/72	18.13.54	50.7N	155.8E	NOR	4.6	S	
KUR/002/05N	01/02/72	05.37.25	49.4N	156.5E	50	4.0	S	
			46.1N	146.2E	NOR	4.0	S	

TABLE I-1

EVENT PARAMETERS

EVENT DESIGNATION	DATE	ORIGIN TIME	LAT	LON	DEPTH	MB	SOURCE BLTN	COMMENT
GRE/002/09N	01/02/72	09.17.53	37.9N	20.7E	NOR	4.2	S	
SIN/002/10N	01/02/72	10.27.35	41.8N	04.5E	19	5.2	S	
KAM/003/06N	01/03/72	06.36.38	51.6N	159.4E	NOR	4.8	P	
KAM/003/19N	01/03/72	19.26.43	52.0N	159.0E	NOR	4.5	N	MBN
KAM/004/02N	01/04/72	02.29.18	55.6N	161.2E	NOR	4.3	S	
KAM/004/10N	01/04/72	10.42.31	55.6N	163.8E	NOR	4.4	S	
TAI/004/12N	01/04/72	12.15.17	22.4N	122.2E	NOR	4.8	P	
KUR/005/02N	01/05/72	02.16.10	43.9N	147.2E	NOR	4.5	P	
AUS/005/04N	01/05/72	04.57.41	47.8N	16.2E	11	4.0	P	
TAD/005/12N	01/05/72	12.02.54	37.8N	73.1E	NOR	4.5	S	
KOM/005/14N	01/05/72	14.26.48	56.6N	169.4E	NOR	4.0	S	ND
KAM/005/16N	01/05/72	16.09.50	57.3N	160.5E	05	3.9	S	
KIR/006/06N	01/06/72	06.30.36	40.7N	72.4E	NOR	4.7	P	
TAI/006/06N	01/06/72	06.33.34	23.3N	123.4E	NOR	4.7	P	MBN
IRA/006/09N	01/06/72	09.41.33	30.3N	50.5E	NOR	5.2	P	
SWR/007/20N	01/07/72	20.37.32	44.1N	45.1E	NOR	4.2	S	
KOM/009/03N	01/09/72	03.23.06	54.4N	164.4E	NOR	3.6	S	ND
KAM/009/14N	01/09/72	14.00.59	55.7N	163.6E	NOR	4.3	S	
KUR/009/14N	01/09/72	14.47.46	45.1N	148.4E	NOR	3.8	S	ND
PHI/010/05N	01/10/72	05.23.52	20.9N	120.4E	NOR	5.0	S	
KOM/011/08N	01/11/72	08.54.34	54.7N	168.2E	28	3.9	S	
GRE/012/13N	01/12/72	13.51.20	35.0N	23.5E	NOR	4.9	P	MBN
KAM/012/20N	01/12/72	20.20.15	55.6N	163.9E	NOR	4.8	S	
SIB/013/17N	01/13/72	17.24.07	61.9N	147.1E	NOR	5.3	S	
SIB/014/03N	01/14/72	03.20.20	67.5N	171.5E	NOR	3.0	P	MBN
IRA/014/22N	01/14/72	22.10.04	32.8N	44.9E	NOR	5.1	P	MBN
KUR/015/00N	01/15/72	00.58.33	49.6N	155.0E	NOR	3.9	S	ND
FRS/015/18N	01/15/72	18.07.59	57.4N	120.7E	13	4.7	P	
SI1/015/20N	01/15/72	20.21.59	40.3N	79.0E	NOR	5.4	S	
SI2/015/20N	01/15/72	20.45.22	39.3N	79.9E	NOR	4.6	P	
KAM/016/04N	01/16/72	04.38.16	55.6N	162.5E	NOR	3.8	S	
KAM/016/11N	01/16/72	11.00.49	55.6N	163.2E	25	3.9	S	
IRA/018/21N	01/18/72	21.12.02	37.5N	48.7E	NOR	4.9	P	MBN
ITA/018/23N	01/18/72	23.16.12	44.2N	8.2E	25	4.1	P	
DOD/020/02N	01/20/72	02.15.07	36.6N	27.1E	NOR	4.8	S	
KUR/022/01N	01/22/72	01.41.24	50.0N	152.0E	NOR	4.2	P	MBN
TUR/022/17N	01/22/72	17.17.31	37.6N	29.9E	13	4.4	P	
KAM/025/10N	01/25/72	10.02.40	53.9N	160.9E	NOR	4.6	P	
ITA/025/20N	01/25/72	20.24.39	43.8N	13.4E	35	4.5	P	
GRE/026/12N	01/26/72	12.54.39	34.5N	25.5E	NOR	4.0	S	
KAM/027/20N	01/27/72	20.37.28	55.7N	162.3E	40	3.8	S	
ECS/028/04N	01/28/72	04.22.28	27.5N	126.5E	NOR	4.4	S	
PAK/028/10N	01/28/72	10.26.54	26.6N	66.3E	NOR	4.0	N	
KIR/028/20N	01/28/72	20.29.19	41.0N	78.0E	NOR	4.4	P	MBN
FRS/028/21N	01/28/72	21.50.00	45.0N	136.0E	NOR	4.0	N	

TABLE I-1

EVENT PARAMETERS
(PAGE 4 OF 6)

EVENT DESIGNATION	DATE	ORIGIN TIME	LAT	LON	DEPTH	MB	SOURCE BLTN	COMMENT
KUR/028/23N	01/28/72	23.42.51	49.3N	157.3E	NOR	3.8	S	
IRA/029/09N	01/29/72	09.50.58	29.0N	62.0E	NOR	3.9	N	
KAM/032/10N	02/01/72	10.16.09	55.8N	162.8E	NOR	4.1	S	
KAM/033/04N	02/02/72	04.26.59	55.7N	162.0E	NOR	3.7	S	
KUR/033/09N	02/02/72	09.58.51	46.8N	146.4E	NOR	3.6	S	
KUR/033/17N	02/02/72	17.56.39	50.7N	160.1E	NOR	3.6	S	
YUN/034/07N	02/03/72	07.22.49	23.4N	102.4E	NOR	4.5	P	
ITA/035/02N	02/04/72	02.42.19	43.8N	13.3E	25	4.9	P	
BAI/035/03N	02/04/72	03.34.56	51.4N	118.0E	NOR	4.2	S	
ITA/035/04N	02/04/72	04.40.55	43.9N	13.2E	NOR	4.8	P	ND
ITA/035/09N	02/04/72	09.18.32	43.9N	13.2E	23	4.4	P	
ITA/035/17N	02/04/72	17.19.52	43.8N	13.2E	23	4.4	P	
ITA/035/19N	02/04/72	19.02.56	43.8N	13.3E	NOR	4.8	P	
ITA/036/01N	02/05/72	01.26.23	43.8N	13.3E	NOR	4.8	P	
ITA/036/03N	02/05/72	03.48.45	43.2N	13.7E	NOR	4.4	P	
ITA/036/05N	02/05/72	05.05.51	43.7N	13.5E	NOR	4.6	P	
ITA/036/07N	02/05/72	07.08.13	43.9N	13.3E	NOR	4.7	P	
ADR/037/01N	02/06/72	01.34.22	44.0N	13.2E	NOR	4.9	P	
KAZ/037/08N	02/06/72	08.03.43	46.0N	80.0E	NOR	4.3	N	
ITA/037/21N	02/06/72	21.44.29	43.8N	13.2E	NOR	4.4	P	
ITA/039/12N	02/08/72	12.19.15	43.8N	13.3E	NOR	4.6	P	
IRA/041/09N	02/10/72	09.04.09	29.6N	50.9E	NOR	3.9	P	
IRA/041/16N	02/10/72	16.40.16	29.5N	50.9E	49	4.1	P	
SIN/042/05N	02/11/72	05.55.46	39.9N	77.4E	23	4.9	P	
TIP/042/12N	02/11/72	12.20.43	29.0N	87.0E	NOR	4.3	N	
KAM/042/21N	02/11/72	21.36.17	56.1N	162.9E	44	4.6	P	
KUR/044/05N	02/13/72	05.24.57	43.5N	147.0E	NOR	3.8	S	
GRE/044/13N	02/13/72	13.07.11	37.1N	24.0E	27	4.5	P	
KOM/044/22N	02/13/72	22.36.54	55.2N	165.5E	NOR	3.9	S	
KUR/046/16N	02/15/72	16.45.22	45.0N	153.0E	NOR	4.1	S	
GRE/047/00N	02/16/72	00.42.24	36.9N	24.2E	NOR	4.5	P	
SIN/047/23N	02/16/72	23.19.20	41.7N	80.7E	29	4.8	P	
KUR/049/18N	02/18/72	18.02.34	43.6N	147.8E	36	4.7	S	
SIN/051/10N	02/20/72	10.22.46	38.5N	90.5E	16	3.9	I	MBN
OKH/051/10N	02/20/72	10.08.46	47.9N	145.9E	97	4.2	I	
KAM/051/20N	02/20/72	20.06.11	50.8N	141.5E	NOR	4.1	I	
KAM/052/22N	02/21/72	22.00.59	54.4N	161.3E	NOR	4.8	I	
YUG/052/23N	02/21/72	23.02.55	41.0N	22.3E	NOR	4.0	I	
MON/053/01N	02/22/72	01.53.36	49.0N	115.0E	NOR	4.1	I	
HIN/053/08N	02/22/72	08.14.26	36.6N	68.6E	NOR	4.0	I	MBN
KUR/054/03N	02/23/72	03.42.41	43.9N	148.3E	39	4.9	I	
KAM/054/19N	02/23/72	19.37.29	55.0N	163.0E	NOR	3.7	I	ND
KUR/055/10N	02/24/72	10.19.37	48.8N	155.7E	NOR	5.0	I	
KUR/055/18N	02/24/72	18.17.34	49.0N	158.0E	NOR	3.5	I	ND
KUR/056/19N	02/25/72	19.59.29	46.0N	147.0E	NOR	3.8	I	

TABLE I-1

EVENT PARAMETERS
(PAGE 5 OF 6)

EVENT DESIGNATION	DATE	ORIGIN TIME	LAT	LON	DEPTH	MB	SOURCE BLTN	COMMENT
WRS/056/22N	02/25/72	22.34.49	50.0N	38.0E	NOR	3.7	I	
KUR/056/22N	02/25/72	22.43.07	49.2N	156.0E	NOR	4.0	I	
KUR/057/05N	02/26/72	05.58.22	46.9N	153.6E	NOR	4.0	I	
KAM/057/09N	02/26/72	09.04.32	55.0N	162.0E	NOR	3.7	I	ND
FRS/057/15N	02/26/72	15.06.42	53.3N	138.7E	NOR	3.	I	MBN
YUN/057/18N	02/26/72	18.46.13	27.1N	100.9E	NOR	4.7	I	
LO1/058/08N	02/27/72	08.42.59	88.0N	74.0W	NOR	3.3	I	ND
LO1/058/10N	02/27/72	10.03.03	87.0N	53.5W	NOR	4.0	I	
LOM/058/11N	02/27/72	11.03.19	90.0N	95.0W	NOR	3.5	I	
LOM/058/17N	02/27/72	17.50.25	86.2N	77.2W	NOR	4.4	I	
BAI/058/22N	02/27/72	22.15.03	55.0N	93.2E	NOR	4.5	I	
KUR/059/01N	02/28/72	01.04.22	46.0N	148.0E	NOR	4.2	I	ND
PAK/059/05N	02/28/72	05.18.56	36.7N	71.4E	NOR	4.2	I	MBN
KAM/059/11N	02/28/72	11.35.31	56.0N	163.0E	NOR	4.1	I	ND
AFG/059/18N	02/28/72	18.12.35	36.0N	68.7E	NOR	4.4	I	MBN
KAM/059/20N	02/28/72	20.04.00	56.1N	164.2E	NOR	3.6	I	ND
IRO/060/08N	02/29/72	08.02.51	32.8N	46.6E	NOR	4.0	I	MBN
IRA/062/14N	03/02/72	14.10.13	31.6N	42.1E	NOR	4.0	I	MBN
ALM/062/19N	03/02/72	19.57.42	43.0N	76.0E	NOR	3.5	I	MBN
KAM/063/00N	03/03/72	00.35.23	53.0N	159.2E	NOR	4.1	I	
NSI/063/05N	03/03/72	05.26.53	77.8N	116.7E	NOR	3.8	I	
KOM/063/08N	03/03/72	08.13.55	55.8N	162.9E	NOR	4.1	I	
YUG/063/21N	03/03/72	21.26.51	44.7N	18.4E	32	4.9	I	
KUR/063/23N	03/03/72	23.10.41	50.2N	155.7E	NOR	4.5	I	
SIN/064/04N	03/04/72	04.00.09	40.2N	79.0E	NOR	4.5	I	
KAM/066/06N	03/06/72	06.05.09	53.5N	160.9E	NOR	3.9	I	ND
KUR/066/09N	03/06/72	09.59.09	45.0N	150.0E	NOR	3.7	I	
OKH/066/19N	03/06/72	19.13.25	56.0N	140.0E	NOR	4.2	I	
CHI/066/23N	03/06/72	23.17.53	40.0N	103.0E	NOR	4.5	I	ND
YUG/067/05N	03/07/72	05.21.21	43.0N	21.0E	NOR	2.7	I	MBN
OKH/068/02N	03/08/72	02.38.11	51.2N	151.9E	NOR	4.2	I	
IRA/068/21N	03/08/72	21.49.11	27.6N	56.7E	45	4.9	I	
BUL/068/22N	03/08/72	22.04.02	40.8N	22.8E	NOR	3.5	I	MBN
KAZ/070/04N	03/10/72	04.56.57	49.9N	78.2E	0	5.5	I	F
KUR/070/06N	03/10/72	06.50.18	45.1N	149.5E	NOR	3.7	I	
ARC/071/06N	03/11/72	06.47.07	81.0N	157.0E	NOR	4.3	I	ND
KAS/071/13N	03/11/72	13.31.39	35.0N	76.0E	NOR	4.1	I	MBN
KUR/073/02N	03/13/72	02.11.05	49.0N	158.0E	NOR	3.8	I	
AFG/073/05N	03/13/72	05.49.13	37.0N	70.0E	NOR	4.0	I	MBN
TIB/073/18N	03/13/72	18.27.07	34.0N	83.0E	NOR	4.1	I	MBN
TIB/075/06N	03/15/72	06.00.33	30.4N	84.5E	NOR	5.3	I	MBN
KUR/077/07N	03/17/72	07.49.02	49.0N	156.2E	NOR	5.2	I	
TAD/077/09N	03/17/72	09.17.11	40.1N	69.7E	26	5.2	I	
IRA/077/17N	03/17/72	17.11.28	28.0N	54.0E	NOR	3.9	I	MBN
KAS/077/23N	03/17/72	23.33.37	32.0N	75.0E	NOR	3.5	I	MBN

TABLE I-1

EVENT PARAMETERS

(PAGE 6 OF 6)

EVENT DESIGNATION	DATE	ORIGIN TIME	LAT	LON	DEPTH	MB	SOURCE BLTN	COMMENT
KAZ/078/07N	03/18/72	07.11.55	47.0N	81.0E	NOR	3.6	I	MBN
KAM/078/13N	03/18/72	13.52.14	57.0N	163.0E	NOR	3.6	I	
KAM/078/18N	03/18/72	18.29.37	50.6N	156.7E	NOR	4.7	I	
OKH/078/19N	03/18/72	19.17.25	54.0N	150.0E	NOR	3.7	I	
KIR/078/19N	03/18/72	19.54.18	41.0N	72.0E	NOR	3.2	I	MBN
CAU/079/03N	03/19/72	03.34.31	42.7N	38.1E	NOR	3.9	I	
KUR/080/14N	03/20/72	14.08.12	47.0N	154.0E	NOR	4.0	I	MBN
SIN/080/21N	03/20/72	21.47.55	40.0N	80.0E	NOR	3.4	I	MBN
CAU/160/17N	06/08/72	17.25.52	43.2N	47.2E	NOR	4.5	P	
PAK/162/11N	06/10/72	11.29.11	28.2N	66.5E	NOR	4.5	P	
SIN/187/04N	07/05/72	04.09.49	43.6N	87.9E	NOR	4.3	P	
KAM/199/08N	07/17/72	08.28.52	55.0N	159.6E	NOR	5.3	P	
GRE/200/13N	07/18/72	13.45.48	41.6N	23.8E	NOR	4.0	P	

ABBREVIATIONS

S :   SAAC/LASA Bulletin

P :   PDE Bulletin

N :   NTNF/NORSAR Bulletin

I :   Bulletin from the International Seismic Month (ISM)

ND :   No Detection at NORSAR (TI Analyst decision).

MBN :   NORSAR Magnitude

E :   Presumed explosion

TABLE I-2

EVENTS AND SENSORS IN WHICH PHASE REVERSALS HAVE BEEN OBSERVED (1971 DATA)

EVENT NAME	06B	05C			08C		10C	14C
	03	01	02	04	00	02	02	01
VAN/072/23N				X				
KIR/082/20N	X			X				
IRA/102/19N	X			X				
KAZ/181/04N	X			X				
HON/228/15N	X	X	X		X	X	X	X
SZE/228/18N	X	X	X		X	X	X	X
KUR/235/21N	X	X	X			X	X	X
SAK/249/13N	X							X
WES/262/11N	X					X		
WRS/295/05N	X					X		
CAN/310/22N	X					X		

SUBARRAY/SEISMOMETER

Data quality was excellent; about one-half of the time all 132 sensors were operational. In most other cases one subarray (six sensors) was dead or contained calibration signals, the worst data loss was 24 sensors. For a total of six events we found spikes in the data, but these events could still be processed. As was stated in Special Report No. 6, it appears that the seismometers are reasonably well equalized across the array.

From about March 20, 1971, to near the end of the year, at least two sensors were observed to have reversed polarities. Sensor 06B03 was in the reversed state throughout this period, and sensor 05C04 was corrected in mid-August only to be followed by a phase reversal of 08C02. For about ten days around this transition, as many as seven sensors were affected by this problem. No phase reversal has been observed in 1972 data. Table I-2 shows the pattern of the reversals and the extent of the data base from which the above conclusions were determined. The effect of the reversals on subarray and array-beam quality will be discussed in Section III.

SECTION II
SIGNAL ANALYSIS

A.   INTRODUCTION

Several large signals recorded by the entire array were analyzed in order to study signal characteristics. Analyses of the following phenomena were performed:

- Variation as a function of epicentral location of signals in both time and frequency domains.

- Variation of SNR (signal-to-noise ratio) from subarray to subarray for a given event, and its relation to subsurface velocity structure.

- Deviation of propagation across the array from a plane-wave model and the variation of this deviation with epicentral location and signal spectral content.

- Discrepancies between body-wave magnitudes (m_b) based on measurements of data processed in TI's Alexandria office and those reported in the NORSAR, LASA, and PDE bulletins and their variation with epicentral region and m_b.

Results of these analyses are discussed in the remainder of this section.

B.   REGIONAL SIGNAL CHARACTERISTICS

A study was undertaken to examine signal waveforms recorded at NORSAR on a regional basis. For this purpose it was found convenient to

apply the short-period discriminants defined in Chapter V to a set of presumed earthquakes from Eurasia. A total of 97 events were selected, all of body wave magnitudes between 4.5 and 5.0. The reason for selecting this narrow range of magnitudes was to minimize side effects on signal complexity and frequency contents caused by magnitude variations. The geographical distribution of these 97 events is shown in Figure II-1.

For each discriminant, the events in our data base were ranked according to their discriminant values. The 25 highest ranking and the 25 lowest ranking events were then plotted in geographical space. Figure II-2 shows the results for the autocorrelation mean square discriminant, which was selected as a representative for the discriminants based on event complexity. Similarly, the dominant period discriminant was selected among the criteria based on signal frequency contents, and the resulting plot is shown in Figure II-3. It should be noted that all complexity discriminants showed similar results, as was also the case with the frequency discriminants.

The following observations on regional signal characteristics may be made from Figures II-1, II-2 and II-3.

- Mediterranean Region

  Not unexpectedly, signal traces from this close-in region (around 20 degrees distance from NORSAR) tend to have high complexity values. It is, however, surprising to find that most of our events from the Mediterranean have a low dominant frequency. In fact, three events from Turkey and one from Italy had a dominant period greater than 1.5 seconds on the adjusted-delay array beam, and all 18 events from Turkey/ Italy exceeded 0.9 seconds.

+ Shallow Earthquakes or Earthquakes of Unknown Depth
△ Earthquakes of Depth at Least 100km
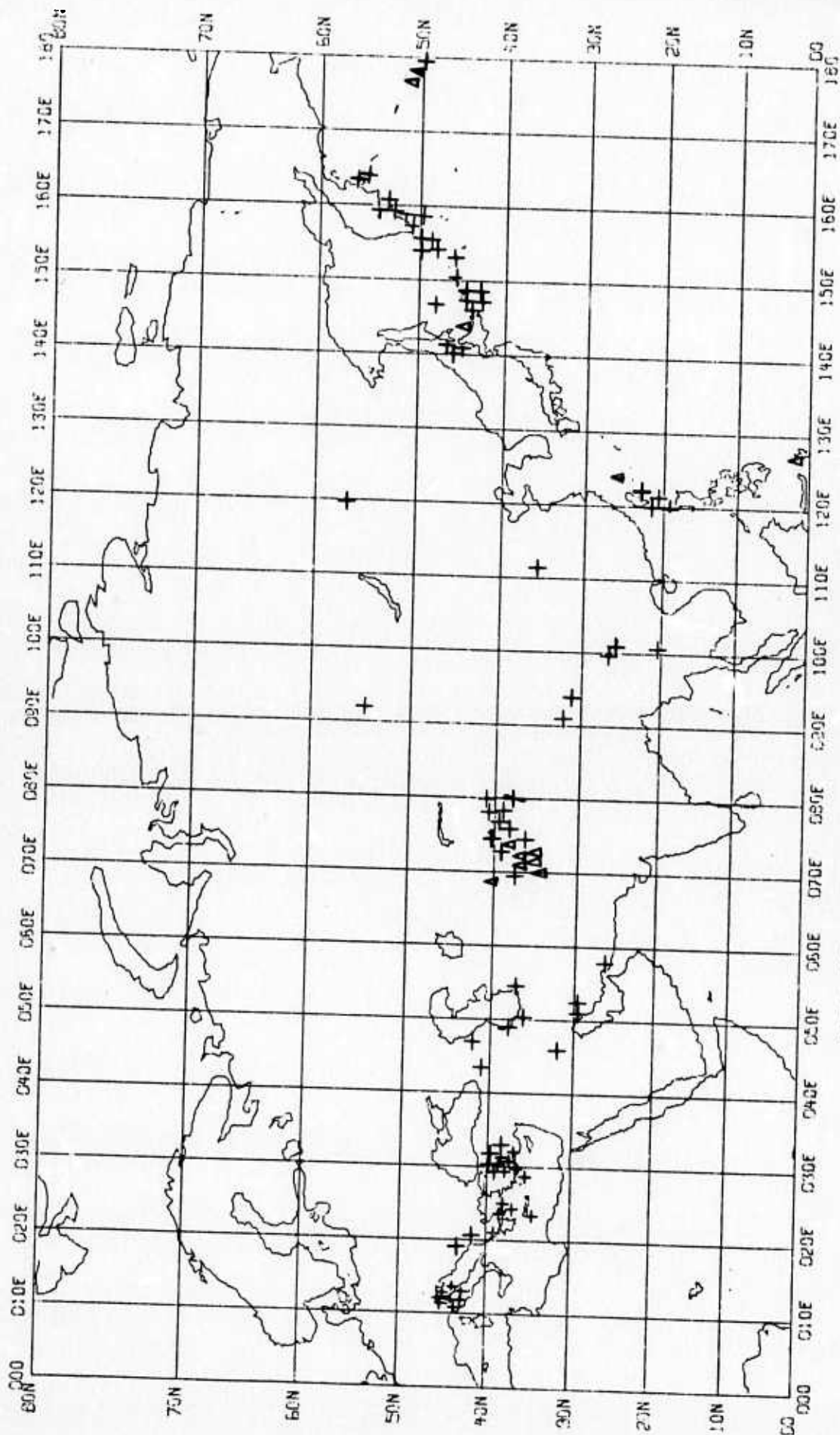
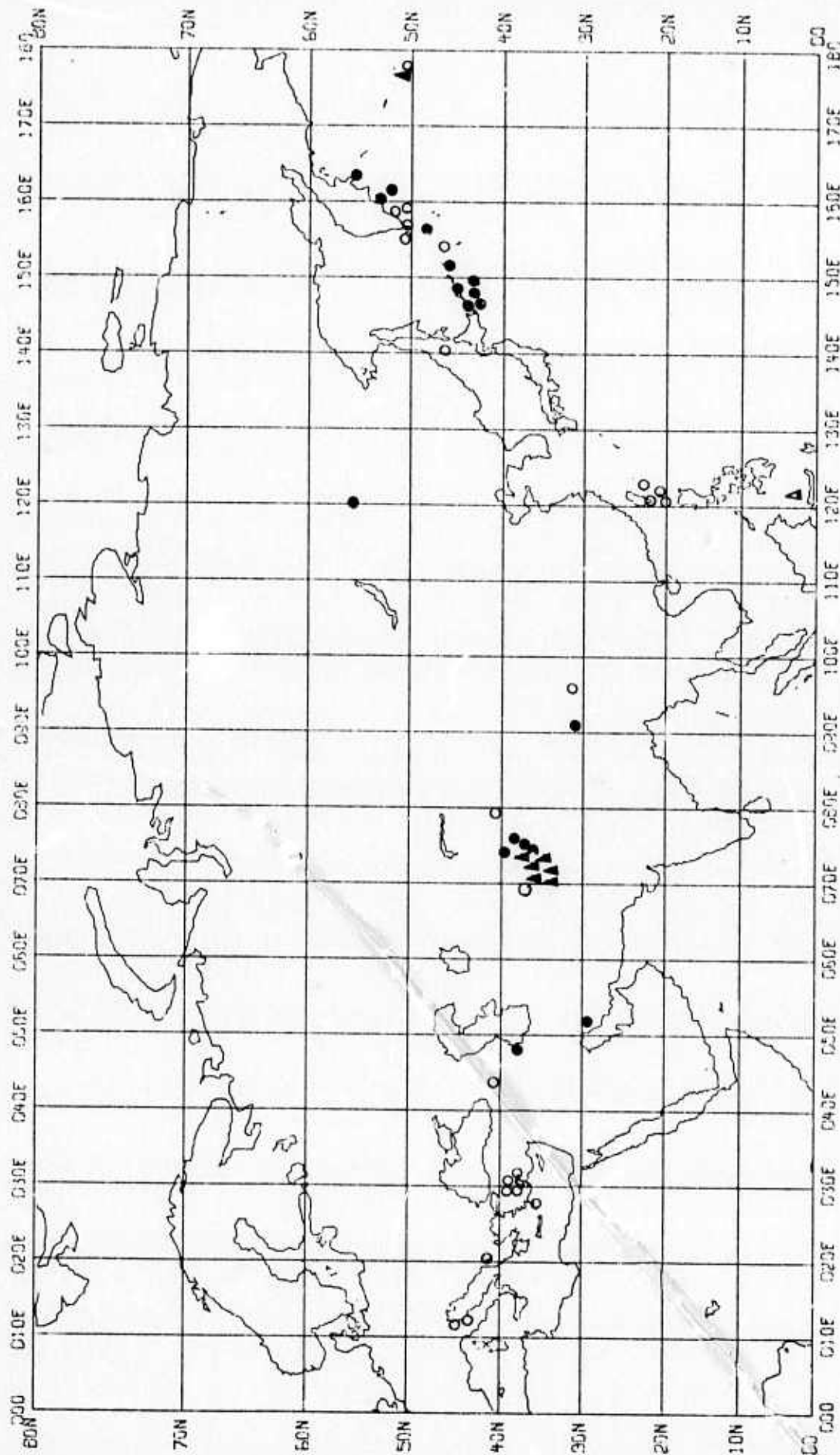MILLER MODIFIED MERCATOR PROJECTION
MAP SCALE: 0.500 IN./ 10 DEG. LONGITUDE

FIGURE II-1

GEOGRAPHICAL DISTRIBUTION OF 97 EARTHQUAKES SELECTED
FOR REGIONAL SIGNAL CHARACTERISTICS STUDY

MILLER MODIFIED MERCATOR PROJECTION
MAP SCALE: 0.500 IN. / 10 DEG. LONGITUDE

FIGURE II-2

REGIONAL SIGNAL COMPLEXITY AS MEASURED BY THE
AUTOCORRELATION MEAN SQUARE DISCRIMINANT

● : Low Complexity (▲ : Deep Earthquakes)
○ : High Complexity (△ : Deep Earthquakes)

II-4

MILLER MODIFIED MERCATOR PROJECTION
MAP SCALE: 0.500 IN./ 10 DEG. LONGITUDE

● High Dominant Frequency (▲ : Deep Earthquakes)
○ Low Dominant Frequency (△ : Deep Earthquakes)
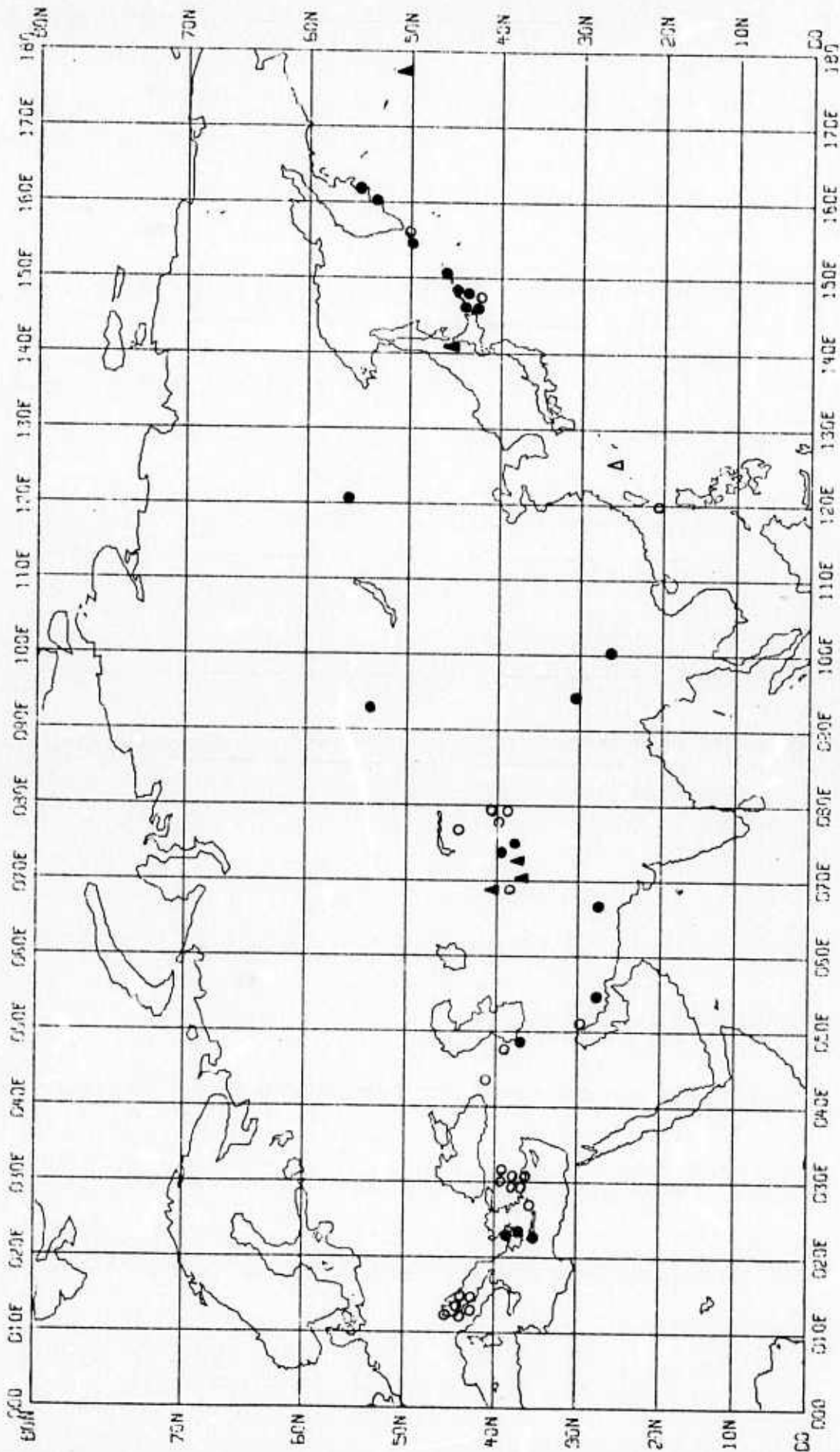
FIGURE II-3

REGIONAL SIGNAL SPECTRAL CHARACTERISTICS AS MEASURED
BY THE DOMINANT PERIOD DISCRIMINANT

II-5

Figure II-4 shows the "average" power spectrum for our Italy events (i.e the average dB value for the selected events for each frequency). The predominantly low frequency content is clearly seen, and individual inspection of the spectra shows furthermore that spectral peaks tend to repeat from one event to another. This is not so surprising in view of the proximity in location of the Italy events.

In contrast to what was observed for Turkey and Italy, events from Greece tend to show significant high frequency content. Four of the five Greece events included in our data base had a dominant period between 0.6 and 0.8 seconds on the adjusted-delay array beam.

- Iran / Middle East

From our limited data base it appears that events from this region generally have low to intermediate complexity. Dominant period for Iran events typically ranges from 0.6 to 0.9 seconds.

- Central Asia

Events from Central Asia have in general low complexity values. This is especially pronounced for the Afghanistan/Tadzhik/Sinkiang region, where 6 deep events were included in our data base.

With respect to dominant period, an interesting transition occurs at about 76 degrees East longitude. Signals from Afghanistan/Tadzhik west of this meridian are generally of high frequencies, with typically 0.5-0.8 seconds dominant period both for deep and shallow earthquakes. To the contrary,

II-6
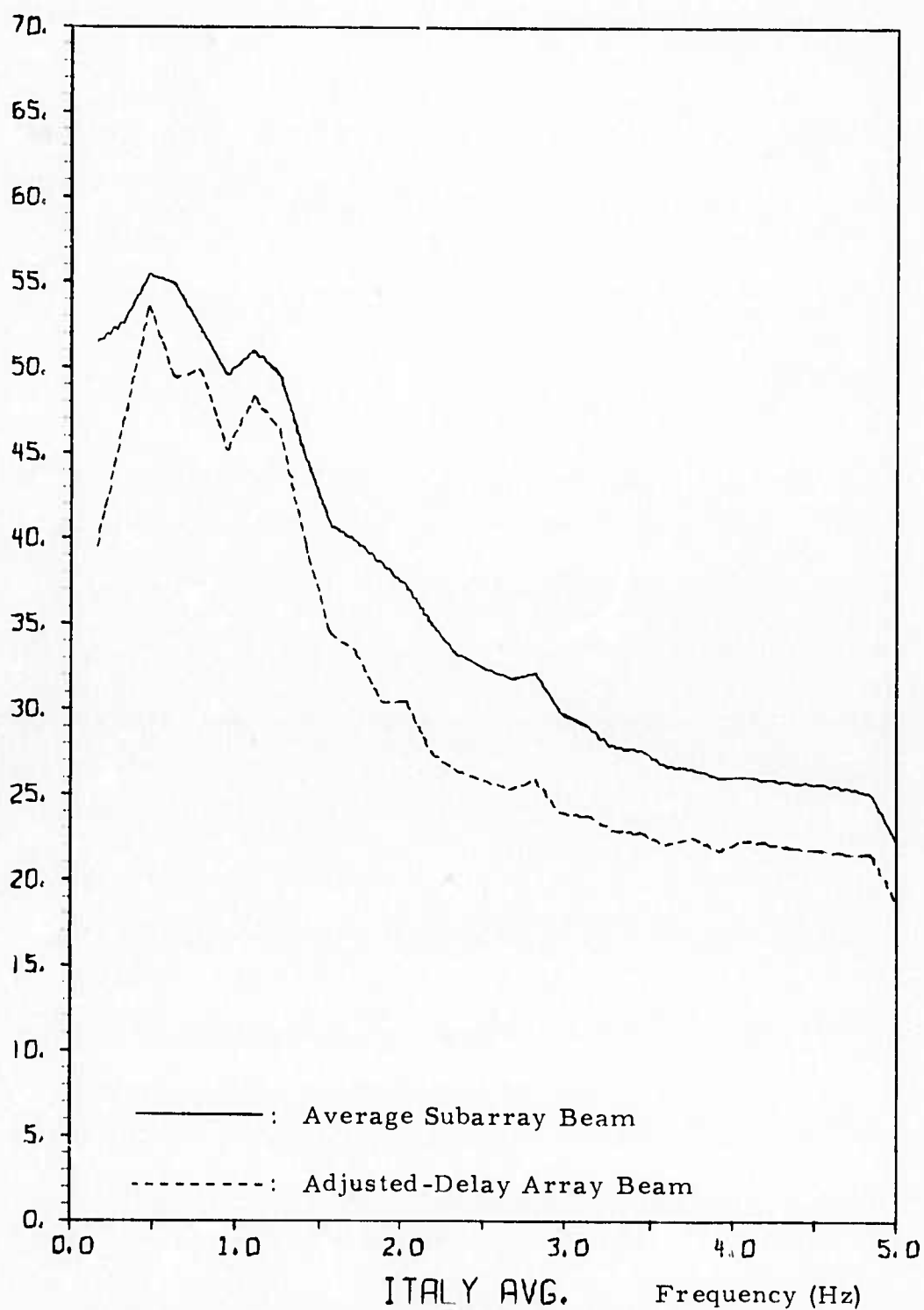
ITALY AVG.
AVBS
ADBS

FIGURE II-4

AVERAGE dB VALUES OF THE POWER SPECTRA FROM
12 ITALY EVENTS BETWEEN FEBRUARY 4
AND FEBRUARY 9, 1972

II-7

signals from the Kirgiz-Sinkiang border region further east
exhibit a dominant period of 1.0-1.3 seconds on the adjusted-
delay array beam.

Signals from earthquakes occurring elsewhere in Central Asia
quite often indicate a significant content of high frequency energy,
but our data base is still to scarce to permit more specific con-
clusions for this general area.

● Southeast Asia

Very few events from this region were included in the data base,
but is interesting to notice the high complexity of our Taiwan
events. Signals from this area tend to have a dominant low
frequency.

● East Asia and Western Pacific

Most events from this region produce low complexity signals at
NORSAR. Some high complexity signals are seen for events
from Kamchatka.

There is a considerable variation in spectral characteristics
for signals from the Kamchatka-Kurile arc. The two extremes
in our event population are KUR/001/16N and KAM/078/18N
with dominant periods of 0.4 and 1.3 seconds respectively
for the adjusted-delay array beams. Both of these events
are of unknown depth. In general events from this region
tend to have a dominant high frequency; this is most pronounced
for earthquakes from the Kurile Islands.

In conclusion, there seems to be significant variations in re-
gional signal characteristics observed at NORSAR. Some of our observations

contrast with the general expectations of decreasing signal complexity and increasing dominant period as the epicentral distance increases.

It is interesting to compare the regional characteristics found in the preceeding study to the corresponding characteristics of underground explosions, which are low complexity and low dominant period (high frequency). The most "explosionlike" earthquakes in this sense are seen to occur in the Tadzhik/Afghanistan region and the Kurile Islands.

C. SUBARRAY BEAM AMPLITUDE VARIATIONS

The striking variations in signal amplitudes from subarray to subarray were discussed briefly in Special Report No. 6. A study was undertaken to investigate this phenomenon in more detail. Several large events from various regions were selected, and signal and noise RMS levels were computed for each event on all subarray beams filtered with the standard filter. The events were grouped by region, and signal-to-noise ratios (SNR) (in dB) were averaged over all events within each region for each subarray. Since the noise level does not vary significantly between subarrays, these SNR values are essentially equivalent to the corresponding signal amplitudes.

The results are presented in Figures II-5 to II-8 for four selected regions: Kuriles, Kazakh, Yunan and Kirgiz. A map of the NORSAR array is shown on each figure together with contours indicating the pattern of signal amplitude variations for each region. The interval between contours is 2 dB, and the numbers represent SNR level in dB relative to the average subarray. Within each region, typical standard deviations for a subarray across the ensemble of events were 2 dB, thus the contour maps should give a reasonably reliable picture of the NORSAR amplitude distribution for the regions selected.
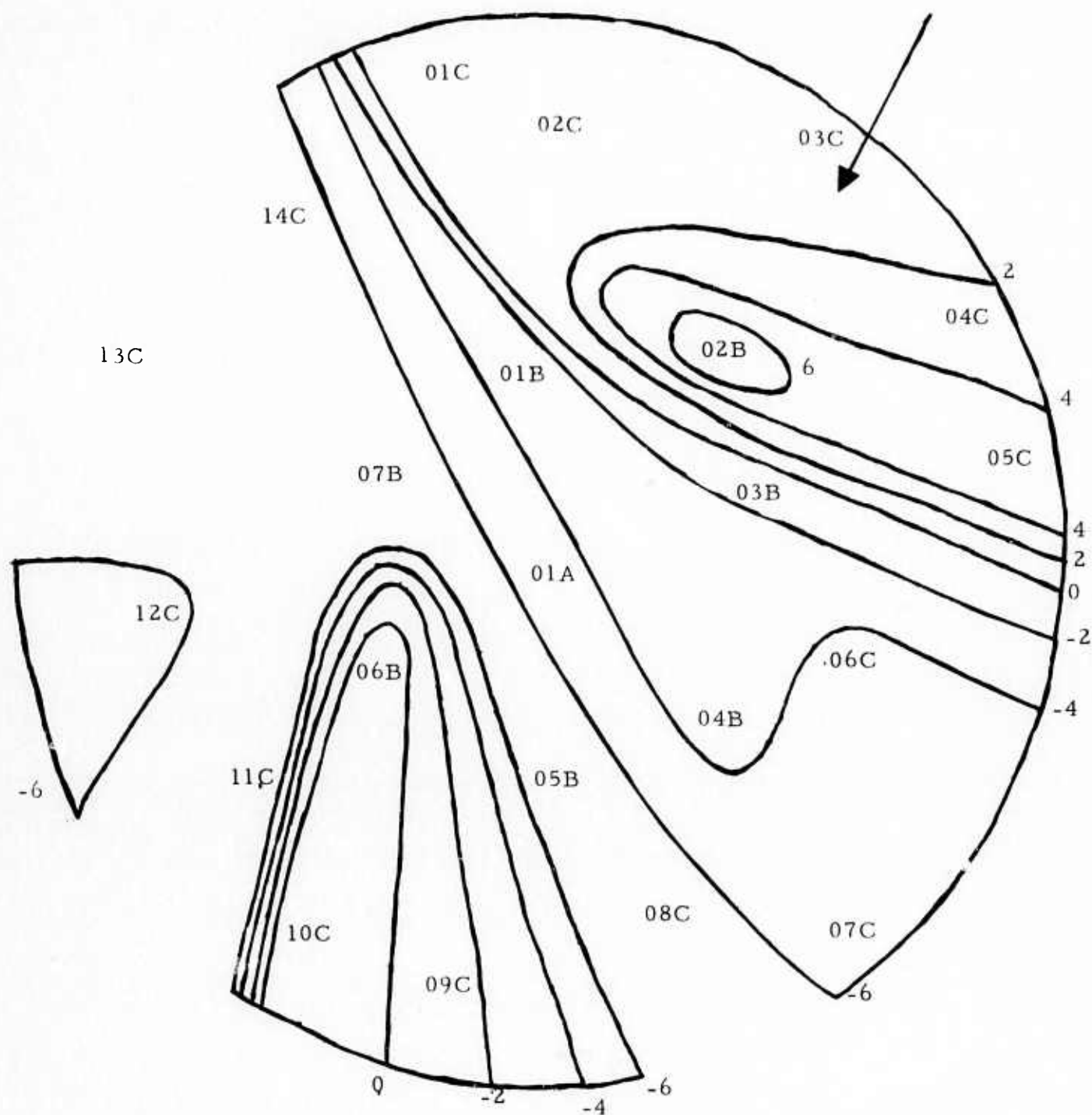
Region: Kuriles; Azimuth: 24 - 32 degrees; Distance: 65 - 70 degrees;
Events: KUR/005/02N, KUR/022/01N, KUR/054/03N, KUR/057/05N, KUR/077/07N

FIGURE II-5

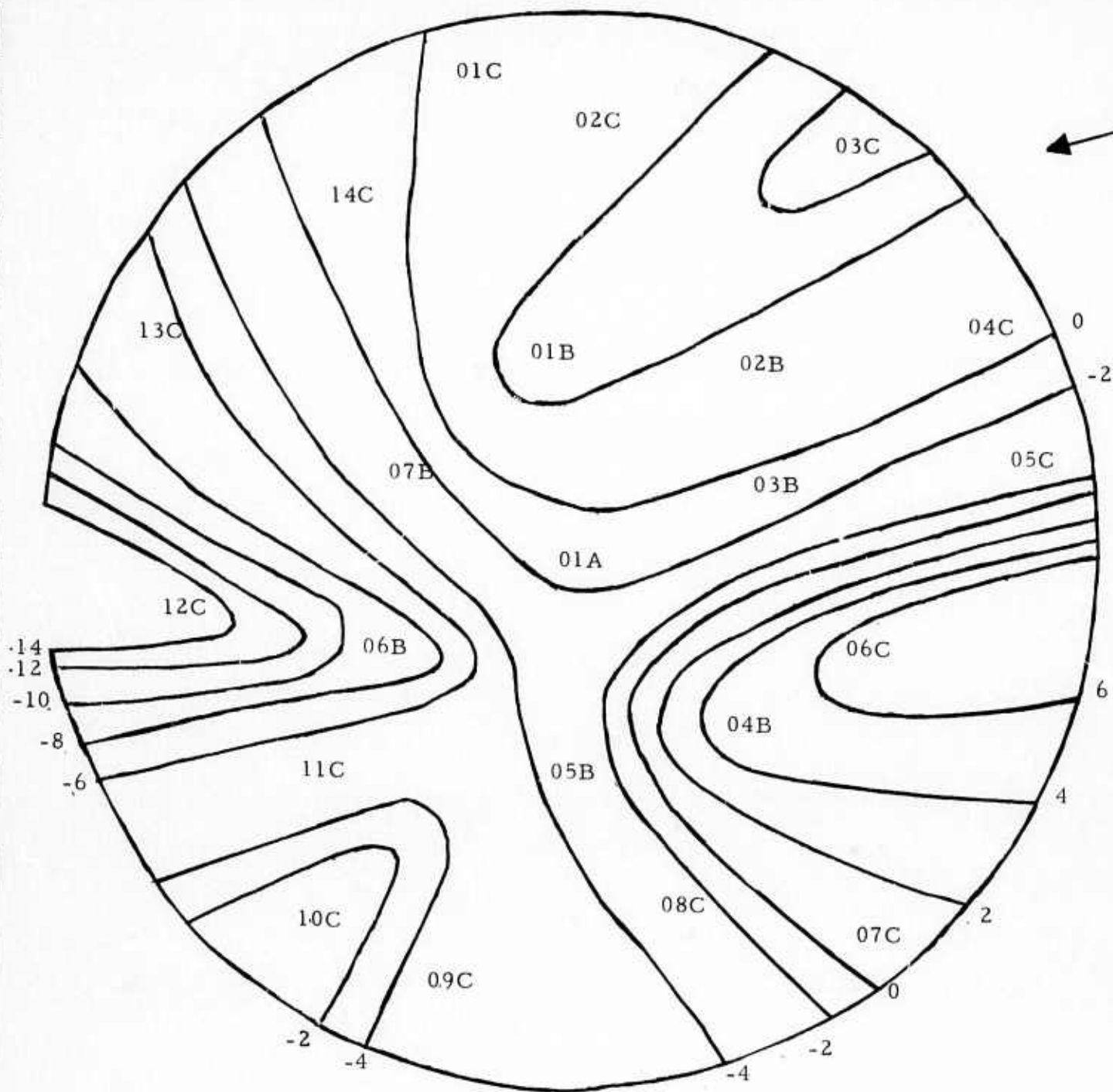CONTOUR PLOT SHOWING SUBARRAY SNR VARIATION
FOR EVENTS FROM KURILES REGION.
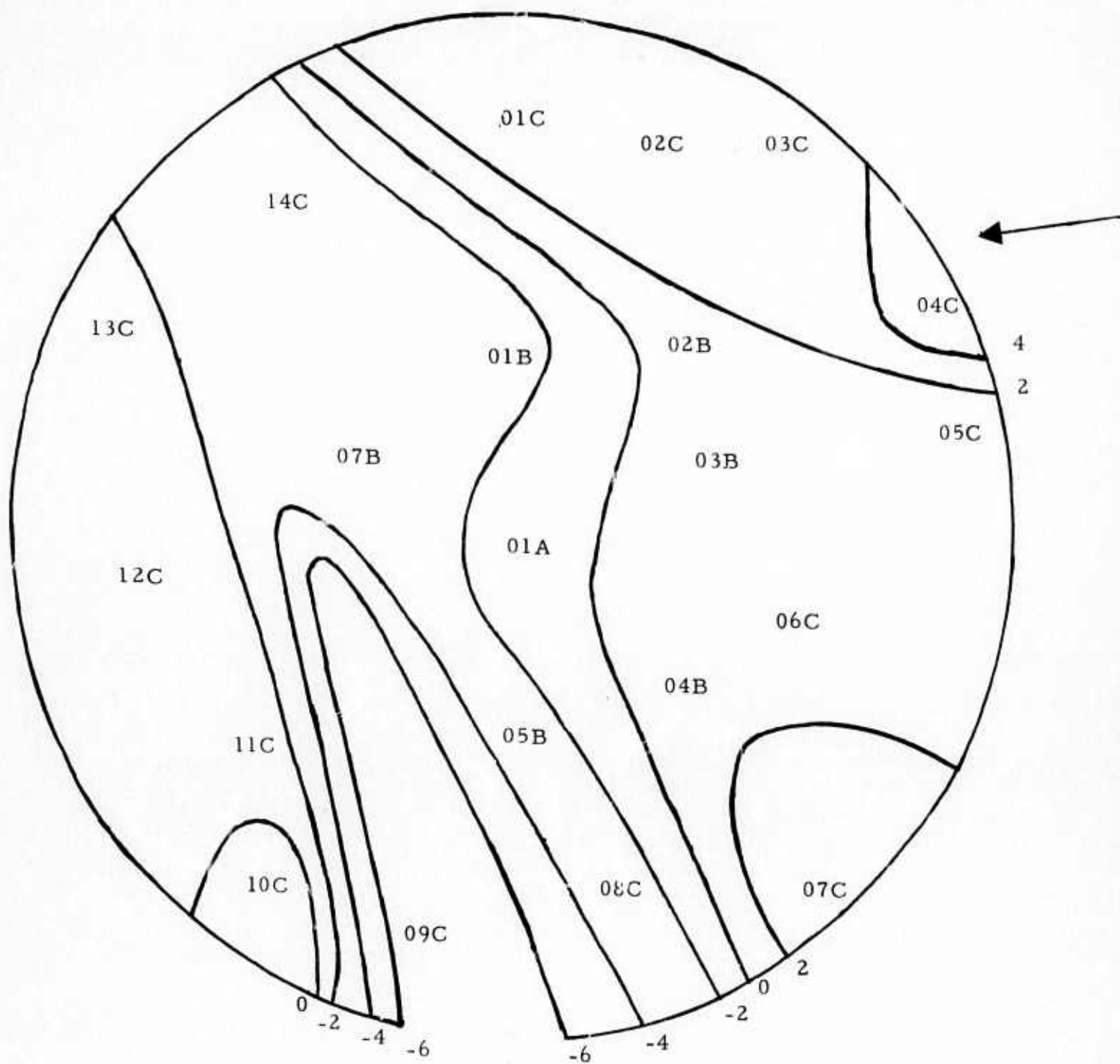
Region: Kirgiz; Azimuth: 83.0 - 83.2 degrees; Distance: 44.4 -44.6 degrees
Events: KIR/082/09N, KIR/082/20N, KIR/083/20N, KIR/166/23N, KIR/170/17N

FIGURE II-6

CONTOUR PLOT SHOWING SUBARRAY SNR VARIATIONS FOR
EVENTS FROM KIRGIZ REGION
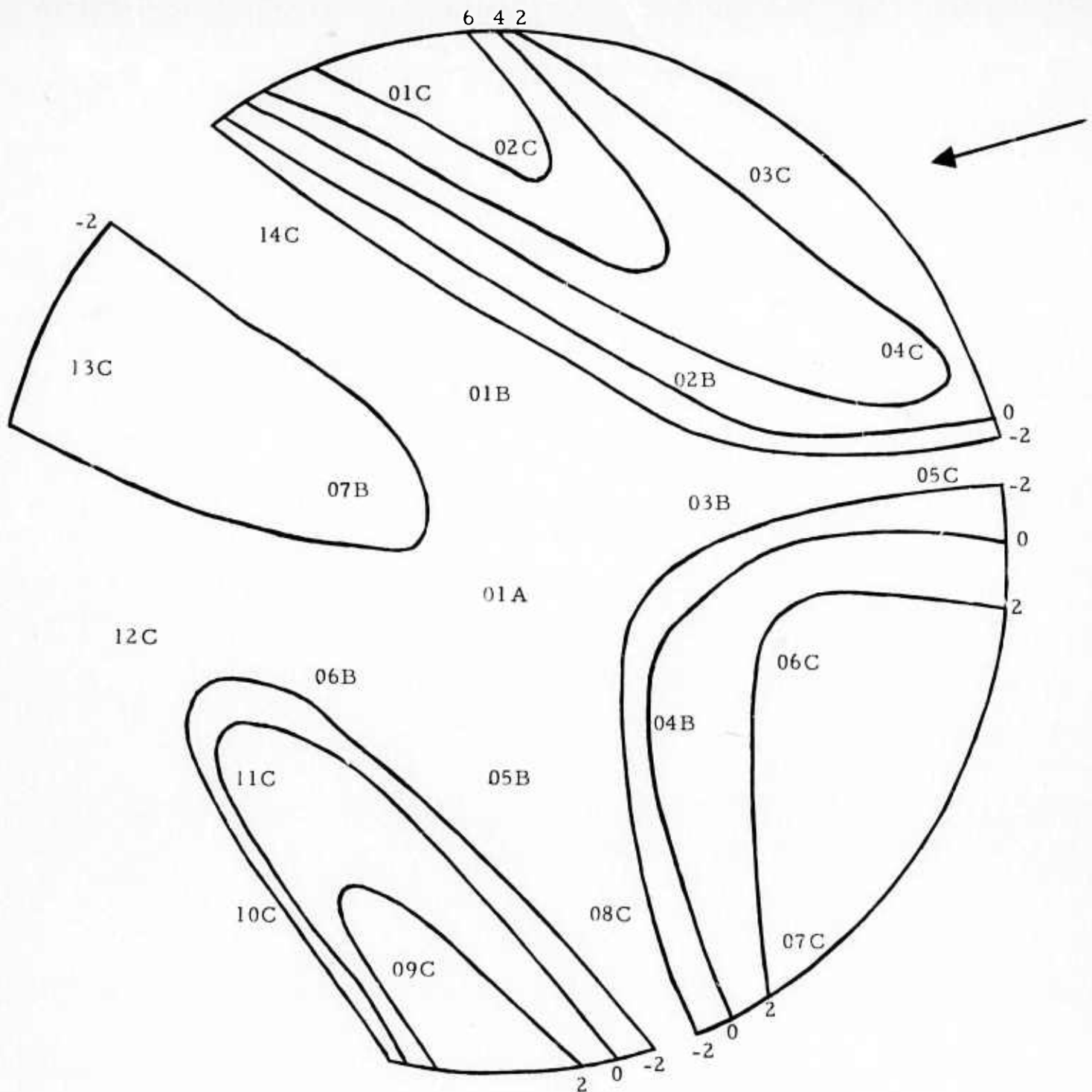
Region: Yunan; Azimuth: 72.6- 75.9 degrees; Distance: 66.4 - 67.4 degrees
Events: YUN/057/18N YUN/141/02N, SZE/228/04N, SZE/228/18N, SZE/246/18N

FIGURE II-7

CONTOUR PLOT SHOWING SUBARRAY SNR VARIATIONS FOR
EVENTS FROM YUNAN REGION

Region: Kazakh; Azimuth: 74.5 - 75.5 degrees; Distance: 37.7 - 38.2 degrees
Events: KAZ/081/04N, KAZ/115/03N, KAZ/145/04N, KAZ/157/04N, KAZ/181/0⁴N

FIGURE II-8

CONTOUR PLOT SHOWING SUBARRAY SNR VARIATIONS FOR
EVENTS FROM KAZAKH REGION

II-13

It appears from these data that the eastern part of the NORSAR array (subarrays 01C through 07C and 01B through 04B) generally show higher signal amplitudes than subarrays located further west. This seems to hold true, with few exceptions, for all of Eurasia; however, our limited data from the Western hemisphere indicates that this pattern is not globally valid.

The great variation in amplitude patterns even for regions fairly close together (like Kazakh and Kirgiz) is striking. Of particular interest is the Kazakh region, (Figure II-8) where subarray 12C exhibits 14 dB lower SNR than the average subarray. This spread is much greater than has been observed for other regions, including other underground nuclear test sites.

An attempt was made to relate the amplitude variations to the structure of the Mohorovicic discontinuity underneath the NORSAR array. Similar studies to explain amplitude anomalies across the LASA array have been performed by Aki (1973) and others.

Depth contours for the Moho underneath NORSAR are presented in Figure II-9, as measured by Kanestrom and Haugland (1971). The arrow on this figure represents the wavefront arrival for Eastern Kazakh events (azimuth 75 degrees), and is seen to follow closely the trend of a ridge in the Moho below subarray 05C. The arrow is furthermore perpendicular to the depth contours corresponding to the sudden depth increase of the Moho in western direction.

Figures II-10 and II-11 are conceptual models of the structure underneath the NORSAR array as seen by applying two vertical sections as indicated in Figure II-9. The directions of wavefront approach indicated in Figures II-10 and II-11 correspond to events from Eastern Kazakh. The refraction effects shown in these figures seem to explain well, in principle,
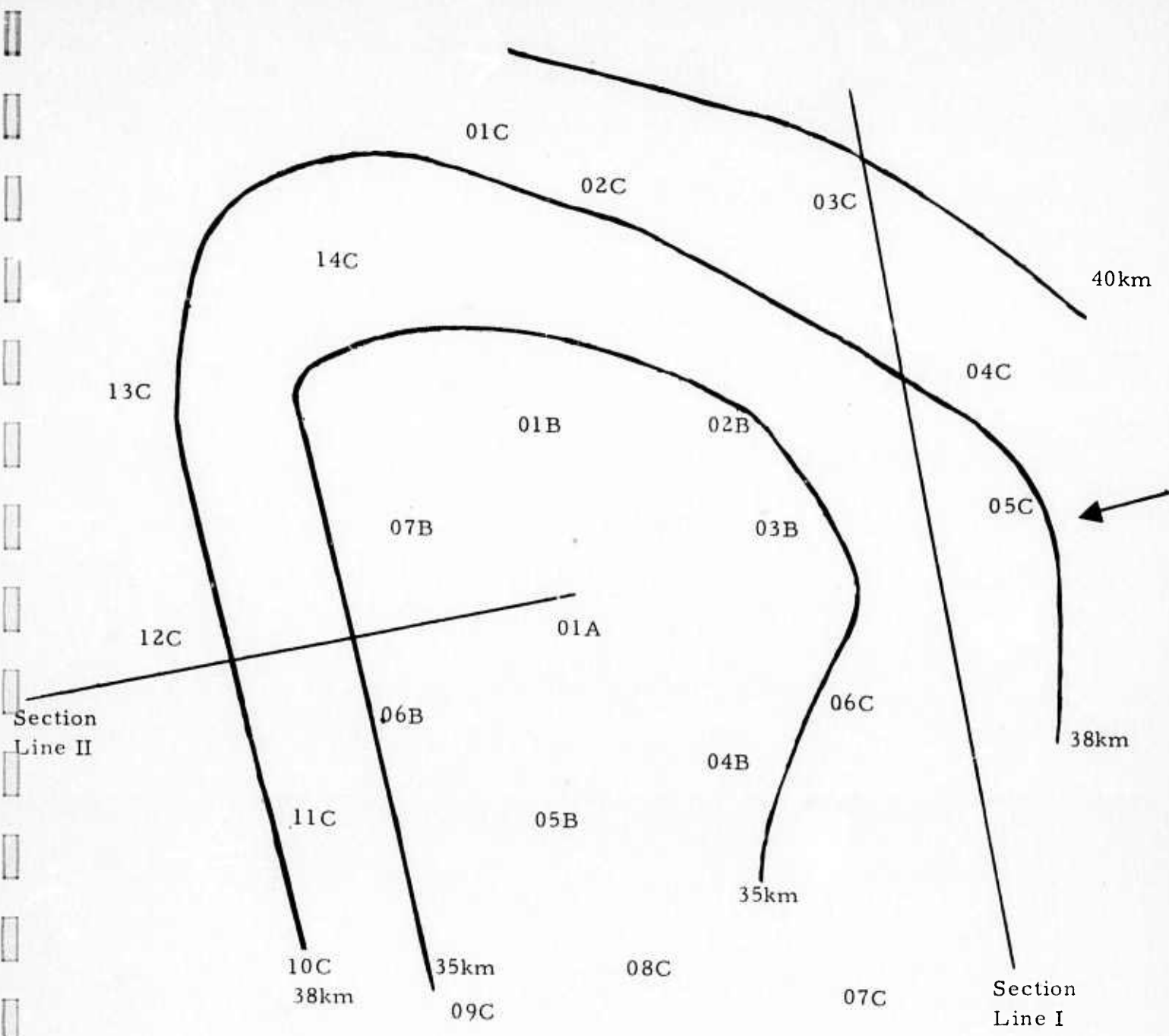
FIGURE II-9

DEPTH CONTOURS OF THE MOHOROVICIC DISCONTINUITY
UNDERNEATH THE NORSAR ARRAY.
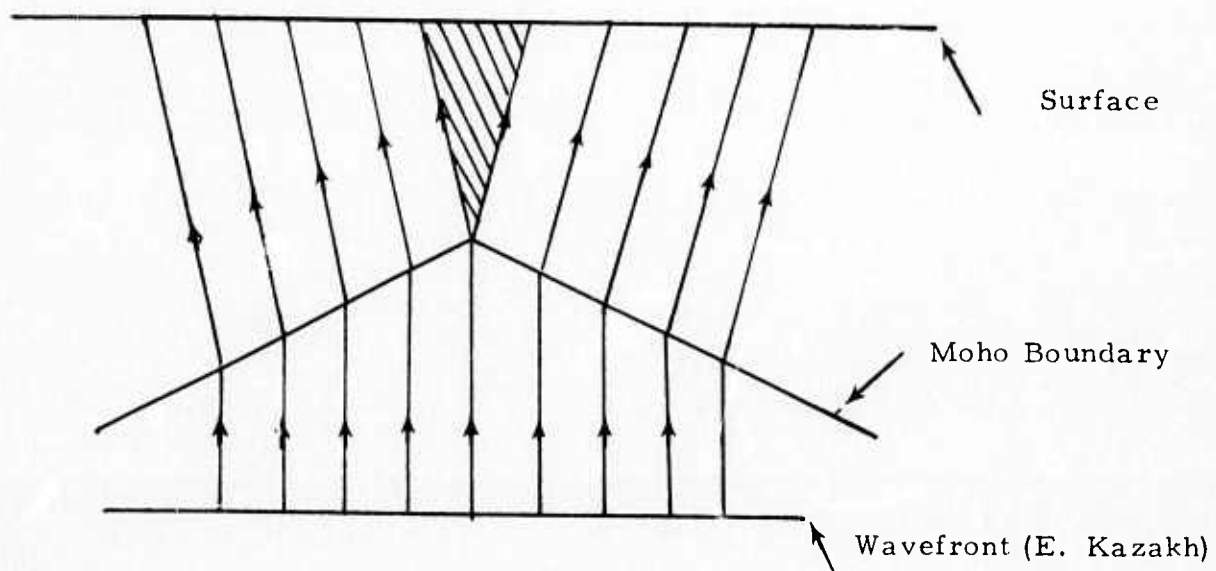
Surface

Moho Boundary

Wavefront (E. Kazakh)

FIGURE II-10

CONCEPTUAL MODEL (SECTION LINE I IN FIGURE II-9)
SHOWING HOW REFRACTION OF P-WAVES MAY CAUSE
LOW SIGNAL AMPLITUDES FOR SEISMOMETERS
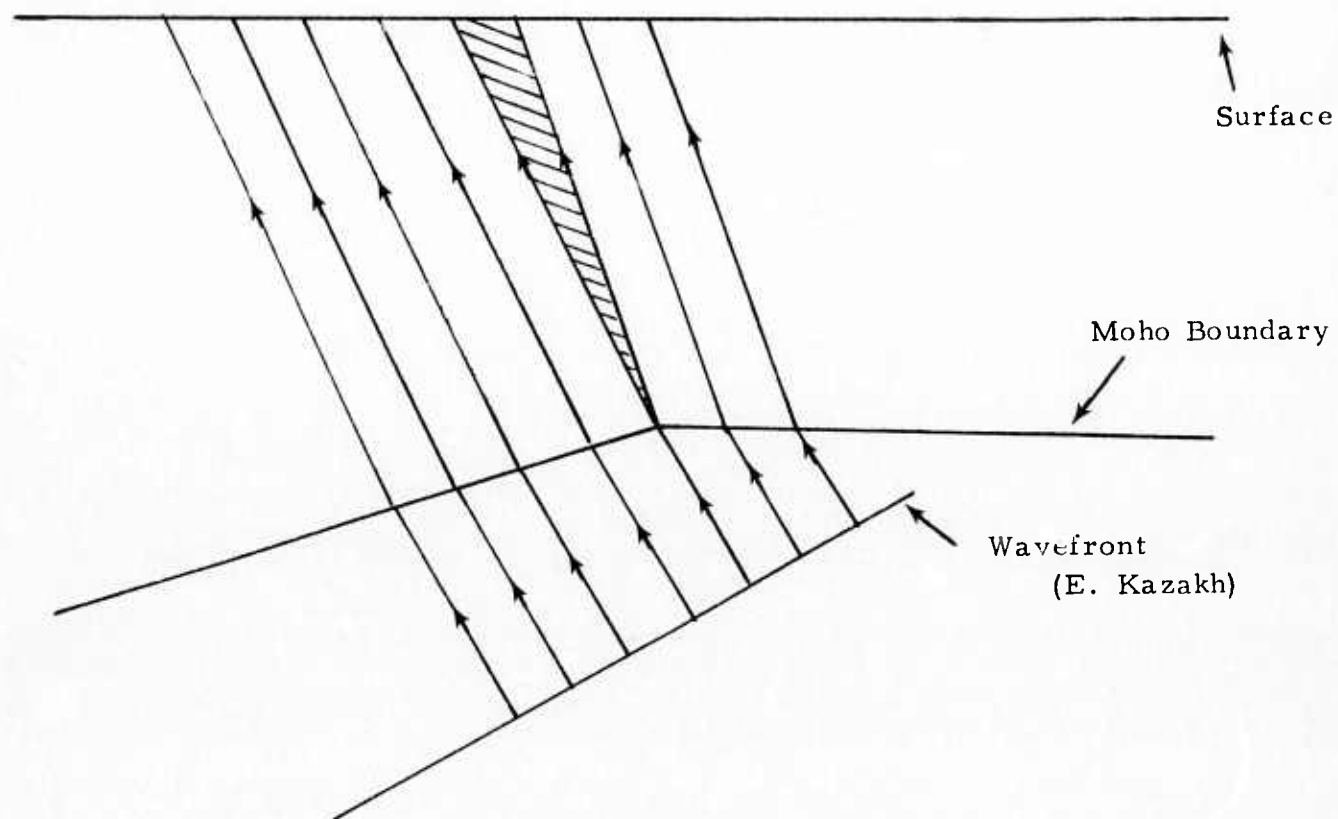SITUATED RIGHT ABOVE A RIDGE IN THE MOHO

FIGURE II-11

CONCEPTUAL MODEL (SECTION LINE II IN FIGURE II-9)
SHOWING THE EFFECTS OF A SUDDEN DEPTH INCREASE
OF THE MOHO. SEISMOMETERS LOCATED AT THE
SHADED AREA WILL SHOW ABNORMALLY
LOW SIGNAL AMPLITUDES.

how the seemingly anomalous behavior of subarray 05C and 12C amplitudes
for Kazakh events may occur.

Note that Figure II-10 will remain unchanged for all wave-
fronts with the same azimuth as the Kazakh events, while the location of the
shaded area in Figure II-11 will vary with the angle of incidence of the wave-
front. This explains why Kazakh is the only region for which extremely low
amplitudes for subarray 12C are seen, while low amplitudes for subarray 05C
are observed also for events from Yunan, which also is at 75 degree azimuth
from NORSAR.

It is conceivable that most of the amplitude variations between
NORSAR subarrays may be explained as caused by curvature of the Moho
boundary underneath the array together with random effects due to scattering.
However, a much more detailed analysis will be required to reach a definite
conclusion with respect to this matter.

An interesting consequence of the regional consistency in the
subarray amplitude variations is that diversity stack beamforming with pre-
defined weights would be a realistic alternative to conventional beamforming
for NORSAR on-line detection processing. Also, the large spread in subarray
amplitudes suggests that forming partial array beams, using only the best
subarrays for each region, might improve signal-to-noise ratios while reducing
computational load for the NORSAR DP. This possibility will be investigated in
future work.

D.   TIME DELAY ANOMALIES

As was stated in Special Report No. 6, significant time delay
anomalies (deviations from plane wave propagation along the great circle
azimuth) are observed for the NORSAR array, and must be taken into account
in array beamforming.

Inter-subarray time delay anomalies were calculated for all large SNR events by computing the cross-correlation functions between the reference subarray beam and the remaining subarray beams. A signal gate of 3 seconds was used in most cases. All computed delays were hand checked for inter-subarray consistency and also compared with delays from nearby events. Whenever a lack of consistency was found, the necessary adjustments were carried out by the analyst.

For the teleseismic regions (distances 30-100 degrees) consistent time delays were generally obtained without difficulty, thus confirming observations reported in Special Report No. 6. The problem mentioned in that report with respect to finding consistent time delays for subarray 7 (06B) for Kirgiz events is now believed to have been caused by the phase reversal in sensor 06B03 discussed in Section I of this report.

As can be expected, the irregular shape of the Mohorovicic discontinuity underneath the NORSAR array described in the preceding sub-section, has ramifications with respect to the travel time anomalies for signals received at NORSAR. As an example, the pattern of measured deviations from a plane wavefront for events from Kirgiz is shown in Figure II-12. The earliest signal arrivals relative to the plane wavefront occur for subarrays 01A and 08C, while subarray 03C has a signal arrival 0.7 seconds too late (relative to the 01A arrival). Time anomalies of up to half this magnitude may be accounted for by the relatively longer path travelled through the earth's crust for rays arriving at 03C than for 01A. The resemblance of this time delay anomaly pattern to the Moho pattern shown in Figure II-9 indicates that the remaining part of the time delay anomalies may come from velocity structures in the earth's mantle related to the shape of the Moho.
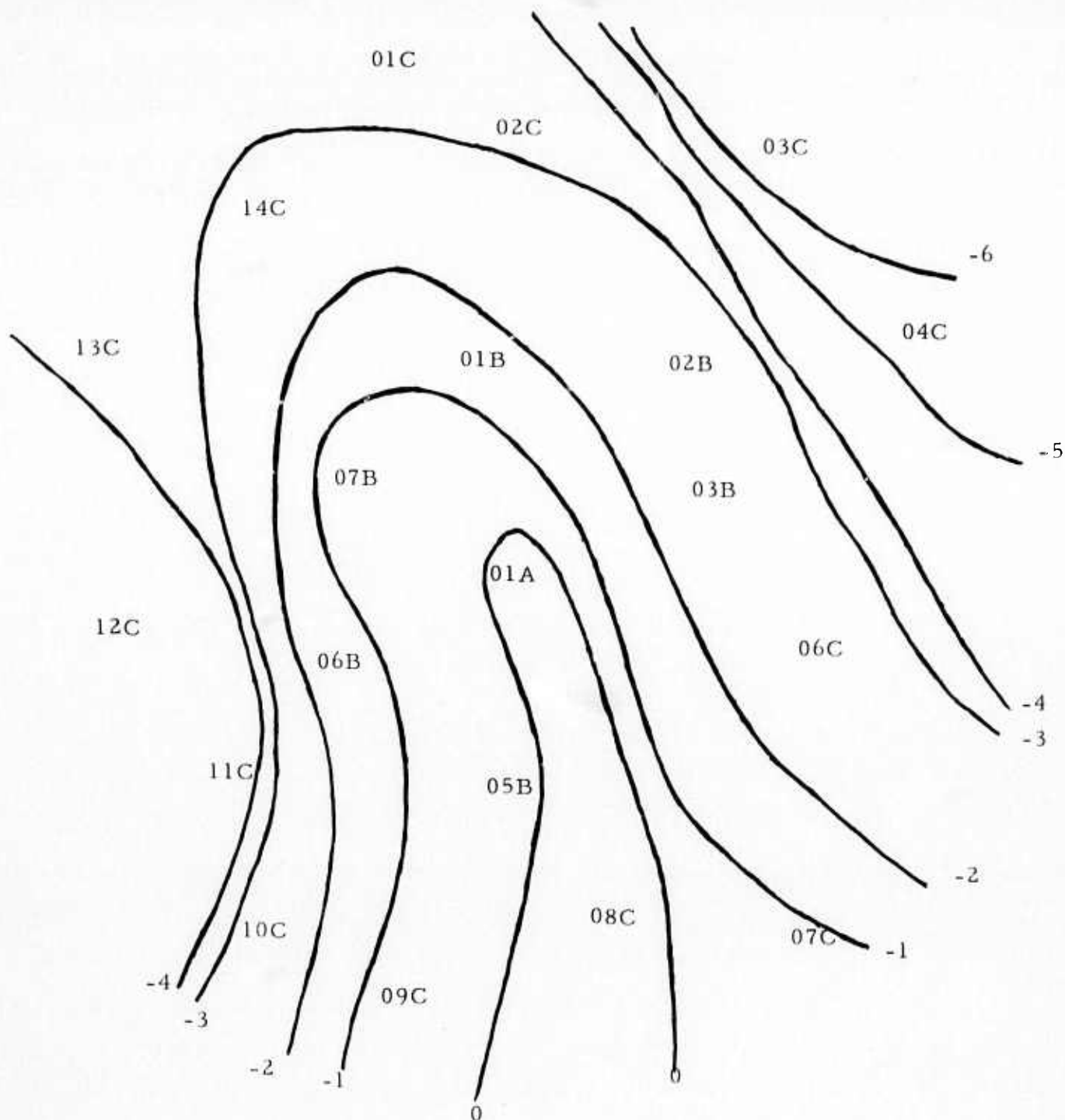
FIGURE II-12

CONTOUR PLOT SHOWING THE MEASURED TIME DELAY
DEVIATIONS FROM A PLANE WAVEFRONT FOR EVENTS
FROM KIRGIZ. THE NUMBERS REFER TO DELAY IN
DECISECONDS, THE EARLIEST ARRIVAL OCCURRING
AT 01A AND 08C.

Near regional events, notably from Western Russia and the Mediterranean area, still represent a considerable problem with respect to finding appropriate inter-subarray time delays. However, the swarm of events from Italy during February 4-8, 1972 has given some insight to the behavior of delay anomalies for Mediterranean region events.

For all the Italy events processed, it was observed on the time domain traces that at least one cycle of 0.5 Hz energy precedes the arrival of a 1 Hz P-wave (e.g., event ITA/036/01N, shown in Figures II-13 and II-14). However, the relative sizes of the corresponding spectral peaks were seen to vary markedly from event to event. For one event, ITA/035/02N, the 0.5 Hz energy completely dominates the spectrum, as seen in Figures II-15 and II-16.

For all Italy events except ITA/035/02N, similar sets of time delay anomalies were found applying the cross-correlation procedure. Interestingly, when the standard filter was applied prior to cross-correlation for ITA/035/02N the resulting time delays were consistent with the other events. (Table II-1). Figure II-17 shows the power spectrum of ITA/035/02N when applying the delays computed from filtered data.

Our conclusions from studying Italy events can thus be stated as follows:

- Energy of distinctly different frequencies arrives at the NORSAR array at distinctly different times. This suggests the existence of two different propagation paths with highly different attenuation characteristics for Italy events.

- Time delay anomalies computed for Italy events vary considerably with frequency. Thus, array beamforming based on delays computed from low frequency energy may cause substantial loss for higher frequencies
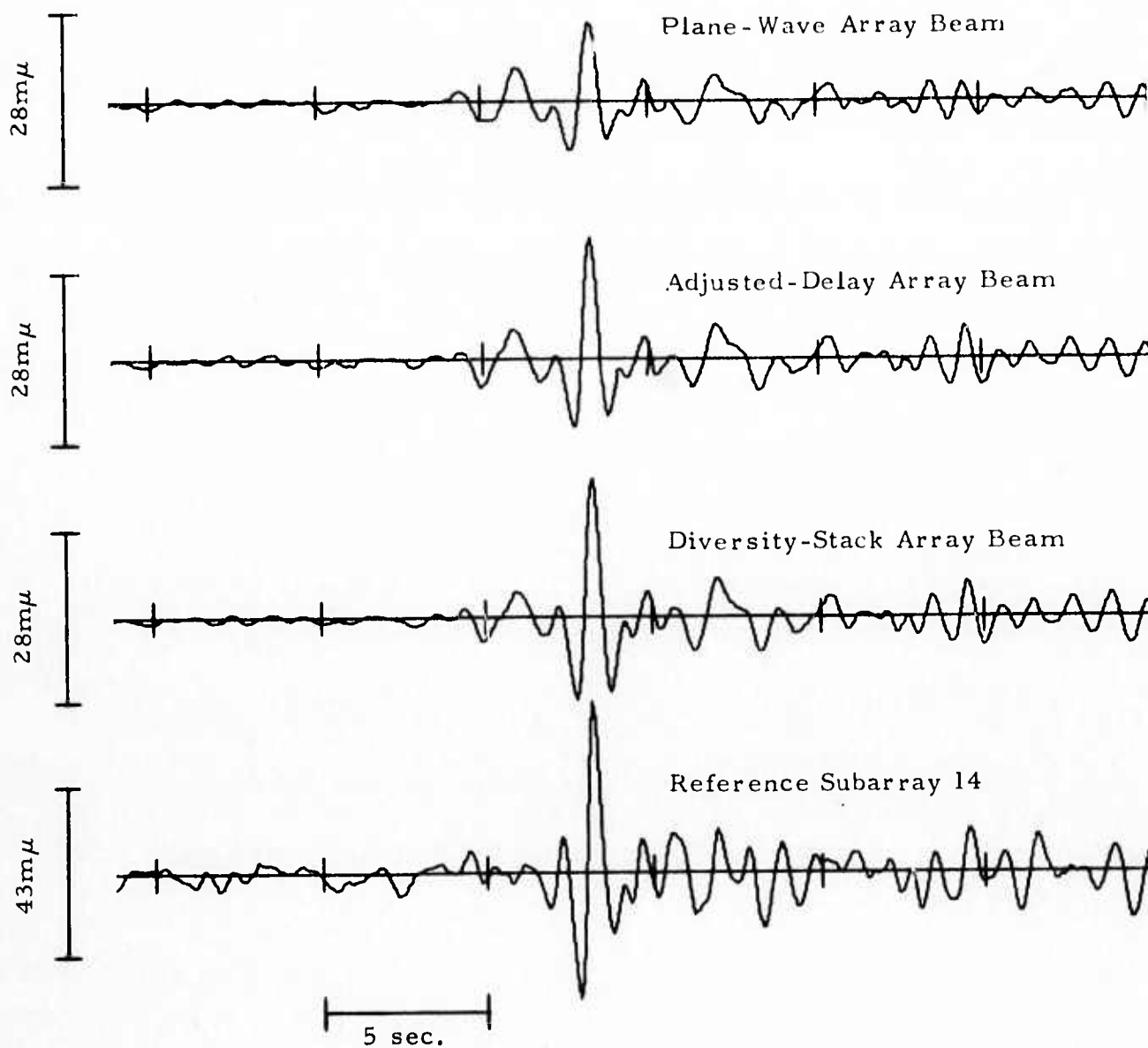
FIGURE II-13
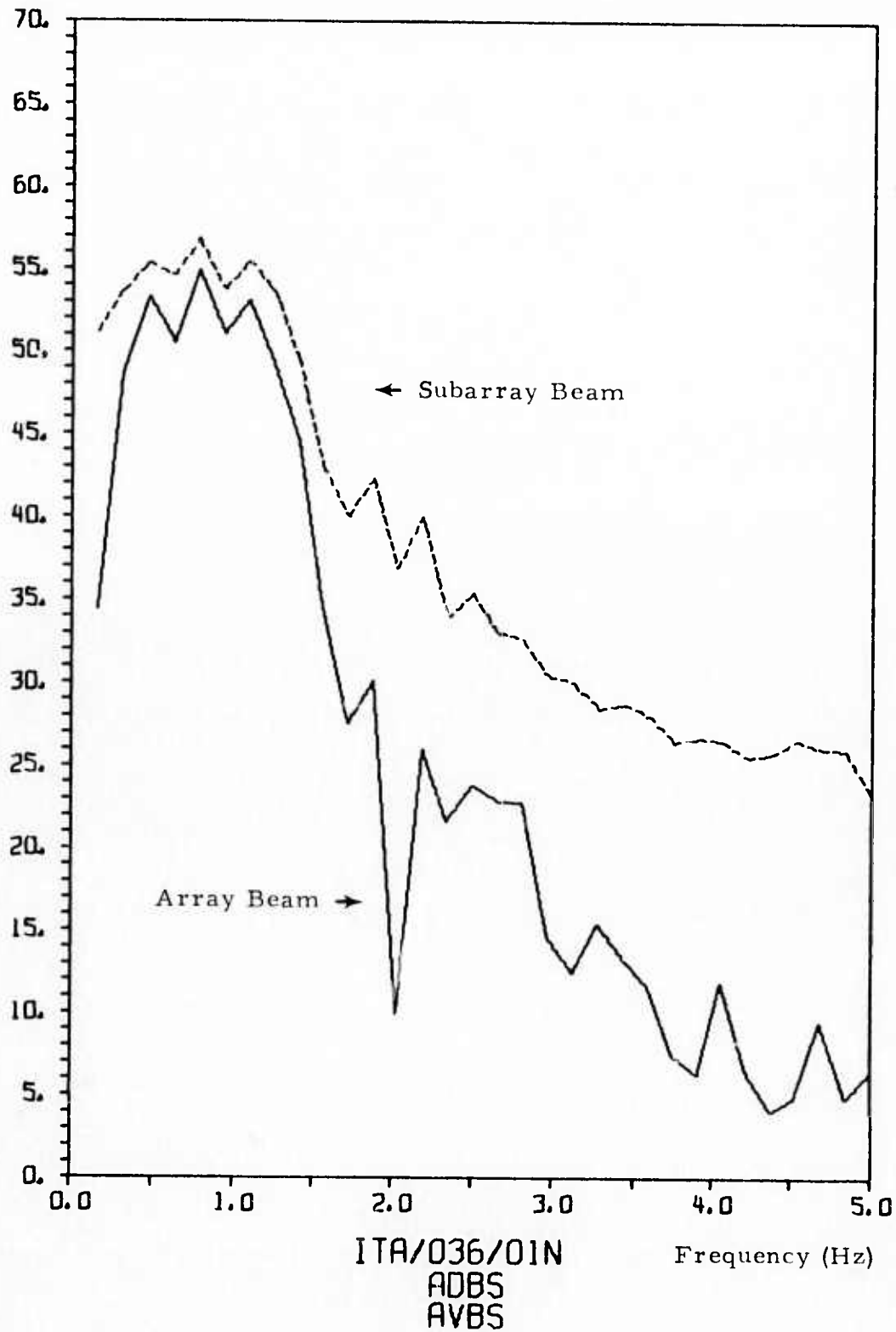
TIME DOMAIN PLOT OF EVENT
ITA/036/01N

FIGURE II-14

SUBARRAY AND ADJUSTED-DELAY ARRAY BEAM SPECTRA
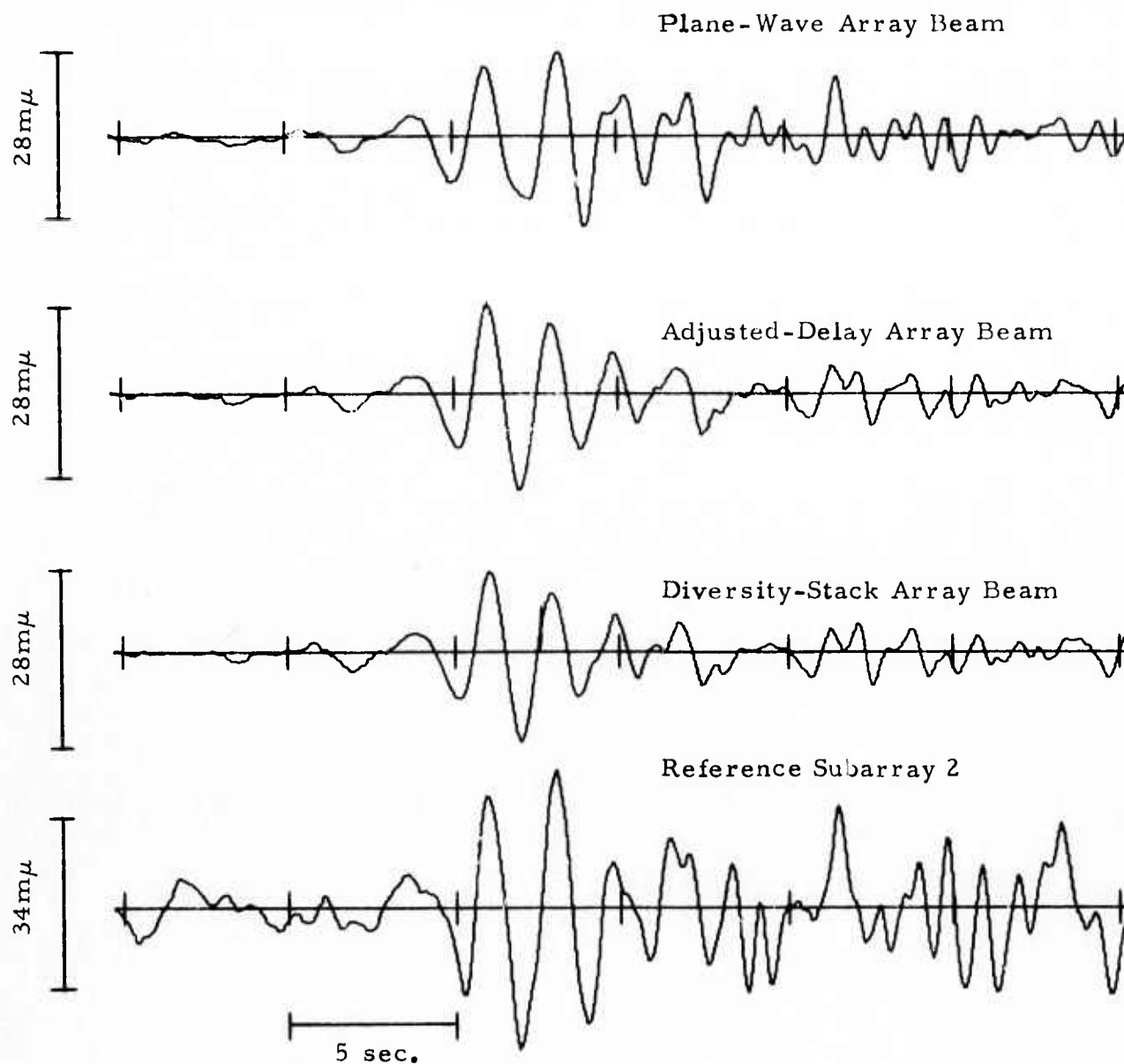FOR EVENT ITA/036/01N
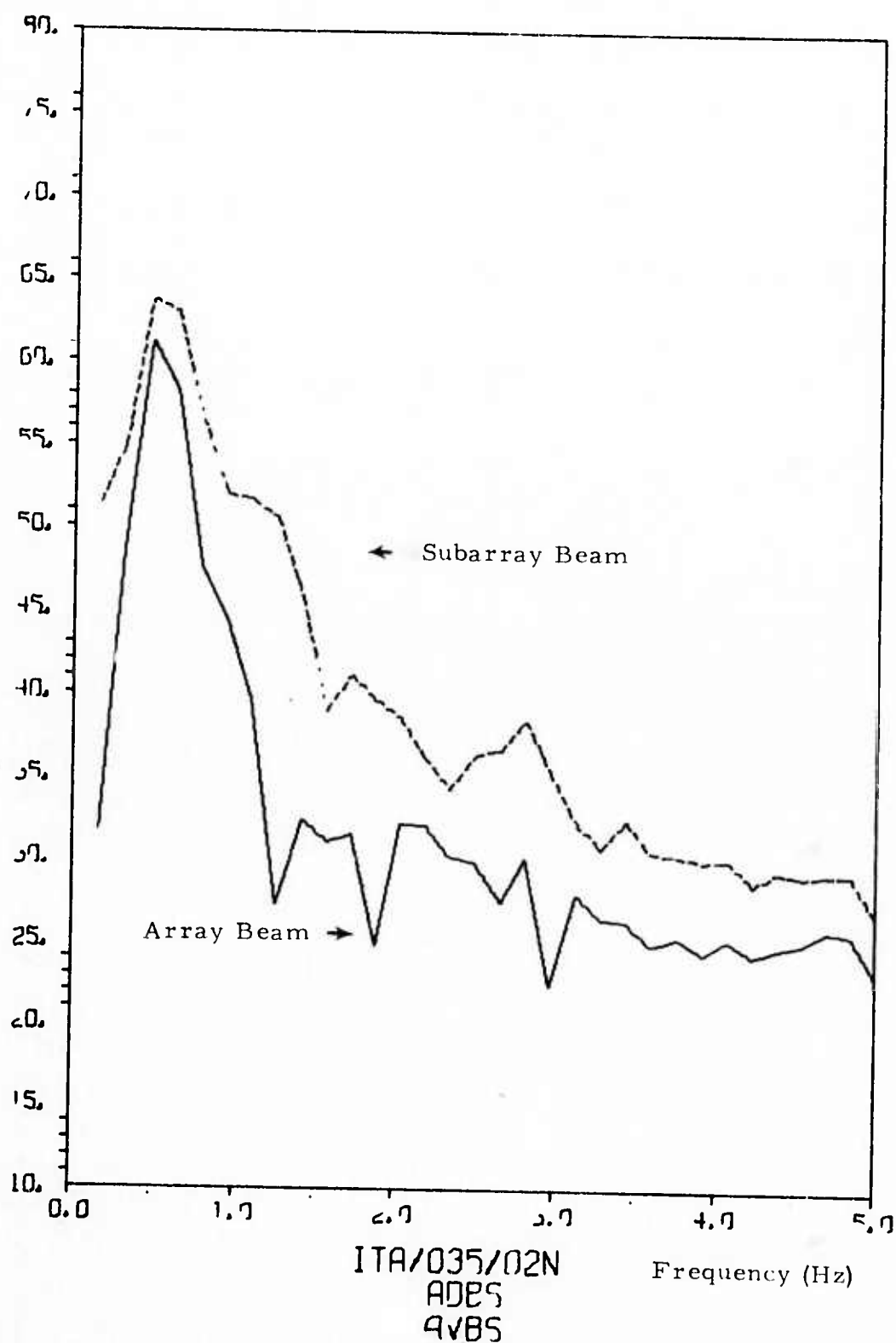
FIGURE II-15

TIME DOMAIN PLOT FOR EVENT
ITA/025/02N

FIGURE II-16

SUBARRAY AND ADJUSTED-DELAY ARRAY BEAM SPECTRA
FOR EVENT ITA/035/02N

II-25

TABLE II - 1

COMPARISON OF DELAY ANOMALIES COMPUTED FROM HIGH AND LOW-FREQUENCY ENERGY FROM ITALIAN EVENTS

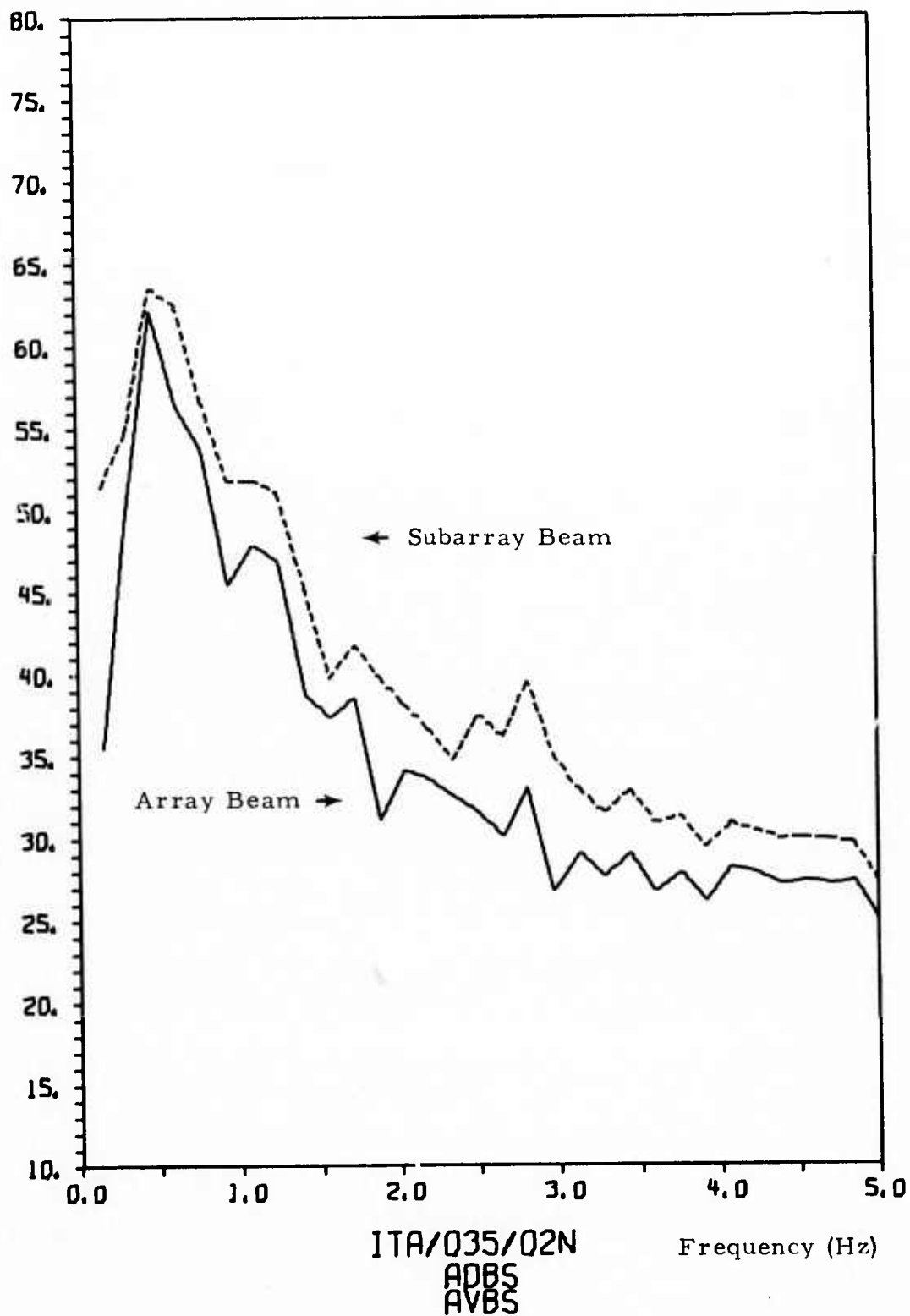| Subarray	ITA/035/02N Unfiltered	Filtered	Modal Values For Other Events
01A	0	0	0
01B	-1	-3	-1
02B	-2	-3	-2
03B	-2	-2	-2
04B	-4	-2	-2
05B	3	0	-1
06B	-1	-3	-3
07B	-1	-3	-2
01C	x	x	x
02C	-2	-3	-2
03C	-3	-2	-1
04C	-3	0	0
05C	-3	0	0
06C	2	-2	-1
07C	3	-3	-3
08C	3	-5	-4
09C	2	-5	-5
10C	1	-4	-5
11C	x	x	-4
12C	-3	-6	-6
13C	-7	-5	-5
14C	-3	-1	-3

FIGURE II-17

SUBARRAY AND ADJUSTED-DELAY ARRAY BEAM SPECTRA FOR
EVENT ITA/035/02N.   ADJUSTED DELAYS IN THIS CASE WERE
COMPUTED FROM FILTERED SUBARRAY BEAMS.

A similar phenomenon of different arrival times for low and high frequency energy, although much less pronounced, has been observed for some other events from the Mediterranean area. Figure II-18 shows as an example the waveforms for an earthquake from Greece, GRE/109/02N.

E.   NORSAR m_b MEASUREMENTS

NORSAR m_b values were measured on a number of detected events from Eurasia using the formula:

$$m_b = \log A/T + B$$

where: A   is the maximum peak-to-peak signal amplitude in $m\mu$ on the adjusted delay array beam (corrected for seismometer response).

T   is the period of the cycle with the maximum amplitude.

B   is the distance factor.

Values for B were given in Special Report No. 6, Table III-4; the same values are also used for the calculation of LASA m_b's.

Figures II-19 and II-20 are plots of NORSAR m_b's versus either PDE m_b's (dots) or LASA m_b's (crosses). Magnitudes reported from ISM are marked as circles. Figure II-19 comprises 67 events from the Japan-Kuriles-Kamchatka region while Figure II-20 is based on 142 events from the remainder of Eurasia.

For the Japan to Kamchatka region NORSAR m_b values appear to be generally slightly lower than LASA/PDE values. The average difference is 0.14 magnitude units, and appears to be independent of event magnitude.
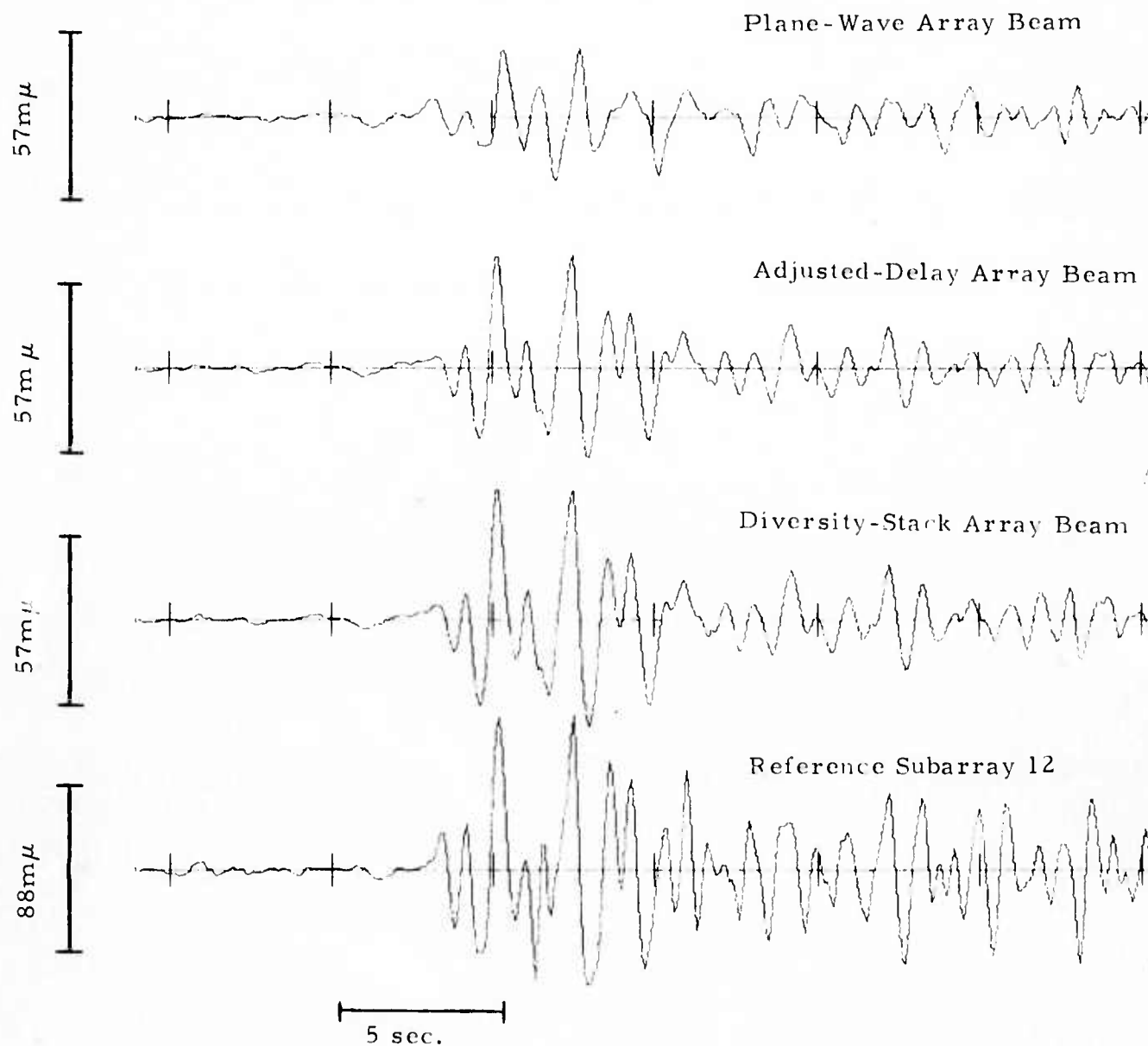
FIGURE II-18

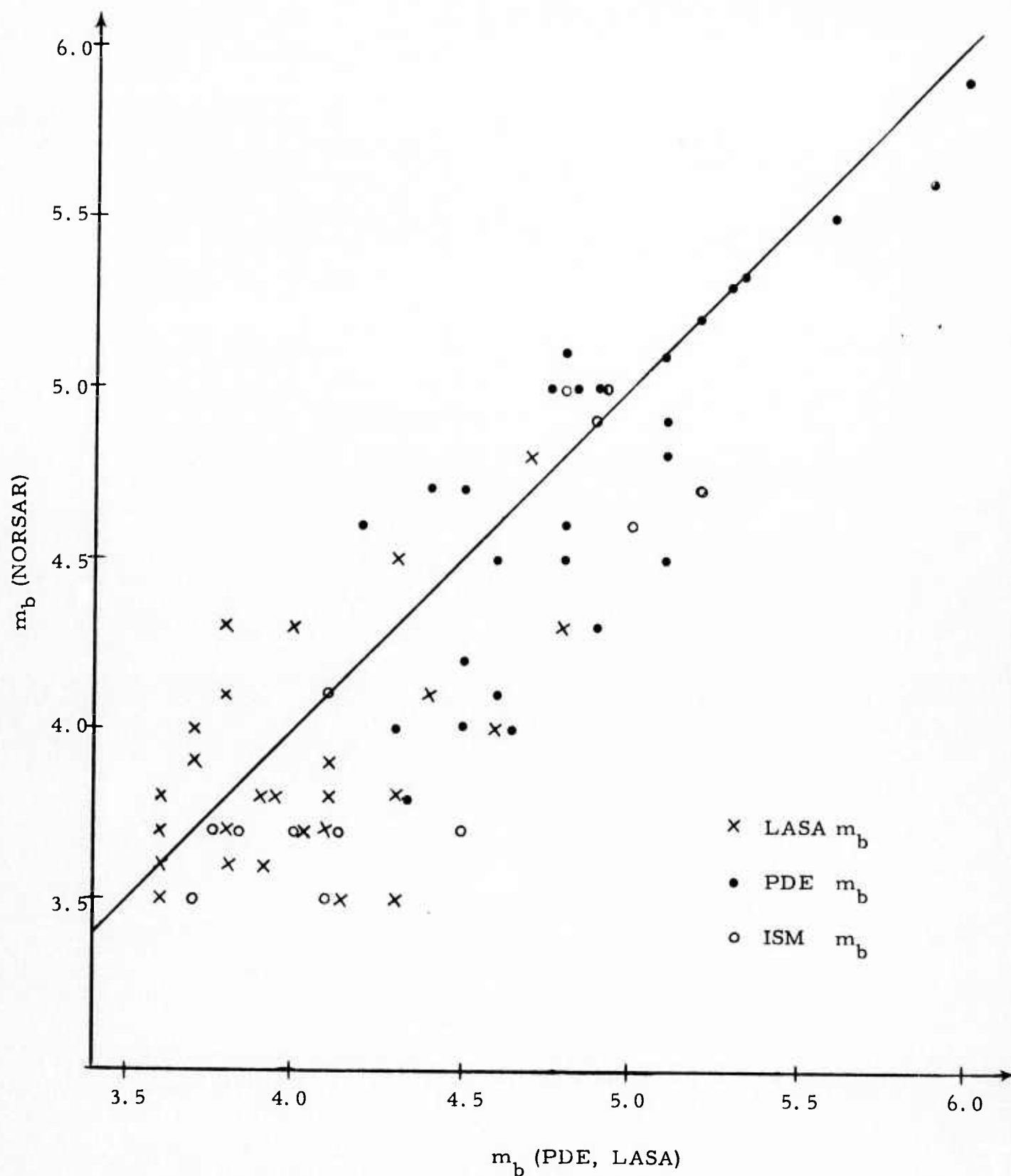**TIME DOMAIN PLOT OF EVENT**
GRE/109/02N

FIGURE II-19

NORSAR MAGNITUDE VERSUS PDE OR LASA MAGNITUDE,
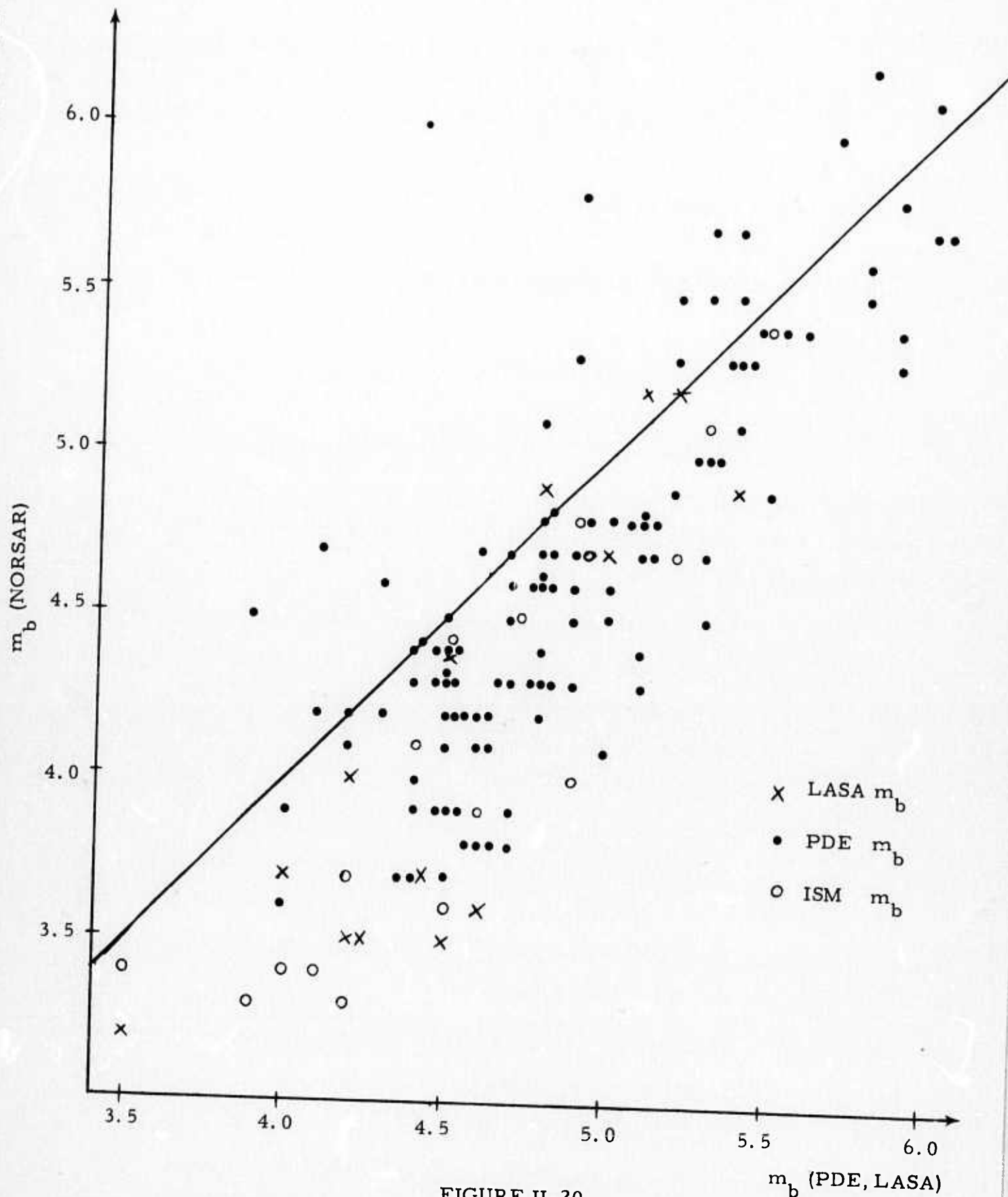KAMCHATKA-KURILES-JAPAN REGION

II-30

FIGURE II-20

NORSAR MAGNITUDE VS. PDE OR LASA MAGNITUDE;
EURASIA APART FROM JAPAN-KURILES-KAMCHATKA

II-31

Note that most of the low magnitude events in this region have magnitudes from LASA, which is located at approximately the same epicentral distance as NORSAR. The spread in the data appears to be considerable in view of this fact. Also, because of the large number of small events not detected by NORSAR, a better estimate of the m_b bias is obtained by only considering events of PDE/LASA m_b greater than 4.0; this yields an average m_b difference of 0.20 m_b units.

All events from other regions of Eurasia have been included in Figure II-20. Again, NORSAR exhibits a generally lower m_b (an average difference of 0.29 magnitude units) but this difference seems to increase as the event magnitude decreases. Since this did not appear to be the case for the Japan to Kamchatka region, it might seem reasonable to relate the problem to the following two factors:

- Several of the low magnitude events in the last case have an m_b from PDE. Stations in the PDE net that report m_b for a small earthquake are likely to have a favorable radiation pattern for this event, and will consequently report a relatively high amplitude.

- While most of the large events in our population are from a distance of 40 degrees or more, where beamforming loss is low, a greater number of the smaller earthquakes are from the Mediterranean region, where large beamforming loss accounts for low NORSAR magnitudes.

However the above problem still requires further investigation before a definite conclusion can be drawn

Figure II-21 gives histograms of the magnitude difference (NORSAR minus PDE or LASA) for the two subregions. The negative bias

Average = -0.14
ST. DEV. = 0.32

Japan-Kuriles-Kamchatka
region (67 events)

m_b (NORSAR) - m_b (PDE, LASA)

Average = -0.29
ST. DEV. = 0.36

Eurasia apart from
Japan-Kuriles-Kamchatka
(142 events)

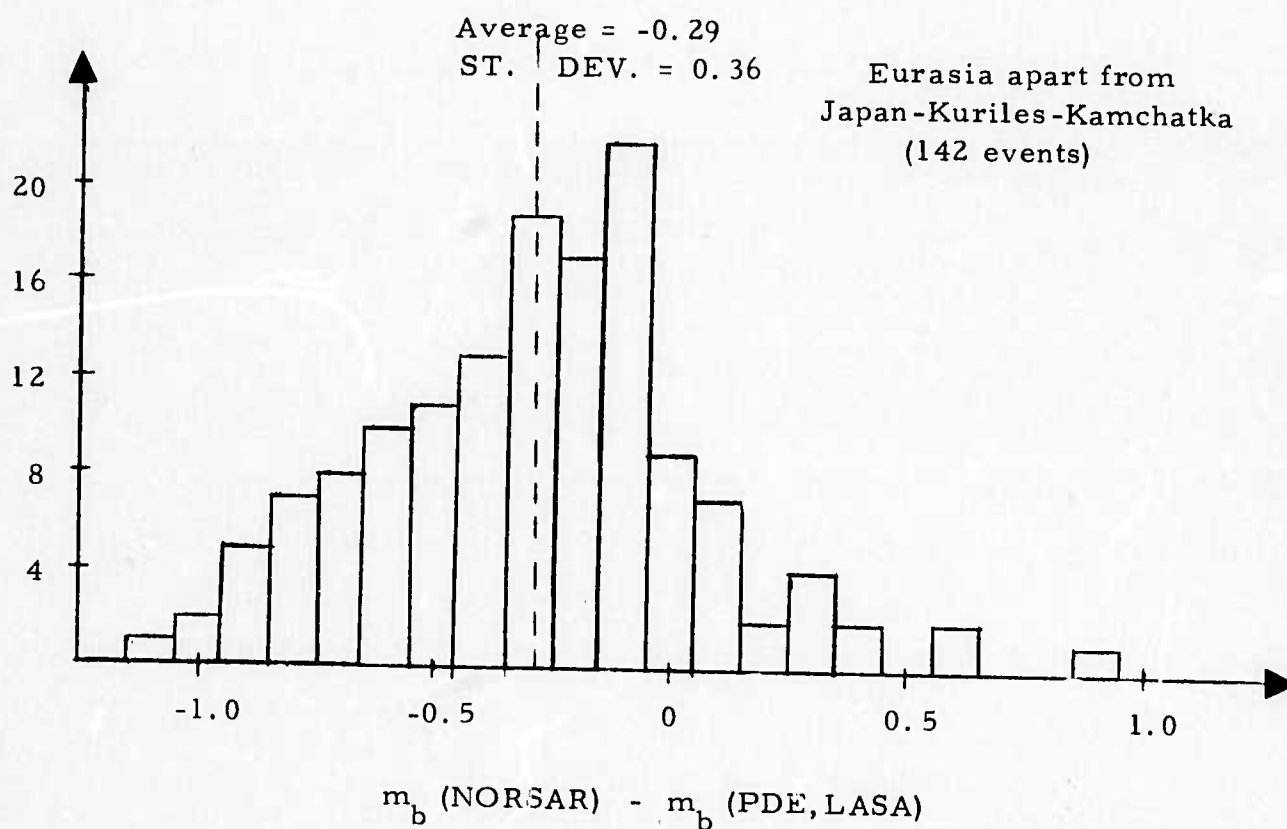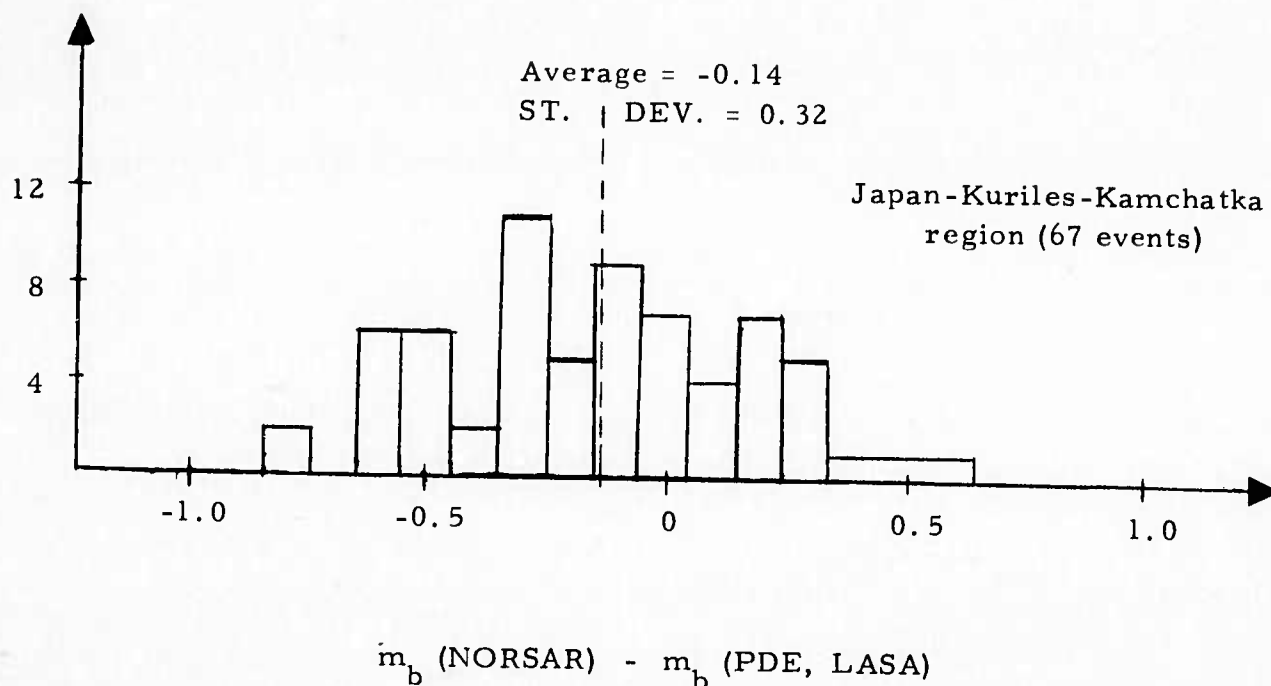m_b (NORSAR) - m_b (PDE, LASA)

FIGURE II-21

HISTOGRAMS OF THE DIFFERENCES BETWEEN
NORSAR AND PDE/LASA m_b FOR 209 EVENTS
FROM EURASIA

could be accounted for by signal loss in array beamforming, which typically is 3 to 4 dB for teleseismic events (0.15 to 0.2 magnitude units). For near regional events the loss will generally be higher, thus explaining the greater negative bias for the continental Eurasian region.

The distribution about the bias appears to be approximately normal, and would reflect normal variation in signal amplitude due to radiation patterns and/or propagation effects. Standard deviations in the two event populations are 0.32 for the Japan to Kamchatka region and 0.36 for the Continental Eurasia.

All the NORSAR magnitudes utilized in the preceding analyses have been measured by TI. For part of the data, m_b values were available from the NORSAR seismic bulletin compiled at Kjeller, Norway. A comparison was carried out to see if any systematic differences were present. Figure II-22 is a histogram of measured deviations for 62 events from distances beyond 30 degrees. It is seen that TI measurements have a slight negative bias (-0.02 m_b units), but that most measurements are consistent. The two events that show particularly large deviations, SIB/014/03N and LO1/058/10N, have significant location differences between the NORSAR bulletin and the PDE epicenter. In general, the observed differences are due to different location estimates, inaccuracies in time delay corrections and lack of precision in m_b measurements.

It is interesting to compare Figure II-22 to the corresponding histograms for NORSAR - PDE/LASA magnitudes (Figure II-21). Figure II-22 may be viewed as expressing the typical uncertainty involved in two independent measurements of the same m_b, and the corresponding standard deviation is approximately 0.15. This contrasts with a standard deviation of slightly above 0.30 for the interstation differences from Figure II-21, thus confirming that

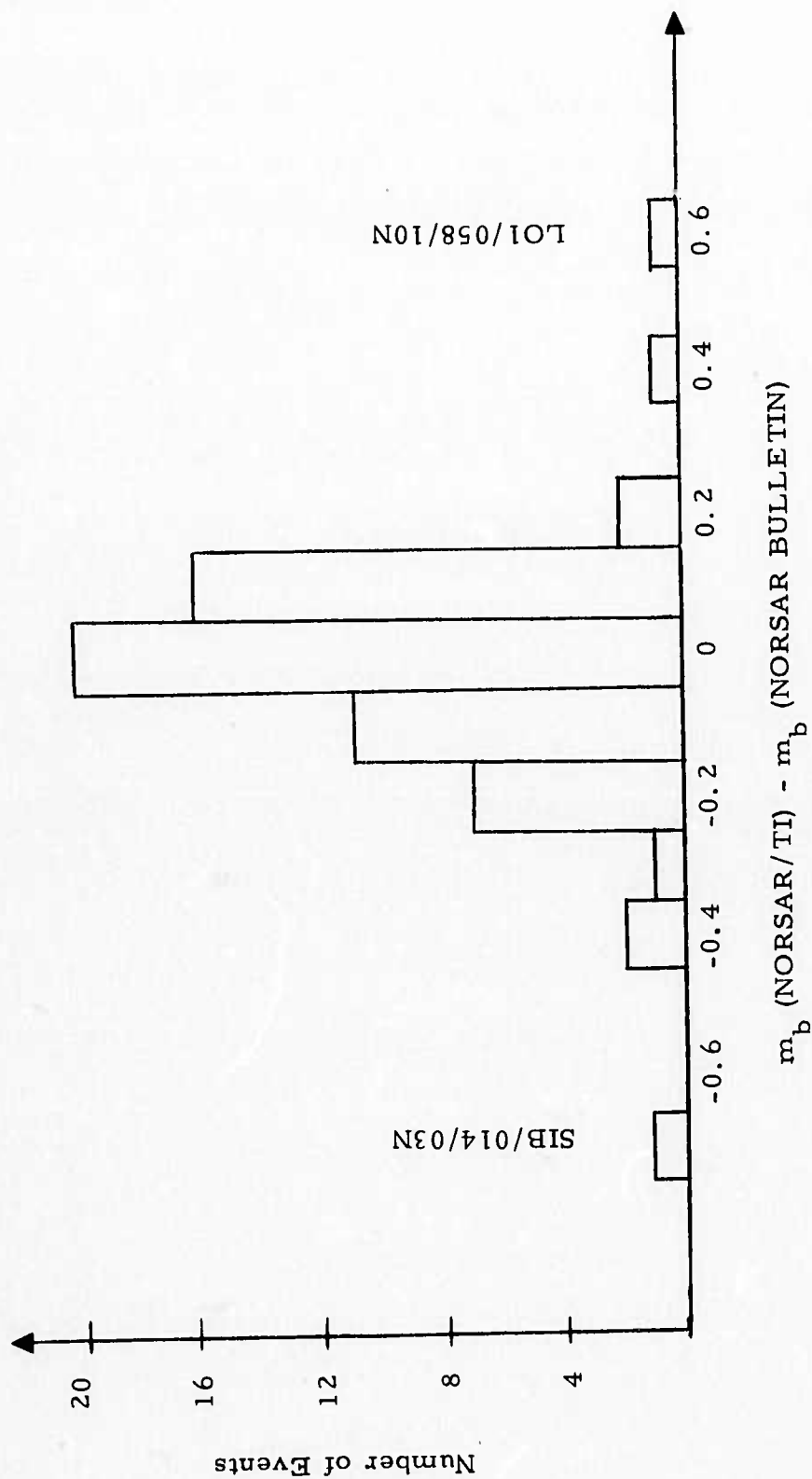m_b (NORSAR/TI) - m_b (NORSAR BULLETIN)

FIGURE II-22

HISTOGRAM OF THE DIFFERENCES IN m_b MEASUREMENTS
BY THE TI ANALYST AND THE NORSAR BULLETIN
FOR 62 TELESEISMIC EVENTS

the observed spread between NORSAR and PDE/LASA magnitudes is mostly real and not due to random measuring effects. (The "real" spread in this case would be approximately: $\sqrt{0.34^2 - 0.15^2} = 0.31$.)

One systematic regional difference was seen in the observed data; the Iran region where 8 events showed an average negative bias of 0.2 for the TI measurement. In fact these 8 events accounted for all of the bias in the total histogram. It thus appears that the time delay corrections used by TI were not optimum for this region.

Our event population was not sufficiently large to enable us to carry out a comparison between m_b values measured by TI and NTNF/NORSAR for near regional events, except for the Italy region. For the 10 events from Italy, the TI measurements averaged 0.4 m_b units higher than NORSAR's and it appeared that the NORSAR Event Processor was operating with poor time delay corrections for this region at the time these measurements took place.

SECTION III
ARRAY PROCESSING RESULTS

A. INTRODUCTION

This section discusses the improvement of signal-to-noise ratio (SNR) and the signal degradation resulting from:

- Subarray Beamforming

- Array Beamforming

- Application of the "standard" filter (Figure III-1)

A total of 71 events from Eurasia were used in these analyses; the magnitude range of these events was from m_b = 4.0 to 6.0.

B. SUBARRAY BEAMFORMING PERFORMANCE

Measurements of signal degradation and SNR improvement from single sensor to subarray beam were made for three events, WRS/295/05N, KAZ/181/04N and GRE/074/15N. The first two of these are presumed explosions. All three contain an appreciably greater than average proportion of high-frequency energy. Previous analysis (Special Report No. 6, 1972) has shown that sub-array beams for other events will in general perform at least as well as those discussed below.

Signal degradation (D) and SNR improvement (I) were computed for each subarray using the formulas:

$$D = 10 \log_{10} (\overline{S} - \overline{N}) - 10 \log_{10} (S_b - N_b)$$
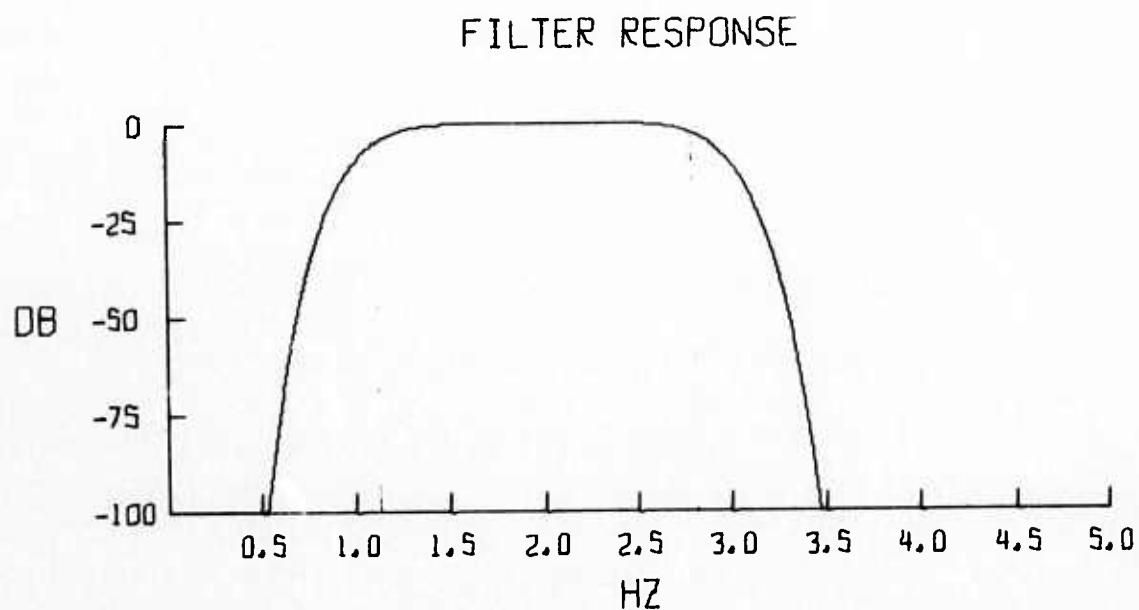
FILTER RESPONSE

FIGURE III-1

FREQUENCY RESPONSE CURVE OF THE STANDARD FILTER
USED FOR P-WAVE DETECTION FOR NORSAR DATA
CORNER FREQUENCIES ARE 1.2 AND 2.8 Hz

$$I = 10 \log_{10} \left(\frac{S_b - N_b}{N_b} \right) - 10 \log_{10} \left(\frac{\overline{S} - \overline{N}}{\overline{N}} \right)$$

where $\overline{S}$ and $\overline{N}$ are signal and noise powers over 6.4 and 70 seconds windows respectively, averaged over all sensors within a subarray; while S_b and N_b are signal and noise powers for the subarray beam over the same windows.

Table III-1 summarizes subarray beamforming results for the three events investigated, using both plane-wave and adjusted delays for subarray beamforming. The adjusted-delay subarray beam shows an average improvement of less than 0.5 dB over the plane wave beam. The gain resulting from using adjusted delays in subarray beamforming is thus only marginal even for close-in, high frequency events.

An interesting observation is that the average subarray beam wide band noise reduction, which is the sum of the SNR improvement and the signal degradation, is 10.5, 9 and 11 dB for the three events respectively. This is well above the expected 7.8 dB corresponding to $\sqrt{N}$ noise reduction. The apparent explanation for this phenomenon is the strong, directional 3-6 second Rayleigh wave noise field generally propagating from the Northwest across the NORSAR array. (Special Report No. 5, 1972). The typical subarray geometry seems to take advantage of the coherency of this noise for beamforming toward the East and Southeast. In fact, when steering the subarray beams toward the Northwest (300 degrees azimuth, 11 km/sec velocity) the wide-band noise suppression for the noise preceding WRS/295/05N averaged only 5.3 dB across the subarrays.

C.   ARRAY BEAMFORMING PERFORMANCE

Array beamforming SNR improvement and signal degradation were computed for 71 Eurasian events in a manner similar to the computations

TABLE III - 1

SUMMARY OF SUBARRAY BEAMFORMING ANALYSIS
RESULTS FOR WIDE-BAND SIGNALS

Event		SNR Improvement (dB)			Signal Degradation (dB)		
		Min	Mean	Max	Min	Mean	Max
WRS/295/05N	P. W.	5.9	8.9	12.0	0.5	1.7	3.7
	A. D	6.7	9.3	12.0	0.5	1.2	2.6
KAZ/181/04N	P. W	3.4	7.0	8.9	0.9	2.1	4.7
	A. D	5.1	7.3	9.3	0.6	1.5	3.0
GRE/074/15N	P. W	5.7	8.5	12.1	1.1	2.5	5.9
	A. D	5.7	8.8	12.1	1.1	2.2	5.9

P. W.   Plane Wave Delays

A. D.   Adjusted Delays

performed in Subsection III-B. Figure III-2 is a histogram showing the distribution of wide-band SNR improvement over the entire event population. More than 80% of the events fall in the 9-12 dB bracket; of the six events with gains less than 7 dB, five are from the Mediterranean region and one is a presumed explosion from E. Kazakh (KAZ/282/06N).

Average SNR gain was 10.1 dB, while signal degradation over the event ensemble averaged 3.0 dB. The sum of these two numbers conforms well to the expected $\sqrt{N}$ noise reduction across the array, which amounts to 13.4 dB for N = 22.

The array beamforming gains were also computed for each event after the standard filter had been applied to the subarray beams. With this procedure, an average SNR gain of 9.3 dB was achieved, while signal degradation averaged 4.0 dB. This higher degradation for filtered signals is to be expected since the filter attenuates the low frequency energy, which is generally the most coherent part of the signal across the array. Figure III-3 shows the average subarray and array beam spectra for a Turkey event, TUR/276/17N, and can serve as a good illustration of the abovementioned point. This event has a low array beamforming loss around 1 Hz, while beamforming loss around 1.5 Hz is close to the 13 dB noise suppression.

Formation of diversity-stack array beams yielded an average improvement over the adjusted-delay beam of 1.0 dB for wideband signals and 1.6 dB for signals to which the standard filter had been applied. Table III-2 shows the distribution of the improvements across the event ensemble.

D.   STANDARD FILTER PERFORMANCE

The SNR improvement and signal degradation obtained by applying the standard filter were computed for the ensemble of 71 Eurasian
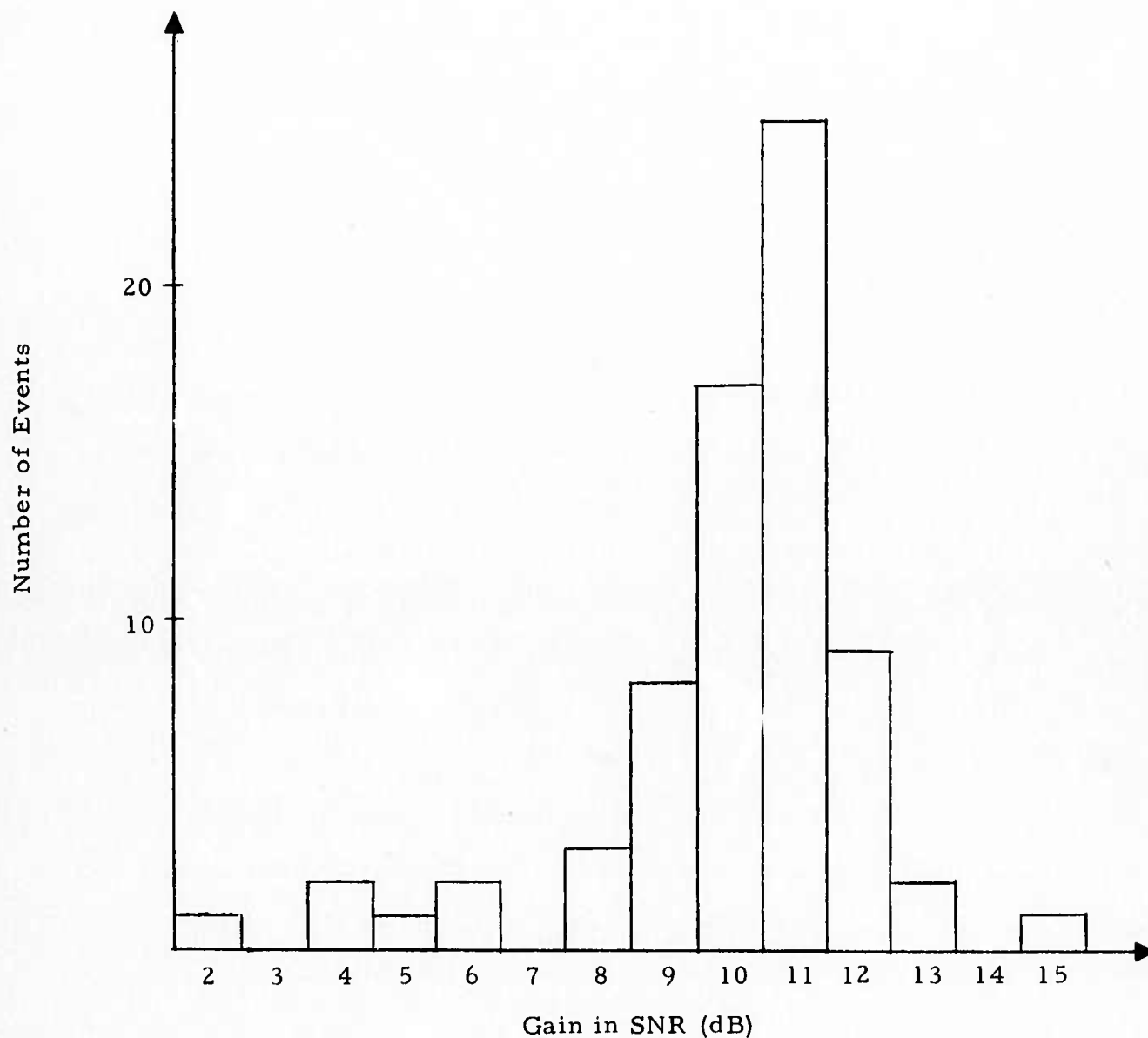
FIGURE III-2

GAIN IN SIGNAL-TO-NOISE RATIO FROM WIDE-BAND
SUBARRAY BEAM TO ADJUSTED-DELAY ARRAY
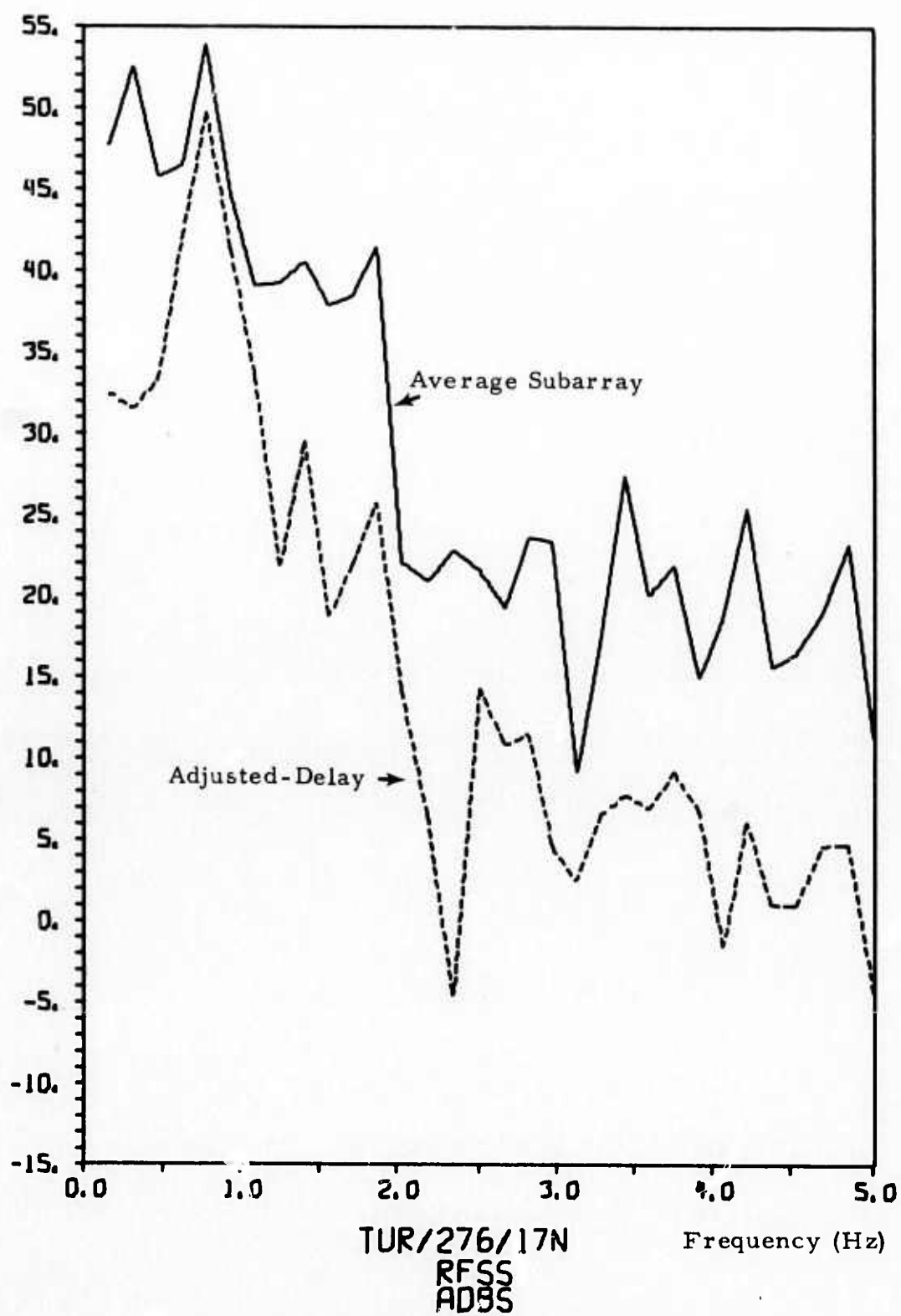BEAM FOR 71 EURASIAN EVENTS

TUR/276/17N
RFSS
ADSS

FIGURE III-3

AVERAGE SUBARRAY AND ADJUSTED-DELAY ARRAY BEAM
SPECTRA FOR EVENT TUR/276/17N

III-7

TABLE III-2

SNR IMPROVEMENT ACHIEVED BY DIVERSITY STACK BEAMFORMING FOR 71 EURASIAN EVENTS

IMPROVEMENT dB NO. OF EVENTS	-2	-1	0	1	2	3	4	5
WIDEBAND	1	2	17	30	19	3	0	0
FILTERED	0	1	11	16	29	13	0	1

events previously referred to in this section. Figure III-4 is a histogram showing the average subarray SNR filtering gain for the individual events; a similar representation of SNR improvements for the filtered array beam is presented in Figure III-5.

Average SNR improvement achieved by the standard filter is 7.5 dB on the subarray beam and 6.8 dB on the array beam level, thus indicating that beamforming tends to decrease the effectiveness of the standard filter. The spread in this data is considerable, with observed SNR gains ranging from -4 to 16 dB for the filtered array beam. In view of the stable spectral characteristics of the short period noise at NORSAR (Special Report No. 6 No. 6, 1972), these fluctuations essentially reflect variation in signal spectral contents. E.g. for the Turkey region, with dominantly low frequency signals (Subsection II-B) standard filter SNR improvement averages only 2 dB, while the average gain for Afghanistan events is 10 dB and for E. Kazakh presumed explosions 14 dB.

Signal power attenuation caused by the standard filter is shown as a histogram in Figure III-6. Average signal loss is 6.5 dB on the filtered array beam, with values for individual events ranging from 1 to 17 dB. This average loss combined with the average SNR gain of 6.8 dB mentioned earlier accounts for an average noise reduction of about 13 dB achieved by the standard filter. This number is consistent with the results from our noise analysis presented in Special Report No. 6, 1972.

Figure III-7 is a plot of the effectiveness of the standard filter as a function of event wide-band SNR. It appears that filter performance is largely independent of event size. There is a slight trend toward higher filtering SNR gains for smaller events when Turkey events are eliminated; this might be attributed to a general tendency for smaller events to contain proportionally more high frequency energy than large events. An enlarged data base will be necessary to study this problem in more detail.

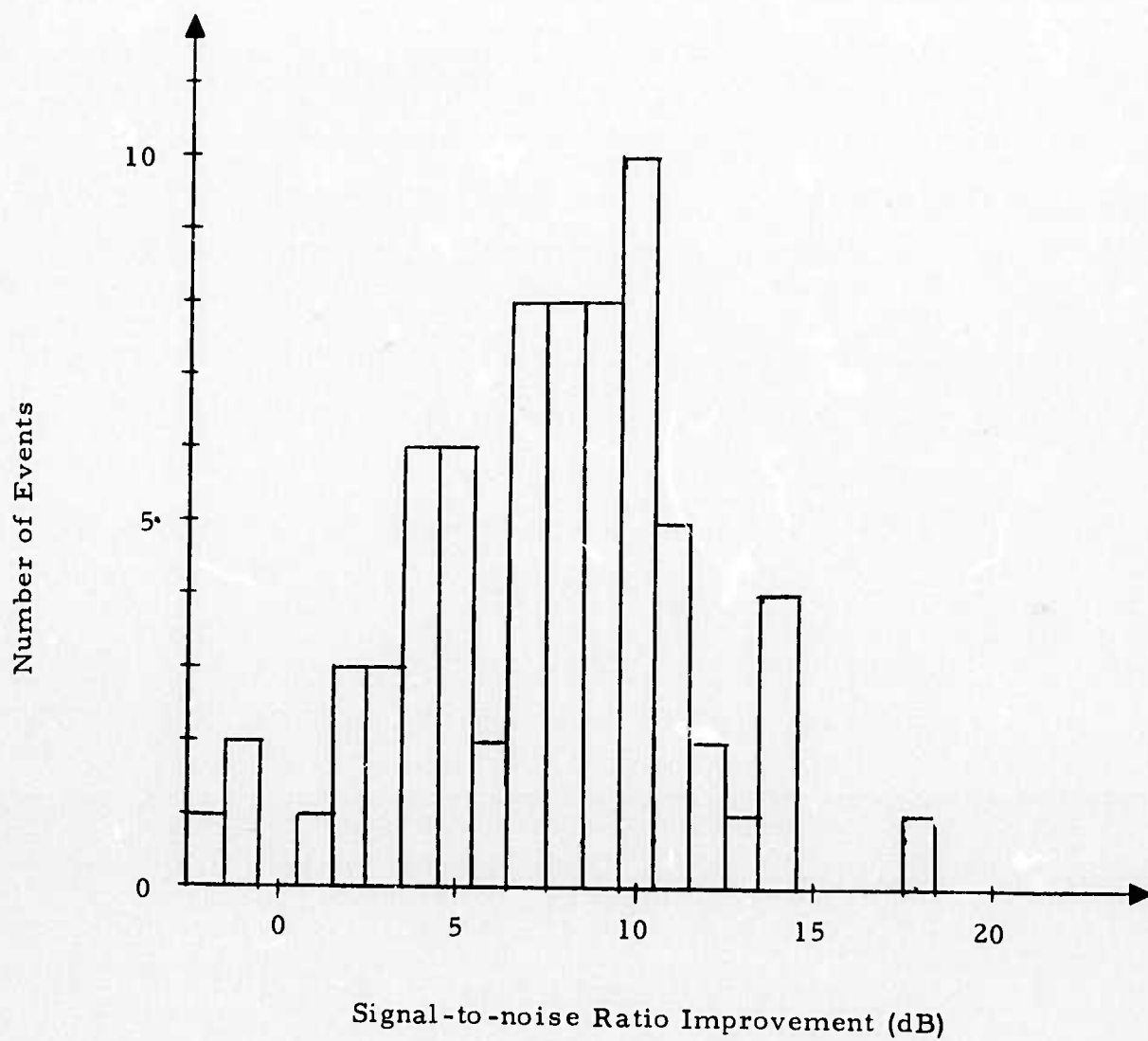Signal-to-noise Ratio Improvement (dB)

FIGURE III-4

AVERAGE SUBARRAY BEAM SNR IMPROVEMENT ACHIEVED
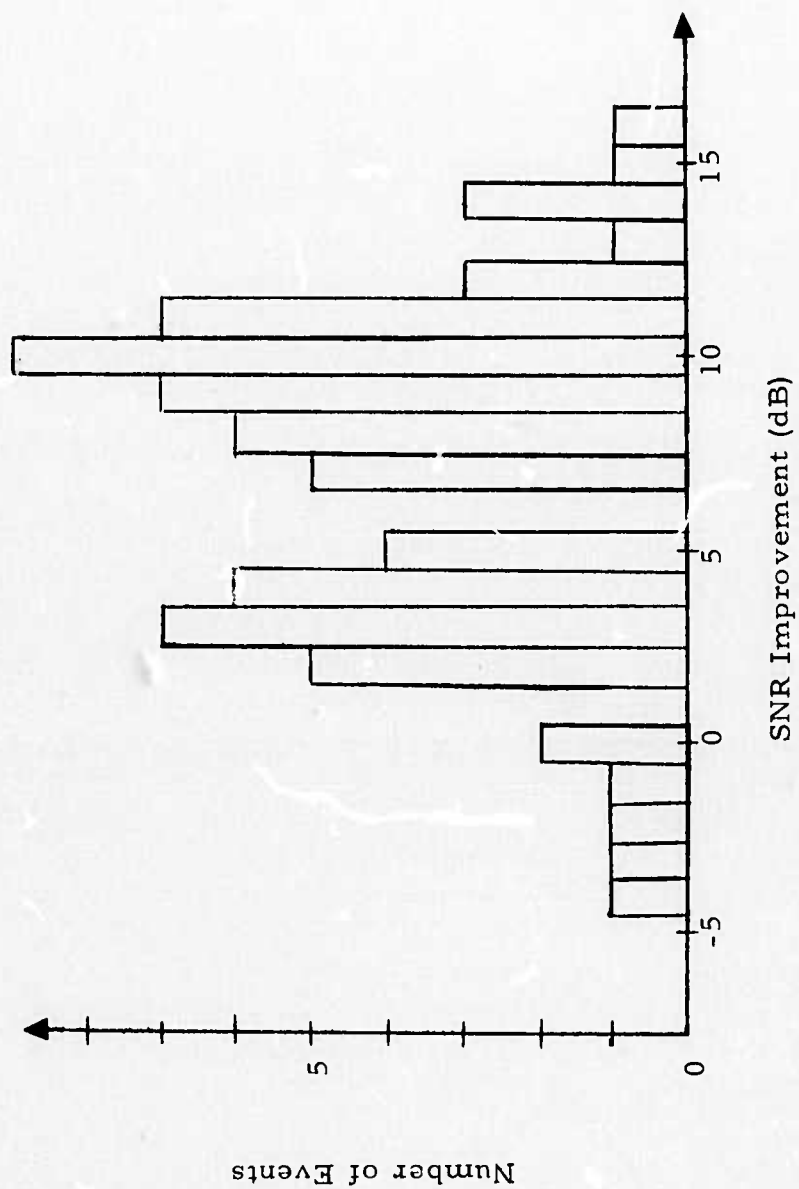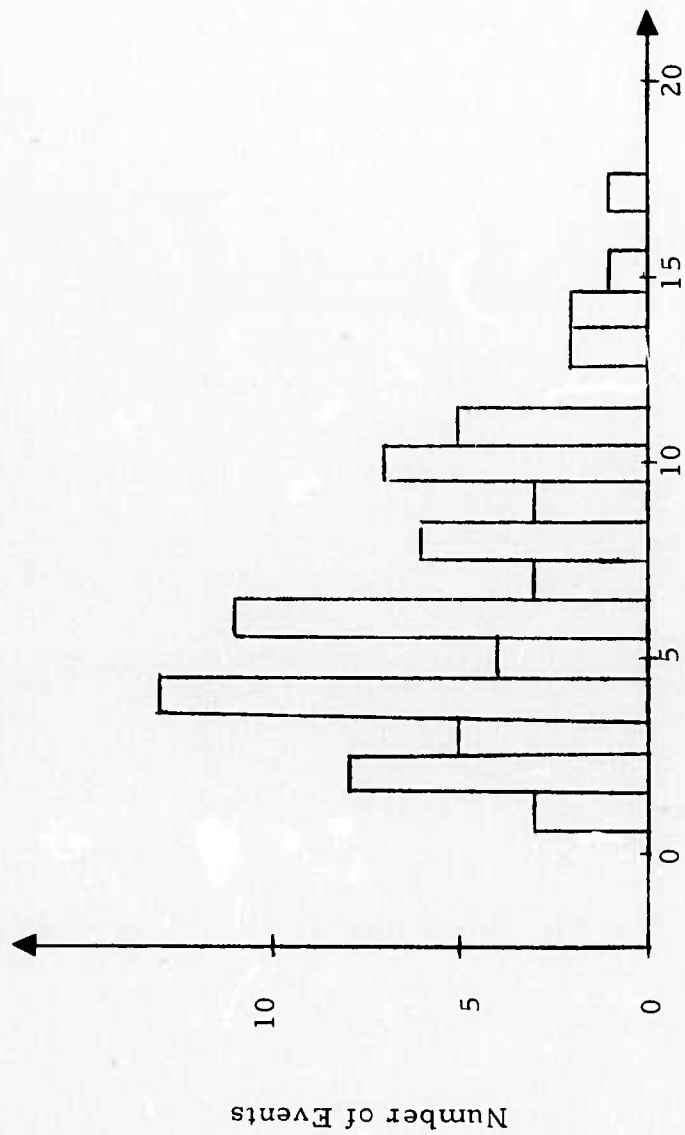BY APPLICATION OF THE STANDARD FILTER

FIGURE III-5

SNR IMPROVEMENT ACHIEVED BY APPLYING THE STANDARD
FILTER TO THE ADJUSTED-DELAY ARRAY BEAM

Signal Power Loss (dB)

FIGURE III-6

SIGNAL ATTENUATION BY THE STANDARD FILTER APPLIED
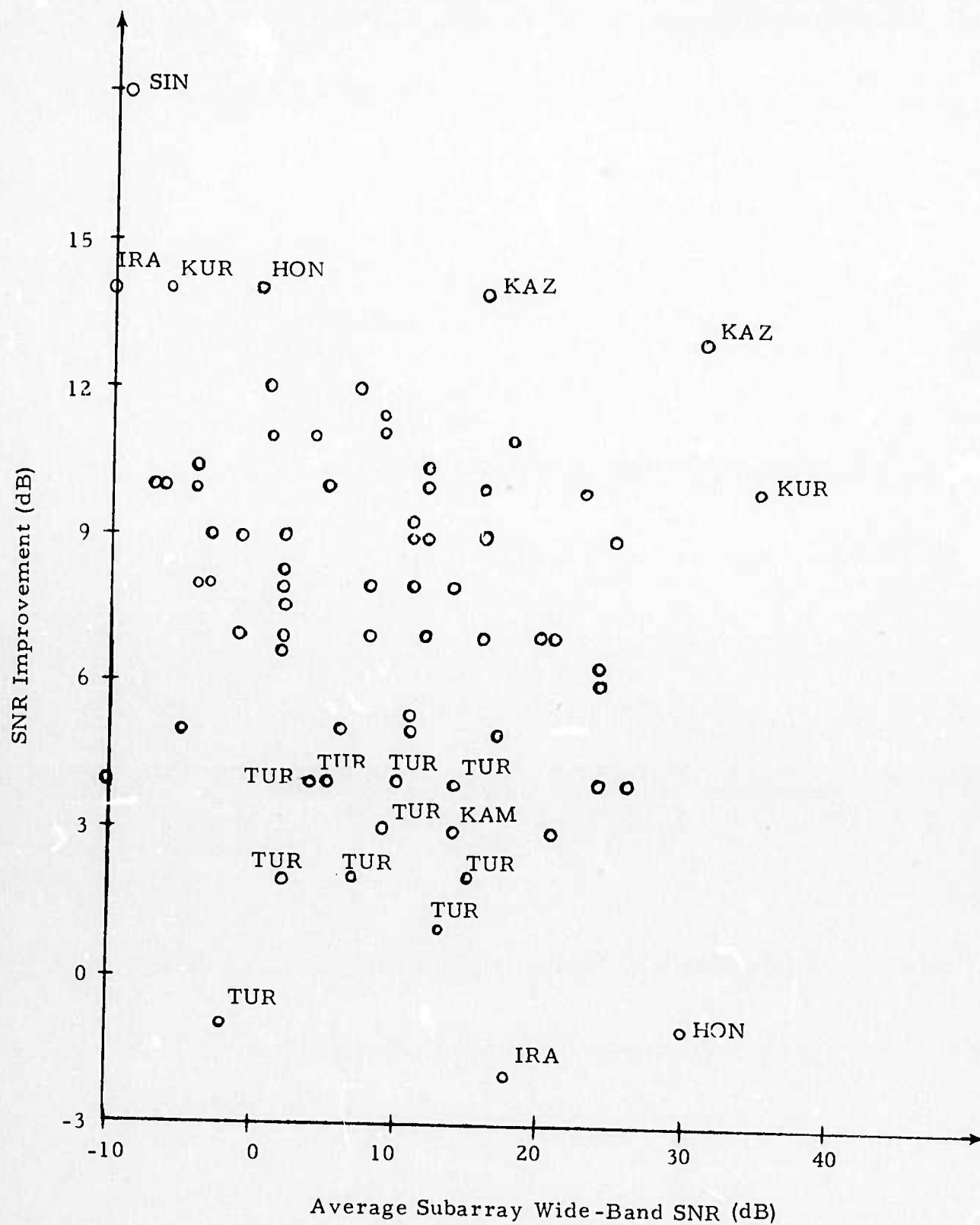TO THE ADJUSTED-DELAY ARRAY BEAM

SNR Improvement (dB)

SIN

15

IRA   KUR   HON   KAZ

KAZ

12

KUR

9

6

TUR   TUR   TUR   TUR

TUR   KAM

3

TUR   TUR   TUR

TUR

0

TUR

HON

IRA

-3

-10   0   10   20   30   40

Average Subarray Wide-Band SNR (dB)

FIGURE III-7

SNR IMPROVEMENT ACHIEVED BY THE STANDARD FILTER ON
THE SUBARRAY LEVEL AS A FUNCTION OF EVENT SNR

SECTION IV
NORSAR TELESEISMIC DETECTION CAPABILITY

A.   ESTIMATE OF THE NORSAR m_b DETECTION THRESHOLD

A study was carried out to determine the detectability of tele-
seismic P- waves using the NORSAR short-period array. The adjusted-delay
array beam was used for P- wave detection. In almost all cases where event
magnitude was below 4.5, a "standard" filter was used (See Figure III-1).
The procedure leading to the selection of this filter was outlined in Special
Report No. 6.

The data base used in this study consisted of a total of 344 events.
The 106 events listed in Special Report No. 6 were supplemented with 238 addi-
tional events listed in Table I-1.

In order to make possible an unbiased estimation of the NORSAR
detection threshold, all events in this population that had been selected using
the NORSAR seismic bulletin as a source were eliminated. Also deleted were
events reported in the bulletin from the International Seismic Month (ISM) where
NORSAR had been listed as the primary source.

We thus arrived at a data base consisting of 303 events from
Eurasia. This population should be a representative set of seismic events from
the Eurasian Continent, including Europe and the Mediterranean all of Continental
Asia and the Kamchatka-Kuriles-Japan arc. The Philippines Islands' region is not
included and only a few Japan events are present. Our event population includes

relatively too many high magnitude events, but this bias will of course not influence our estimate of the NORSAR incremental detection threshold.

The data base was divided into two subsets. 121 events from the Japan-Kuriles-Kamchatka arc (called Japan region) and 182 events from all other regions in Eurasia (called Continental Eurasia). A further regional sub-division would be desirable, but our limited event population so far does not permit this.

Of the 121 events in the Japan region a total of 26 events ranging in body-wave magnitude from 3.3 to 4.4 were not detected by NORSAR. Figure IV-1 is a histogram representing the magnitude distribution of Japan region events processed and indicating how many of these were not detected.

Of the 182 events in Continental Eurasia, a total of 12 events between m_b = 3.3 and 4.8 were not detected by NORSAR. The one event of m_b = 4.8 (ITA 035/04N) not detected may possibly have been assigned too high a magnitude, since only one USCGS station reported a signal amplitude for this event. This station (LOR) averaged 0.7 m_b units higher than the PDE m_b for other Italy events. Figure IV-2 is a histogram representing the magnitude distribution and detection status for events within Continental Eurasia.

Figure IV-3 shows a plot of the detected/not detected status for events from Continental Eurasia of magnitude less than 4.7. There is no def-inite trend towards lower detectability for greater epicentral distance, but our population of small events is scarce above 40 degrees distance. It is still interesting to note the good detection performance between 35 and 55 degrees; most of the events in this group are from Central Asia.

An estimate of the incremental detection probability for the NORSAR array was derived from Figure IV-4 . To stabilize the pictures for
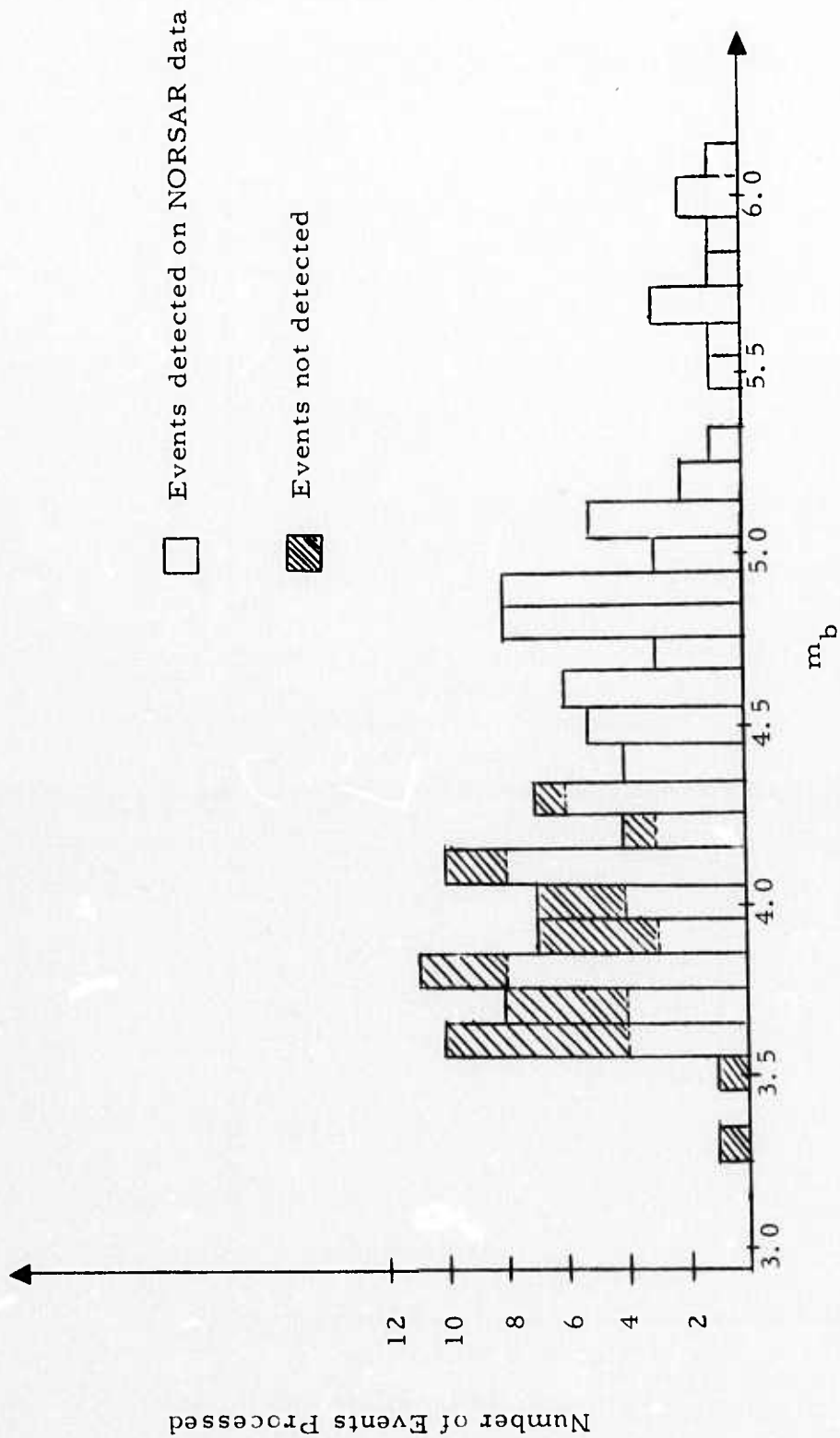
FIGURE IV-1

HISTOGRAM OF P-WAVES PROCESSED AND
DETECTED BY THE NORSAR ARRAY FOR
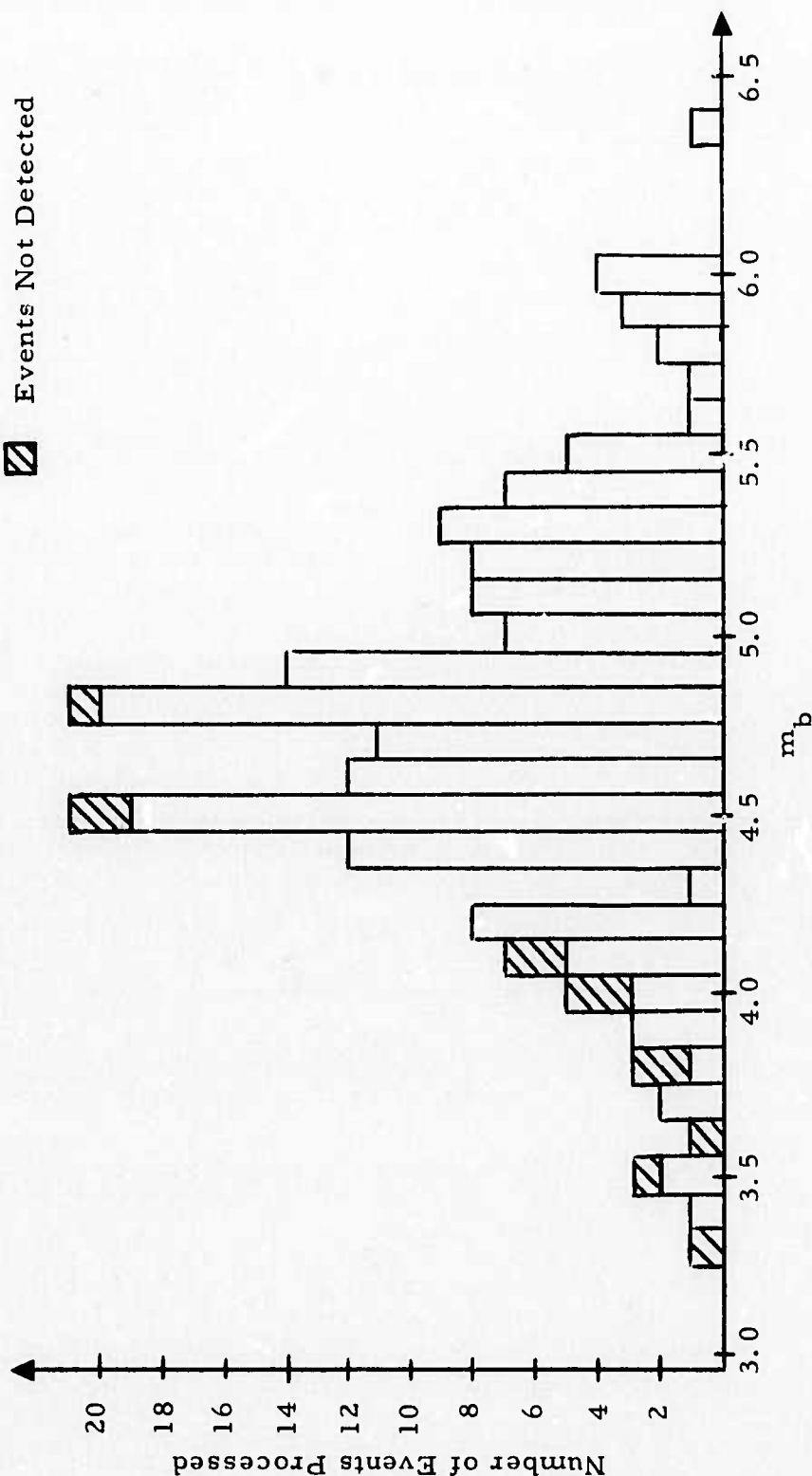THE JAPAN-KAMCHATKA REGION

IV-3

FIGURE IV-2

HISTOGRAM OF P-WAVES PROCESSED AND DETECTED BY
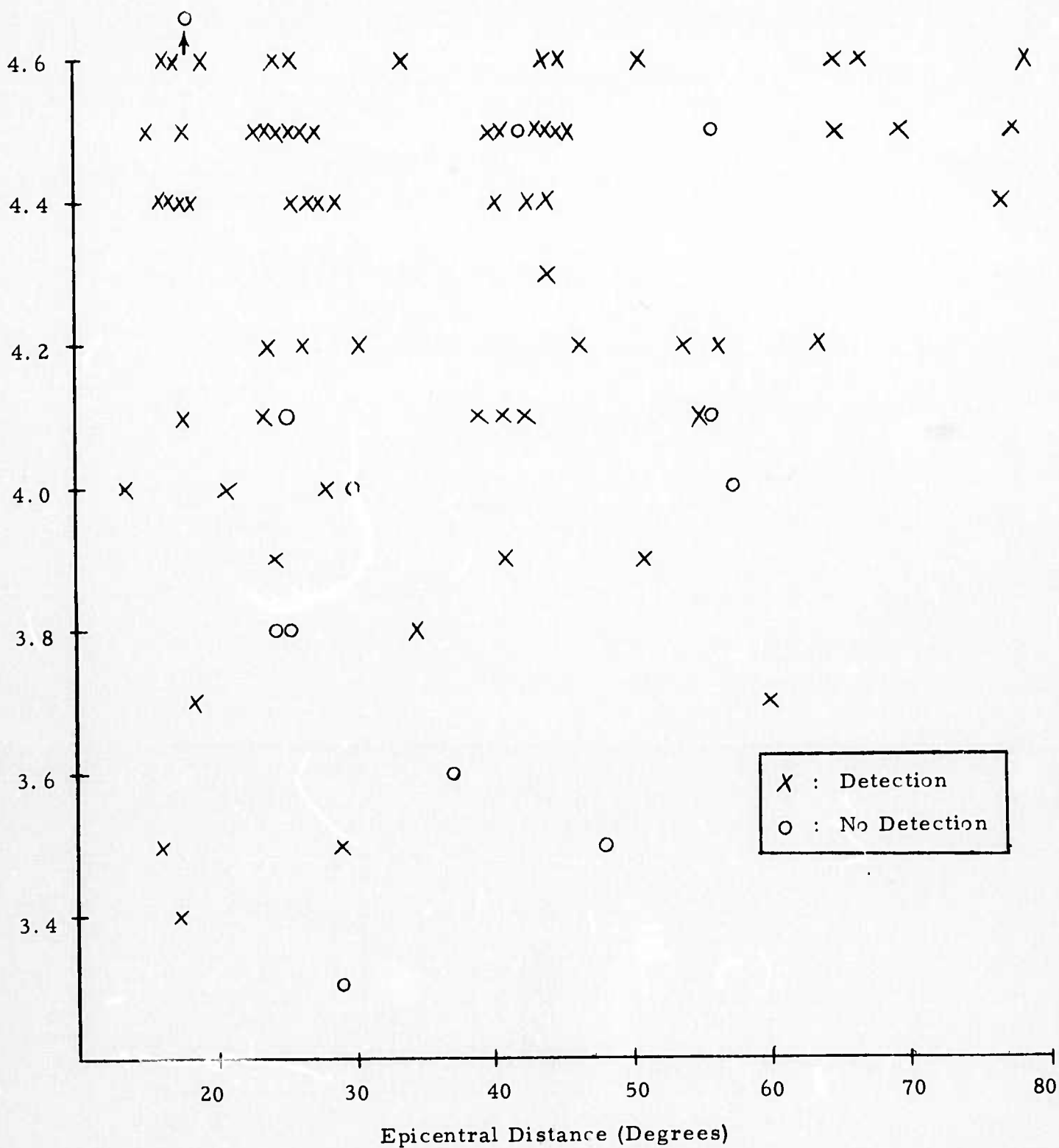THE NORSAR ARRAY FOR EURASIA APART FROM THE
JAPAN-KAMCHATKA REGION

FIGURE IV-3

NORSAR P-WAVE DETECTIONS/MISSES
VS. m_b AND EPICENTRAL DISTANCE
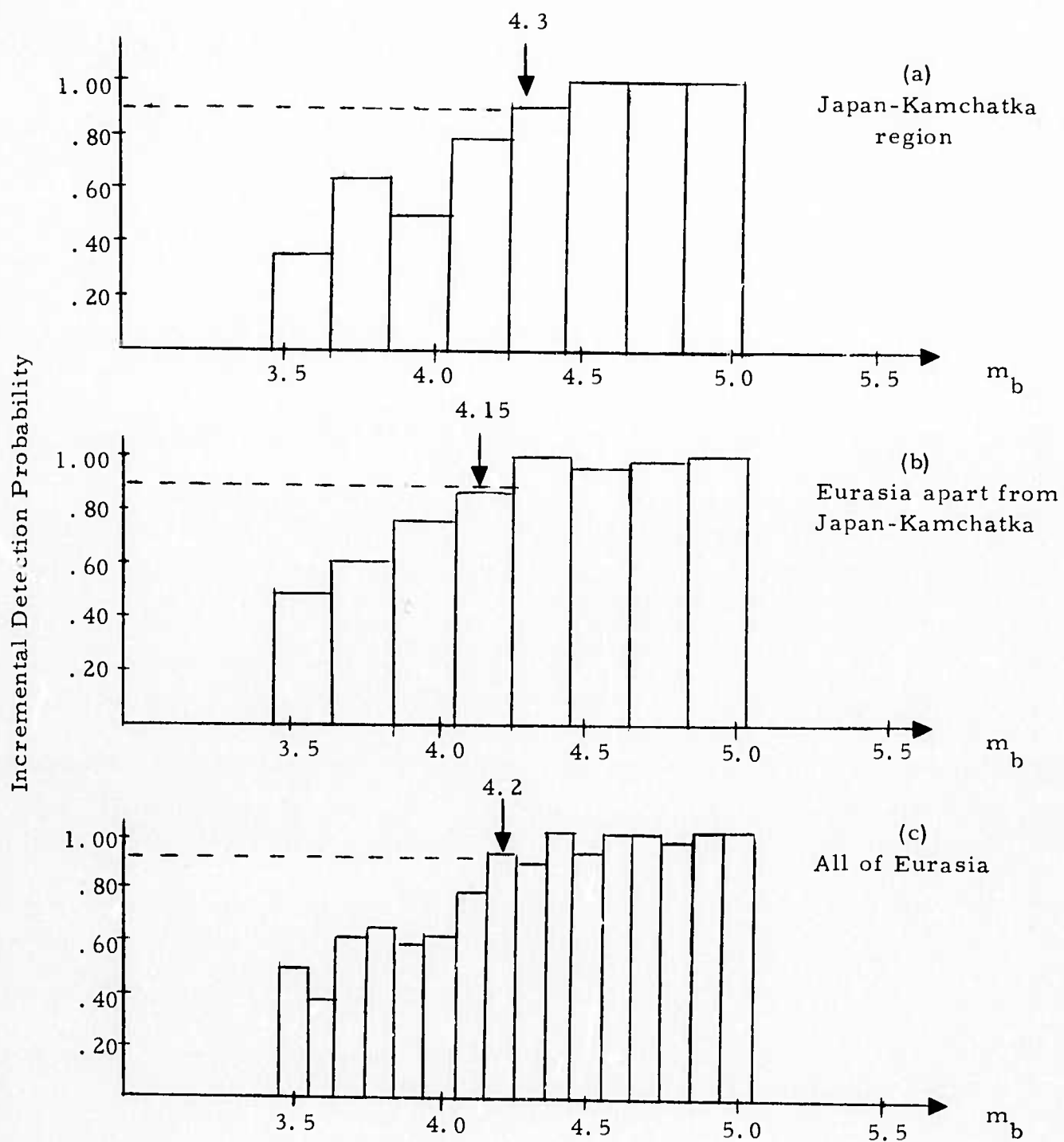(EURASIA APART FROM JAPAN-KAMCHATKA)

IV-5

FIGURE IV-4

INCREMENTAL DETECTION PROBABILITY OF THE NORSAR ARRAY

the two subregions individually, the events were grouped in steps of 0.2 magnitude units. The detection probability in each bin is the ratio of the number of events detected to the total number of events processed. It appears that the 90% incremental detection level is around m_b = 4.3 for the Japan-Kamchatka region and between m_b = 4.1 and 4.2 for the remainder of Eurasia. The histogram representing all events is somewhat more stable, and suggests a 90% incremental detection threshold near m_b = 4.2 for all of Eurasia.

The apparent discrepancy between this result and the m_b threshold of 4.3 - 4.4 suggested in Special Report No. 6 seem to be attributed to lack of data and also the fact that most of the low magnitude events were from the Japan-Kuriles-Kamchatka region where detection capability is somewhat poorer.

Our 90% m_b threshold of 4.2 agrees well with the corresponding LASA threshold of 3.9 considering that the NORSAR RMS noise levels through the standard filter is about a factor of 2 higher than those observed at LASA (Special Report No. 6); (Dean 1971). This accounts for a difference of about 0.3 m_b units in detection threshold between the two arrays.

Some qualifications still exist with respect to the above estimates First of all, the event population is still scarce, and should be expanded further. Notably more events of magnitudes 4.0 - 4.5 are needed. Secondly, all decisions regarding detection/no detection have been made by an analyst looking for a signal with a known source location and arrival time; thus the degradation inherent in an automatic detection system has not been a factor here.

B.   COMPARISON OF TI AND NORSAR DETECTION RATES

For the time period 1 January to 20 March 1972 a study was carried out to compare the number of events reported in the NORSAR seismic bulletin to the number of detections claimed by the TI analyst. A total of 122

events reported from PDE/LASA/ISM were available for this time period, 53 from the Japan to Kamchatka region and 69 from other parts of Eurasia. The results are presented in Table IV-1.

It appears that the NORSAR bulletin reported almost all detectable events of magnitude greater than 4.2 for the Japan region , while several events up to magnitude 4.6 from other parts of Eurasia were missed. Some reservations must be made due to the scarcity of events from the Japan region, but our data still reflects the excellent beam coverage of this area for the NORSAR on-line Detection Processor.

Several low magnitude events have not been reported in the NORSAR bulletin, this is in part due to a conservative acceptance threshold for the NORSAR Event Processor at the time, but may also reflect the inherent limitations of an automatic event detector.

Based on our analysis of NORSAR data so far, it is possible to establish a simple theoretical model for the NORSAR detection capability and to give tentative estimates of the parameters as follows:

For an arbitrary earthquake of PDE/LASA body-wave magnitude m, NORSAR can be expected to see this signal as a magnitude m_N event where m_N is sampled from a Gaussian distribution with mean $m - \Delta$ and standard deviation σ_1 . (e.g. for the Japan to Kamchatka region, $\Delta \approx 0.2$ and $\sigma_1 \approx 0.3$ according to subsection II-E).

Whether or not an event is detected at NORSAR is dependent upon noise level and processing losses. In Special Report No. 6 the average RMS filtered array beam noise was found to be 0.12 $m\mu$, and a tentative standard deviation is 2 dB. Signal attenuation by the standard filter varies considerably; values from 1 to 7 dB are typical for teleseismic region. If signal-to-noise ratio (SNR) required for detection is set at 11 dB (which is consistent

TABLE IV-1

COMPARISON OF THE NORSAR SEISMIC BULLETIN TO EVENTS VERIFIED BY TI USING NORSAR DATA

Magnitude Bracket	Japan-Kamchatka Arc			Remainder of Eurasia		
	Total Events	TI Detection	NORSAR Bulletin	Total Events	TI Detection	NORSAR Bulletin
3.3 - 3.4	1	0	0	1	0	0
3.5 - 3.6	6	2	0	2	1	0
3.7 - 3.8	11	8	3	3	3	0
3.9 - 4.0	10	6	3	6	6	3
4.1 - 4.2	8	6	4	9	8	3
4.3 - 4.4	3	3	3	8	8	4
4.5 - 4.6	5	5	4	12	11	7
4.7 - 4.8	5	5	5	12	11	11
4.9 -	4	4	4	16	16	15

with the NORSAR detection processor), we find that the smallest signal generally detectable on an unfiltered array beam has a RMS value of 0.7 mμ or a peak-to-peak amplitude of 2 mμ. At a 65 degrees range this corresponds to an earthquake of NORSAR magnitude of approximately 3.75 if a period of 1.0 seconds is assumed. This limiting magnitude m_L varies with background noise and as a function of system loss, and we will assume that it follows a Gaussian distribution with expectation m_0 and standard deviation σ_0. Values of $m_0 \approx 3.75$ for the Japan-Kamchatka region and $\sigma_0 \approx 0.2$ are suggested by the preceding considerations.

We are now able to formulate the probability of NORSAR detecting an event of PDE/LASA magnitude m as follows:

$$\text{Pr (Detect m)} = \text{Pr}(m_N \geq m_L) = \Phi \left(-\frac{m - \Delta - m_0}{\sigma} \right)$$

$$\text{where } \sigma^2 = \sigma_1^2 + \sigma_0^2$$

since $(m_N - m_L)$ is Gaussian with expectation $(m - \Delta - m_0)$ and standard deviation σ. Φ denotes here the cumulative normal distribution function.

The detectability curve with the above parameters for the Japan-Kamchatka area is sketched in Figure IV-5. It is seen to agree reasonably well with the observed detection rates shown in Figure IV-4, although the 90% detection level is slightly higher (around 4.4) for the theoretical curve.

The above model may be used for estimating the total number of detections N by the NORSAR array for a given seismic region, using the

Probability of Detection (Incremental)

1.0

90%

.8

.6

50%

.4

.2
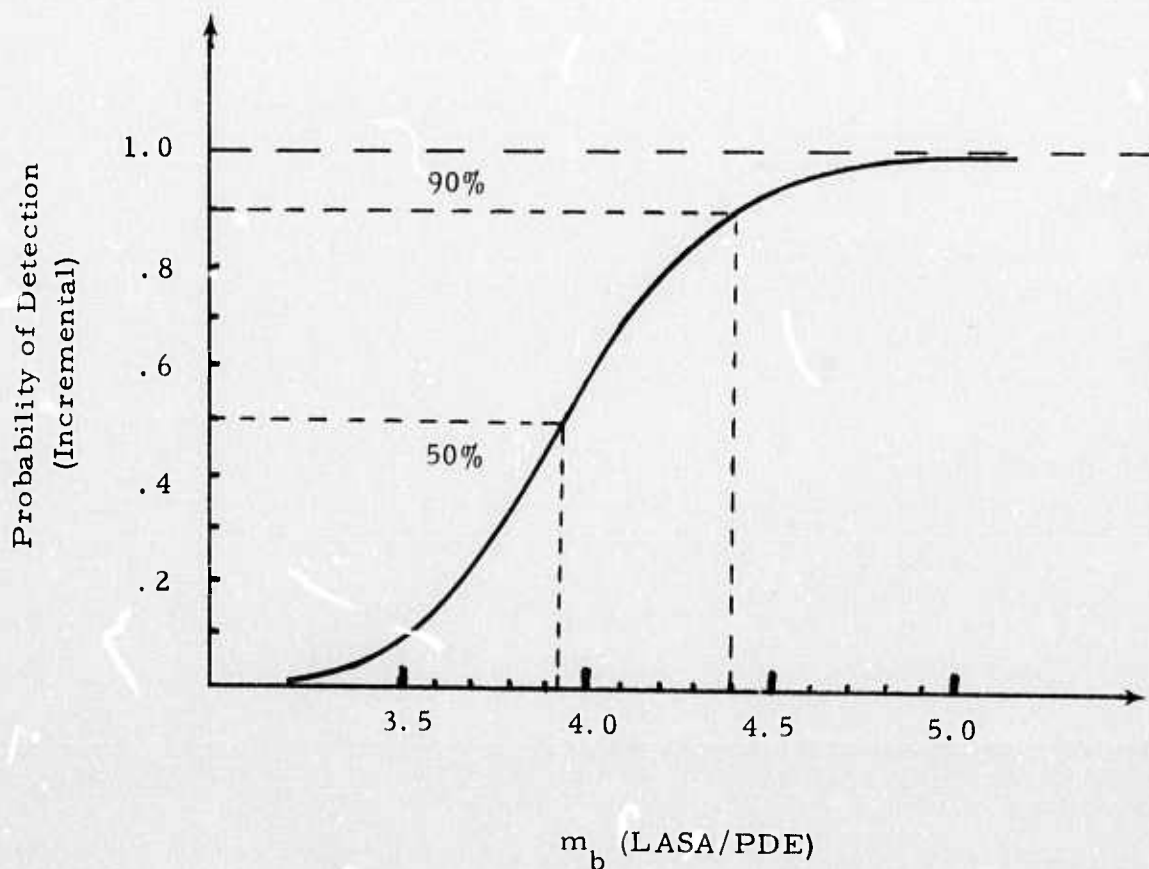
3.5   4.0   4.5   5.0

m_b (LASA/PDE)

FIGURE IV-5

EXPECTED DETECTION CAPABILITY OF THE NORSAR ARRAY
FOR THE JAPAN-TO-KAMCHATKA REGION BASED ON
MEASURED SEISMIC NOISE LEVEL
AND PROCESSING LOSSES

IV-11

standard seismicity formula for the cumulative number N_c of earthquakes above a given magnitude m:

$$\log N_c = a - b \, m$$

N is then determined by

$$N = \int_{-\infty}^{\infty} \frac{dN_c}{dm} \; \Phi \left(\frac{m - \Delta \cdot m_0}{\sigma} \right) \, dm$$

which yields

$$\log N = a - b \, (m_0 + \Delta) + \frac{b^2 \sigma^2}{2} \ln 10$$

Values of a = 6.85 and b = 1.04 for the year 1965 have been obtained by Evernden (1970) for the Kamchatka/Kuriles region of the USSR. Based on this our estimate of the NORSAR optimum detection capability for this area becomes approximately 800 events annually. Of course some uncertainty in this number is caused by variable seismicity from year to year. Apart from this, one significant possible error source is our estimate of the 50% incremental detection threshold $m_0 + \Delta$. An error of 0.1 in this estimate will cause our estimate of N to be wrong by 20-25%.

The model developed here does not apply directly to the general Eurasian region since distance factors vary greatly when near regional events are included and also the NORSAR magnitude bias seems to show a significant regional dependence. More data will be needed to analyze theoretical detection capability for the remainder of Eurasia on a regional basis.

SECTION V
SHORT - PERIOD DISCRIMINATION

A.   DEFINITION OF DISCRIMINANTS

1.   P30 Mean Square

This discriminant, which is a measure of event complexity, is computed by crosscorrelating 4 sec of the waveform (beginning a few points before P-wave onset) with the next 30 seconds of the waveform and with the noise preceding the signal. A mean square, weighted by the lag, is then computed from the correlations over both 30 seconds of the noise and 30 seconds of the signal. The noise mean square is subtracted from the signal mean square to obtain the discriminant used (Texas Instruments Incorporated, 1971).

2.   Autocorrelation Mean Square

This discriminant is also a measure of complexity. The autocorrelations of a 30-second noise gate and of a 30-second signal gate are computed and a weighted mean square then derived from these correlations for the noise and signal. The discriminant is derived from the signal mean square minus the noise mean.

3.   Envelope Difference

This discriminant is also derived from the P30 correlation by computing the mean-square difference between the envelope correlation and a fixed decaying exponential, the decay rate of which is the average rate for an ensemble of 16 explosions recorded at LASA. As with the first two statistics, envelope difference is a measure of complexity.

4.   Dominant Period

This discriminant is computed by finding the cycle in the wave-
form with the maximum absolute amplitude; the dominant period is the duration
of this cycle in seconds.   This parameter can be estimated with some confidence,
even for events with a relatively low signal-to-noise ratio.   The dominant period
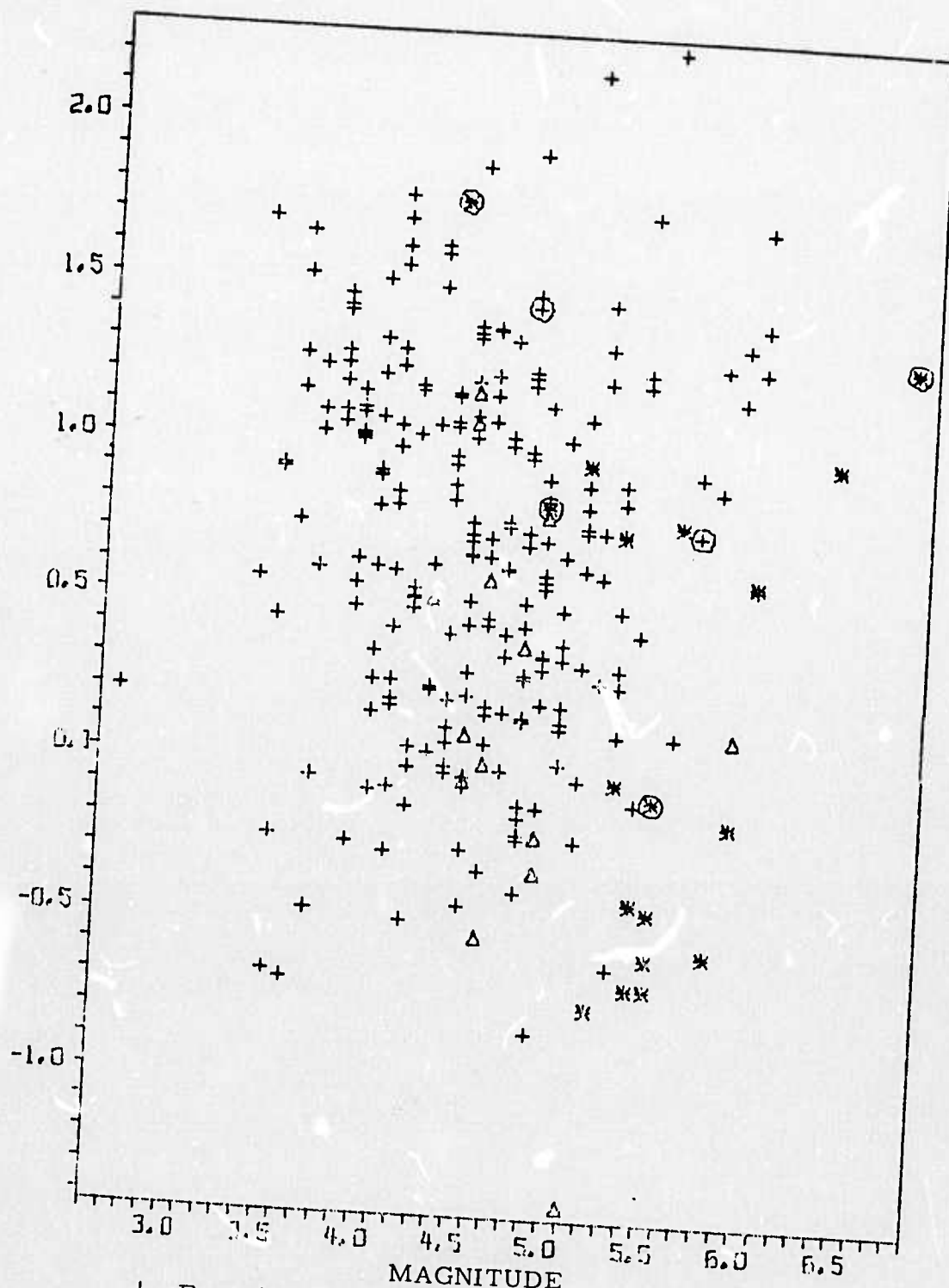discriminant is a rough measure of spectral energy distribution.

5.   Spectral Ratio

This discriminant is derived from the signal power spectrum
over a gate beginning just before the signal arrival.   The power spectrum is
smoothed over three frequency points, and the power in three bands is com-
puted; Band 1: 0. - 0.55 Hz; Band 2: 0.55 - 1.5 Hz; Band 3: 1.5 - 5.0 Hz.
These bands have been selected based on NORSAR data.   Spectral ratios
computed were Band 3 to Band 2 and Band 3 to Band 1 respectively.

The spectral ratio that seems to produce the best separation
for LASA data, (0.35-0.85Hz to 1.45-1.85Hz) also was computed for each event,
but did not appear to be as effective for NORSAR data.

B.   NORSAR SHORT-PERIOD DISCRIMINATION RESULTS

Short period discriminant values for the discriminants defined
in V A are plotted as a function of body-wave magnitude for a total of 269 events
in Figures V-1 to V-12.   Shallow earthquakes and earthquakes of unknown depth
are represented by a cross.   Deep earthquakes (of depths greater than 100 km)
are denoted by a triangle.   Presumed explosions are indicated by an asterisk.
Events from the Western Hemisphere are surrounded by a circle.

FIGURE V-1

REFERENCE SUBARRAY P30 MEAN SQUARE DISCRIMINANT

V-3
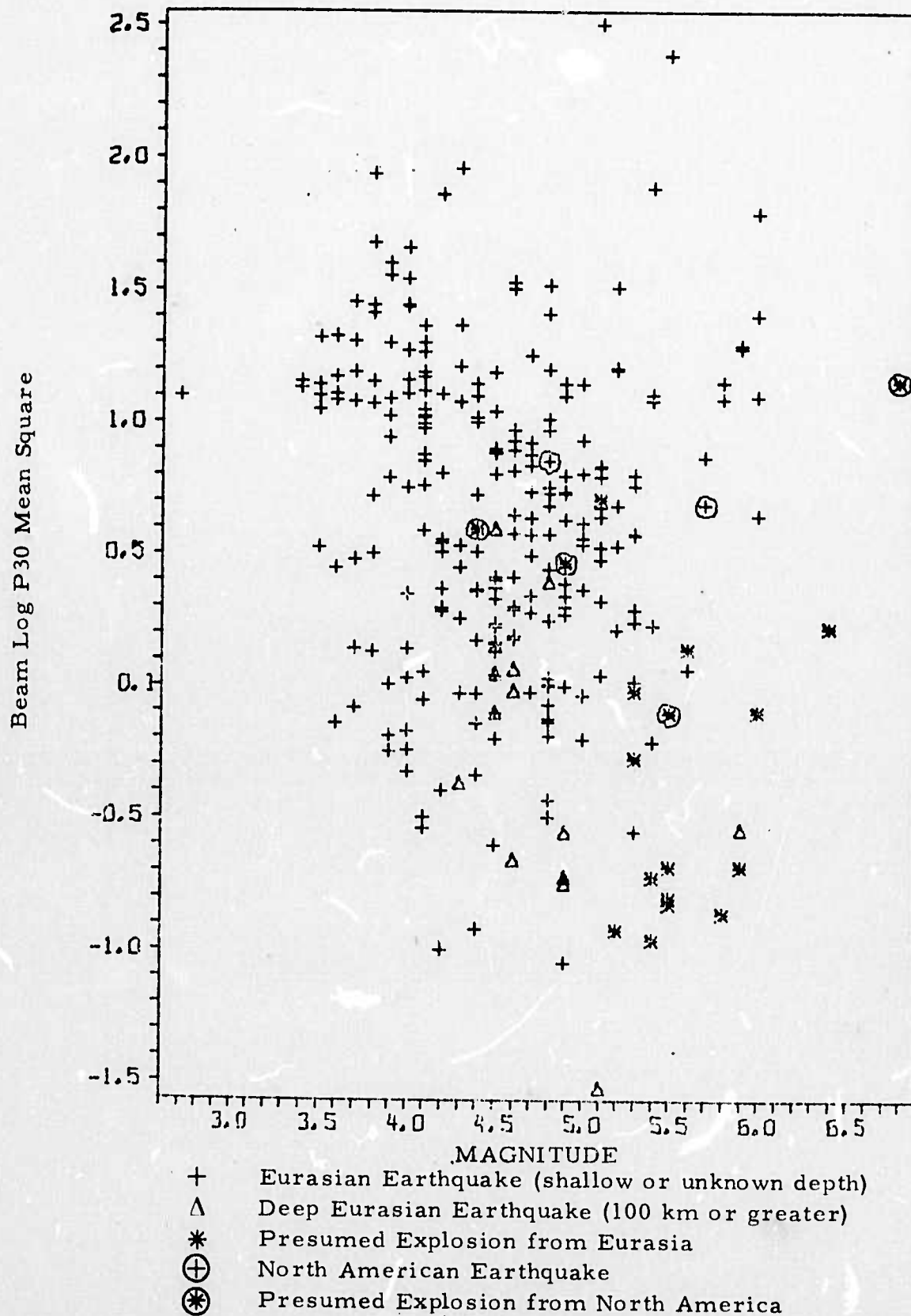
FIGURE V-2

ADJUSTED-DELAY BEAM P30 MEAN SQUARE DISCRIMINANT

V-4

FIGURE V-3

REFERENCE AUTOCORRELATION MEAN SQUARE

V-5

FIGURE V-4

ADJUSTED-DELAY BEAM AUTOCORRELATION MEAN SQUARE

V-6

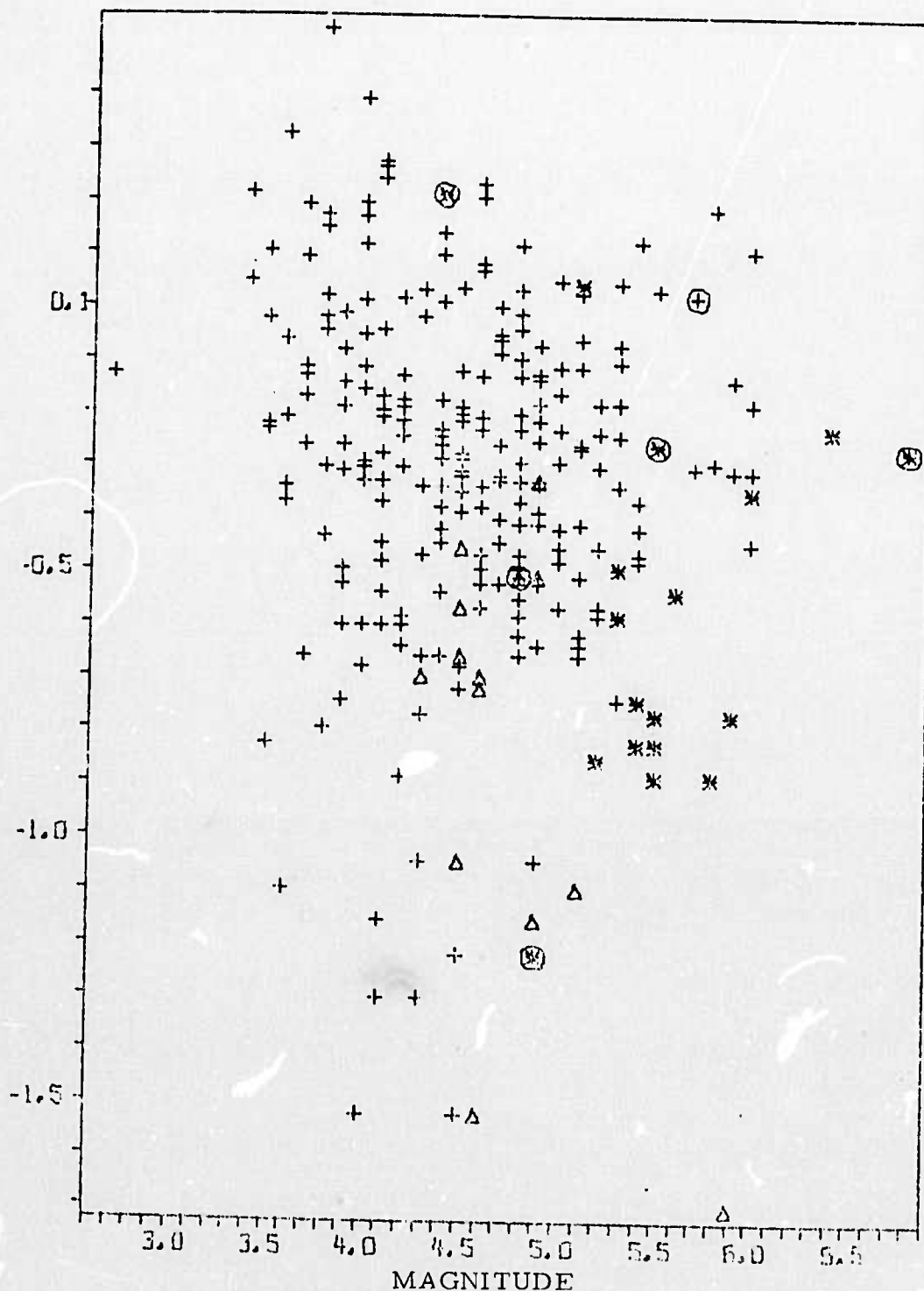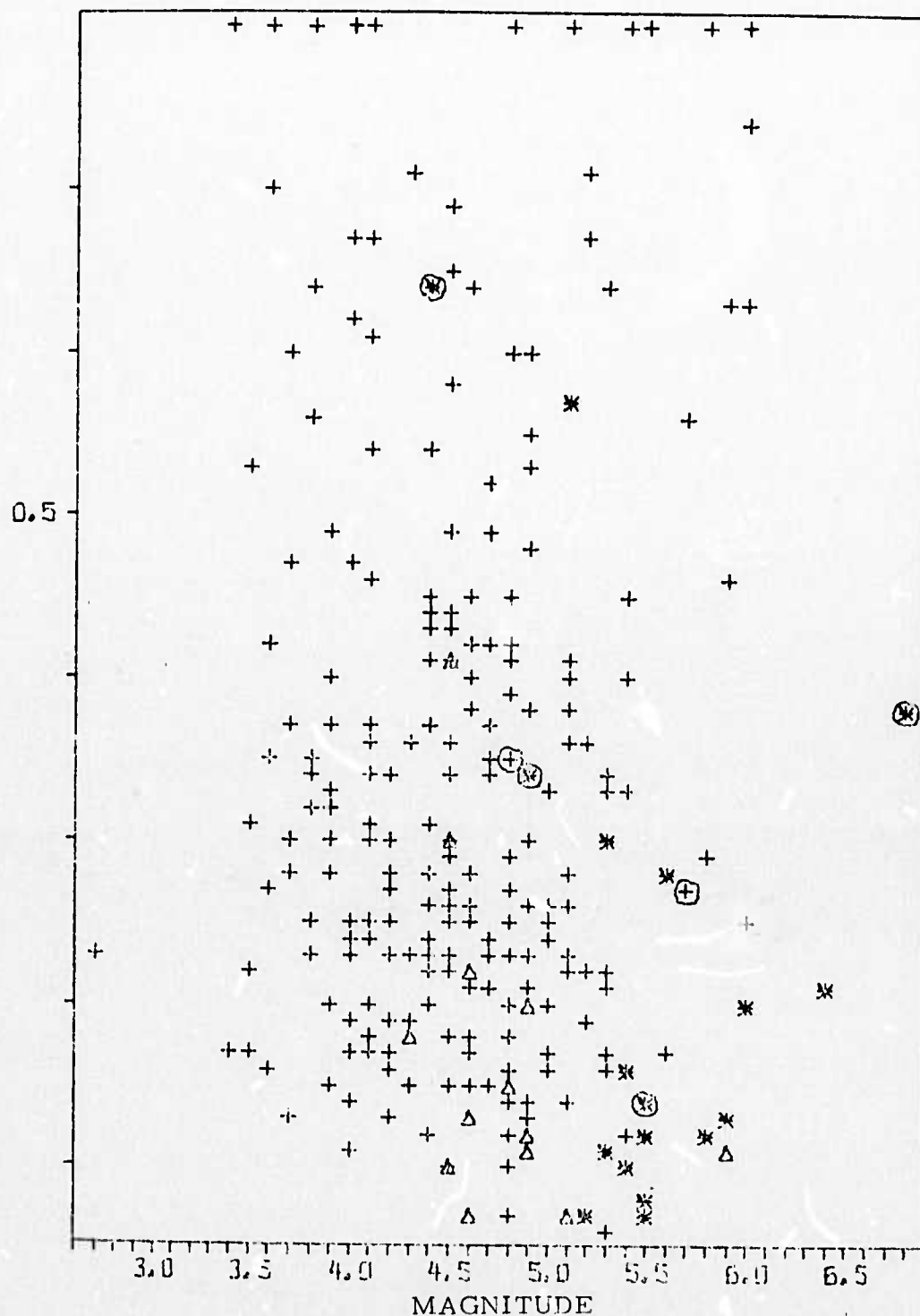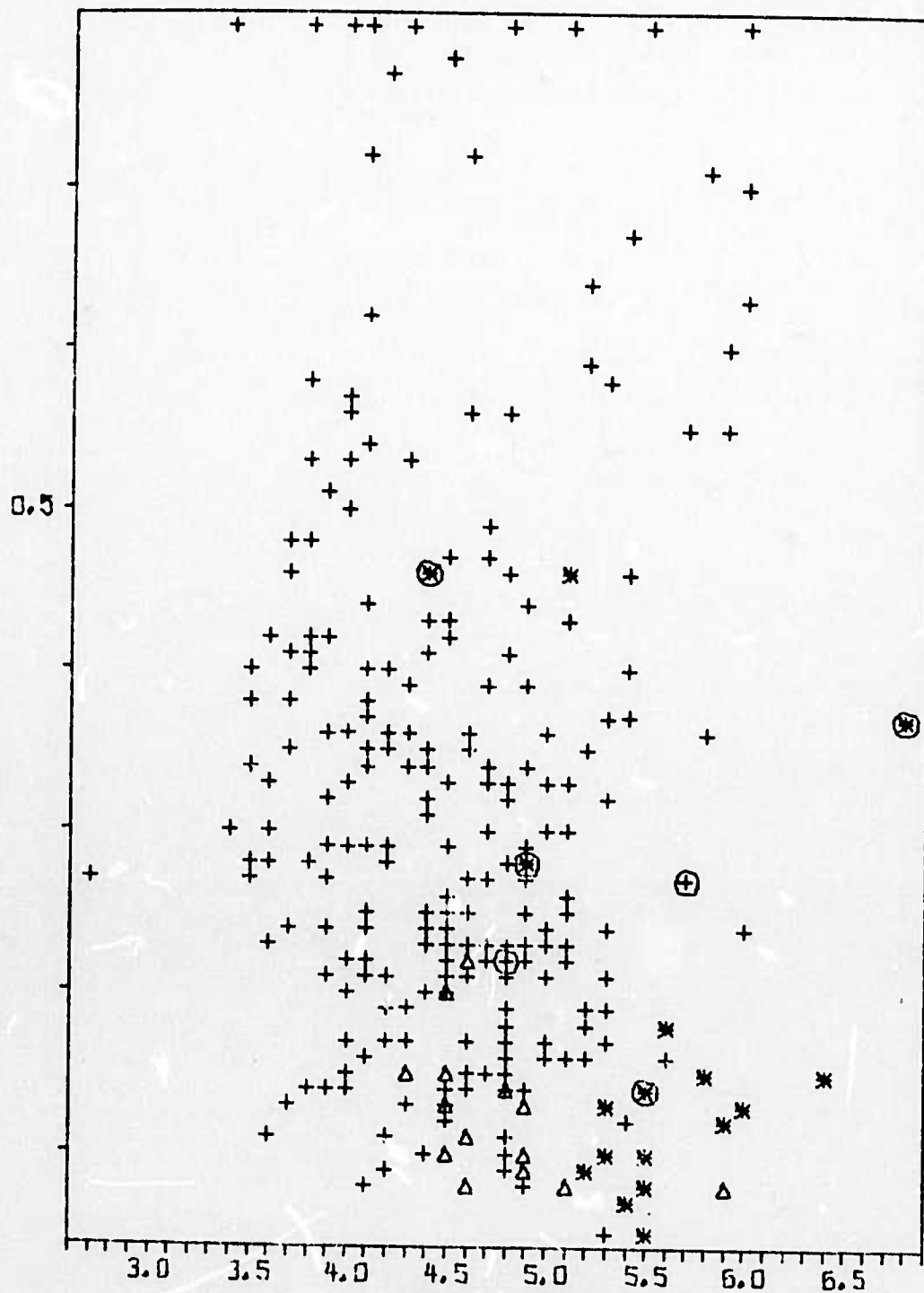Reference Envelope Difference (Counts Squared)

MAGNITUDE
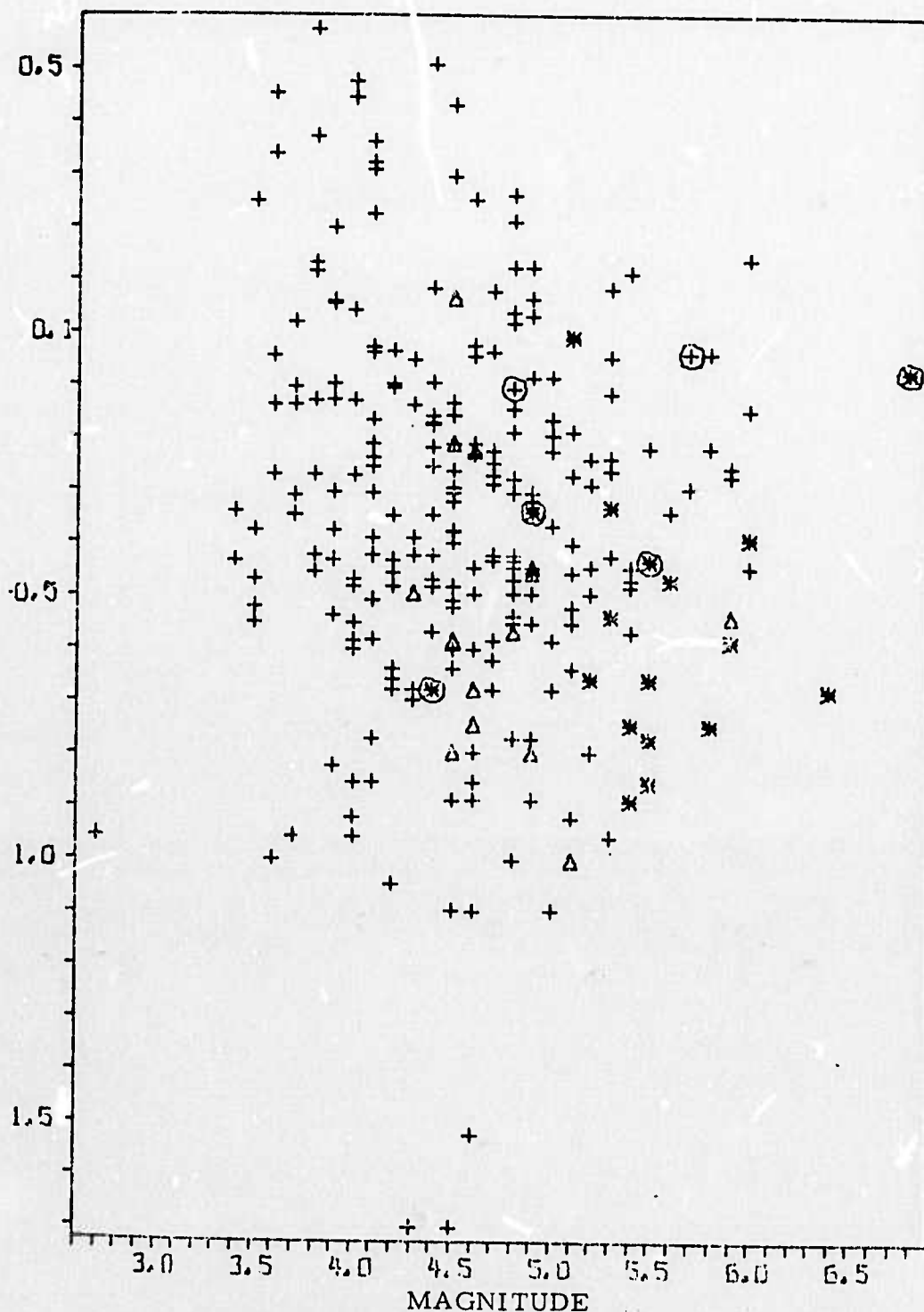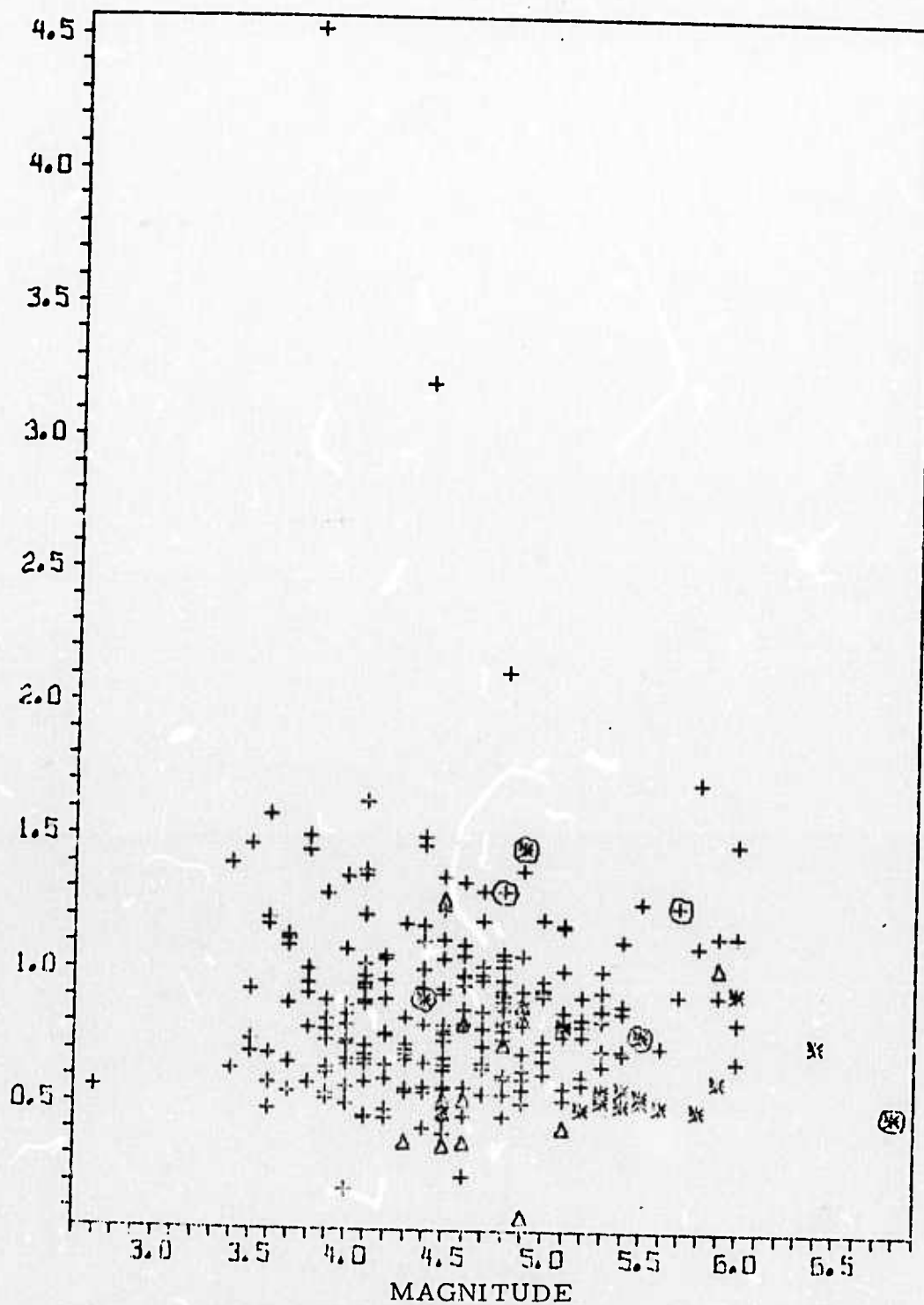
+   Eurasian Earthquake (shallow or unknown depth)

Λ   Deep Eurasian Earthquake (100 km or greater)

✳   Presumed Explosion from Eurasia

⊕   North American Earthquake

⊛   Presumed Explosion from North America

FIGURE V-5

REFERENCE ENVELOPE DIFFERENCE (COUNTS SQUARED)

FIGURE V-6

ADJUSTED-DELAY BEAM ENVELOPE DIFFERENCE (COUNTS SQUARED)

V-8

FIGURE V-7

REFERENCE DOMINANT PERIOD (SECONDS)

V-9

FIGURE V-8

ADJUSTED-DELAY BEAM DOMINANT PERIOD (SECONDS)

V-10

FIGURE V-9

REFERENCE SPECTRAL RATIO [(1.5-5)/(0-0.55)] (dB)

V-11

FIGURE V-10

ADJUSTED-DELAY BEAM SPECTRAL RATIO

$[(1.5-5)/(0-0.55)]$ (dB)

FIGURE V-11

REFERENCE SPECTRAL RATIO

$[(1.5-5)/(0.55-1.5)]$ (dB)

FIGURE V-12

ADJUSTED-DELAY BEAM SPECTRAL RATIO

$[(1.5-5)/(0.55-1.5)]$ (dB)

V-14

As was observed in Special Report No. 6, the discriminants appear to be not very effective for deep earthquakes. In particular this applies to the autocorrelation and envelope difference criteria, while the spectral ratio discriminants seem to perform better in this case. Also, it is evident that presumed explosions from the Western Hemisphere do not follow the same patterns as Eurasian ones, thus we will confine the remainder of this section to the discussion of NORSAR short period discriminants applied to Eurasian events.

A comparison between the corresponding plots for the discriminants applied to the reference subarray beam versus the adjusted delay array beam reveals that the array beam yields consistently as good or better separation between Eurasian earthquakes and presumed explosions. Table V-1 was compiled by visually inspecting the plots shown and listing all "difficult" events of magnitude 5.0 and greater, i.e., events that would appear to be within the wrong population by at least one of the criteria applied to the array beam.

It is seen from Table V-1 that the classification of an event may vary considerably from one discriminant to the other . The presumed explosions that appeared to be most difficult to classify were from Western Russia. WRS/277/10N and WRS/295/10N. These two events both had complex waveforms and significant energy content below 1.5 Hz. Only the spectral ratio criterion that compared high frequency energy to very low frequency energy was able to classify these events properly.

One deep earthquake, KUR/099/15N, consistently behaved as an explosion with respect to all the discriminants. One other deep earthquake, TAL/271/14N, and one shallow earthquake KM1/073/12N, were misclassified by the signal complexity criteria, but behaved normally with respect to the spectral content discriminants. The three remaining "difficult" earthquakes were misclassified by only one of the six discriminants.

TABLE V-1

EFFECTIVENESS OF VARIOUS SP DISCRIMINATION CRITERIA FOR SELECTED EVENTS RECORDED AT NORSAR

EVENT	DEPTH	m_B	BEAM LOG P 30	BEAM LOG AUTO	BEAM ENV DIFF	BEAM PERIOD	SP. RATIO 1.5-5/0-.55	SP. RATIO 1.5-5/.55-1.5
PRESUMED EXPLOSIONS								
WRS/277/10N	13	5.1	Q+	Q+	Q+	Q	E+	Q
WRS/295/05N	0	5.3	Q	Q	ND	Q+	E+	Q+
KAZ/181/04N	0	5.4	E+	E	E+	E+	ND	Q+
URA/082/06N	0	5.6	Q	ND	ND	E+	E+	E+
KAZ/356/06N	0	6.0	E	O	E+	E+	ND	E
EARTHQUAKES								
KUR/099/15N	126	5.1	E+	E+	E	E+	E	E+
KM1/073/12N	35	5.3	ND	E	E+	Q	ND	Q
TIB/123/00N	16	5.4	ND	Q+	E	Q+	Q+	Q
KUR/213/02N	20	5.6	Q	Q+	ND	Q	E	ND
TAL/271/14N	169	5.9	E+	E+	E+	Q+	Q+	Q+
KUR/252/23N	7	6.0	Q	ND	ND	E	Q+	Q

E+ (Q+) Definitely within explosion (earthquake) population

E (Q) Appears to be within explosion (earthquake) population

ND Borderline case, no decision made.

It appears from our data that the discriminants based on spectral contents generally separate better between earthquakes and presumed explosions than the discriminants based on waveform complexity. However some kind of a multivariate criterion would probably give the most reliable performance. For example, selecting all events that definitely belong to the presumed explosion population for at least one of the spectral contents discriminants (code E + in Table V-1) would cause all the 14 Eurasian presumed explosions to be included, while only 1 of the 51 Eurasian earthquakes of magnitude 5.0 and greater would satisfy the criterion. This one earthquake is KUR/099/15N of depth 126km.

More data from presumed explosions of magnitudes below 5.0 is needed to determine the capabilities of short period discriminants applied to low magnitude events and to determine what kind of multivariate discriminants would be most effective on NORSAR data.

A comparison between the performance of these Short Period discriminants and the three combined Short Period-Long Period discriminants ($Ms - m_b$, $AR - m_b$, $AL - m_b$) described in Special Report No. 5 was carried out. However, only 49 events, 8 of which are presumed explosions, have been processed in common for the SP and LP evaluation programs, thus our present data is sufficient only to yield a tentative indication of the relative efficiency of the two types of criteria. Of the eleven "difficult" events listed in Table 3, three had been selected for LP discrimination; KAZ/356/06N, TIB/123/00N and KUR/213/02N. All of these events were very clearly assigned to the proper category by the three SP-LP discriminants. In fact no event in our limited common population failed any of the combined SP-LP discrimination criteria, but one event appeared to be a borderline decision, BLS/210/19N. This presumed earthquake of $m_b = 4.5$ had a surface wave magnitude of $M_s = 2.5$.

However, all our short period discriminants placed this event definitely in the earthquake population.

As expected these preliminary data indicate that the Long Period discriminants yield better separation between earthquakes and presumed explosions than our Short Period criteria. The question of to what degree SP discriminants can supplement LP criteria when those fail cannot be fully answered from our present data base. Future efforts will be directed towards increasing the number of common events for SP and LP discrimination, as well as extending the total data base for discrimination studies.

SECTION VI
CONCLUSIONS AND FUTURE PLANS

A.   CONCLUSIONS

Conclusions about the performance of the short period NORSAR array, based on analysis of more than 300 signals (primarily from Eurasia) are given below.

Data quality is excellent. For about one-half of the samples all 132 sensors were operational. The worst data loss encountered was 24 sensors. For six events spikes were found in the data, but these events could still be processed. Phase reversals were observed for a few seismometers during parts of 1971, but this problem had been corrected for 1972 data.

Major conclusions from the signal analysis are:

- Amplitude variations across the subarrays are generally large (typically 4:1) and show strong dependance upon source region. However, within narrow regions a high degree of consistency is seen, and it appears that most of the amplitude variations may be explained by scattering effects due to the irregular structure of the Mohorovicic discontinuity underneath the NORSAR array.

- Time delay anomalies (deviation from plane wave propagation along the great circle path) are significant between subarrays, but a consistent set of anomalies can in general be obtained

for events of epicentral distance greater than 30 degrees from NORSAR. Part of the observed anomalies, but not all, can be explained from the variations in depth of the Moho below NORSAR.

- For certain close-in events, notably events from Italy, low and high frequency signal energy appear to follow different paths; the 0.5 Hz energy arriving at NORSAR 1 - 2 seconds before the 1 Hz energy. Significant differences were found in this case between time delay anomalies for the low and high frequency signal bands.

- Considerable variation in regional signal characteristics has been observed. Signal waveform complexity showed the expected decrease with increasing distance, except for some high complexity events from Taiwan and South Kamchatka. Signal spectral contents was more unpredictable, with low frequency signals being observed mainly from Italy, Turkey, Kirgiz and Taiwan while Greece, Tadzhik and Kurile Island events generally produced high frequency signals.

- Significant spread has been observed between LASA/PDE and NORSAR magnitudes (as measured by the TI analyst). NORSAR magnitudes are generally lower, with an average negative bias of 0.2 - 0.3 m_b units, and with a standard deviation of 0.3 around this bias.

The following conclusions were derived concerning array processing performance:

- Average wide band subarray beam-to-array beam SNR improvement was 10 dB, with 80 percent of all examined events having

VI-2

values between 9 and 12 dB. As expected, array gain is considerably lower for close-in events and presumed explosions with high dominant frequency.

- Average wide-band signal degradation from subarray to array level is 3 dB. Together with the 10 dB SNR improvement, this is consistent with the expected 13.4dB noise reduction for a 22-element array.

- Diversity stack array beamforming yielded an average improvement over the adjusted-delay array beam of 1.0 dB for unfiltered and 1.6 dB for filtered signals (standard filter).

- Compensating for time delay anomalies on the subarray level yielded an average of only 0.5 dB SNR improvement for three close-in events compared with plane wave subarray beams. Thus plane wave delays appear to be adequate on the subarray level.

- SNR improvement achieved with the standard filter averaged 7 dB, with values for individual events ranging from -4 to 16 dB. Significant regional dependence was seen in these numbers. Filter signal suppression averaged around 6 dB, and also showed a large variability between events.

Our conclusions concerning NORSAR detectability are:

- 90% incremental detection threshold is close to 4.2 for all of Eurasia combined, and slightly higher (4.3) for the Japan to Kamchatka arc.

- The number of events reported in the NORSAR seismic bulletin for January-March 1972 appears to be considerably lower than

would be expected from our analysis of NORSAR detectability. Presumably, this is due partly to conservative prethreshold for operation of the NORSAR Event Processor, partly to the inherent limitations of the automatic signal detector.

- A theoretical model based on NORSAR seismic noise level and processing losses seems to give detectability estimates which are consistent with our experimental results.

Conclusions with respect to short period discrimination are:

- Discriminants based on spectral energy distribution seem to be superior to discriminants based on the complexity of the signal waveform.

- No single discriminant was able to separate completely between presumed explosions and earthquakes. The best separation was obtained by considering the spectral ratio of energy in the bands 1.5 to 5.0 Hz and 0 - 0.55Hz, although reservations must be taken due to possible bias caused by the high signal-to-noise ratios for all events in the presumed explosion population.

- It appeared possible to improve separation significantly by considering a combination of discriminants. However, no formal multivariate model was established to determine an optimum criterion.

- A preliminary study of the performance of short period discriminants versus that of $M_s - m_b$ and other SP-LP discriminants gave the expected result that the latter ones in general produce a better separation between earthquakes and presumed explosions.

B.   FUTURE PLANS

Future NORSAR short period evaluation efforts will concentrate on increasing the ensemble of low and intermediate magnitude Eurasian events. As the event population increases, more emphasis will be laid upon obtaining regional estimates of signal processing losses, time delay and amplitude anomalies and detection thresholds.   Regional signal characteristics will be investigated in further detail.

The effects on array gain from eliminating subarrays that give consistently low signal amplitudes for certain regions will be investigated.

Measurements of short period discriminants will be updated, and more investigation will be performed to find the optimum bands for computing spectral ratio.   The possibilities of multivariate short period discrimination will be studied as well as the combination of short and long period discriminants.

SECTION VII
REFERENCES

Aki, K., 1973, Scattering of P Waves under the Montana LASA, Journal of Geophysical Research, 78, 1334-1345.

Barnard, T. E. and R. L. Whitelaw, 1972, Preliminary Evaluation of the Norwegian Short Period Array, Special Report No. 6, Extended Array Evaluation Program, Contract Number F33657-71-C-0843, Texas Instruments Incorporated, Dallas, Texas.

Dean, W. C., R. O. Ahner and E. F. Chiburis, 1971, Evaluation of the SAAC - LASA system, SAAC Special Report No. 1, AFTAC Contract Number F33657-71-C-0510.

Evernden, J. F., 1970, Study of Regional Seismicity and Associated Problems, Bulletin Seismological Society of America, 60, 393-446.

Eyres, J. S., F. R. Laun and W. H. Swindell, 1972, Preliminary Evaluation of the Norwegian Long Period Array, Special Report No. 5, Extended Array Evaluation Program, Contract Number F33657-71-C-0843, Texas Instruments Incorporated, Dallas, Texas.

Kanestrom, R. and K. Haugland, 1971, Crustal Structure in Southeastern Norway from Seismic Refraction Measurements, Scientific Report No. 5, Seismological Observatory, University of Bergen, Norway.

Texas Instruments, Incorporated, 1971, Documentation of NORSAR Short Period Array Evaluation Software Package, Contract Number F33657-69-C-1063, Dallas, Texas.